

**NASA**  
**Technical Memorandum 84664**

**AVRADCOM**  
**Technical Report 83-D-21**

NASA-TM-84664

19830024247

# **Interior Noise and Vibration Measurements on Operational Military Helicopters and Comparisons With Various Ride Quality Criteria**

**Sherman A. Clevenson, Jack D. Leatherwood,  
and Daniel D. Hollenbaugh**

**AUGUST 1983**



25th Anniversary  
1958-1983

**NASA**





# **Interior Noise and Vibration Measurements on Operational Military Helicopters and Comparisons With Various Ride Quality Criteria**

**Sherman A. Clevenson and Jack D. Leatherwood**  
*Langley Research Center*  
*Hampton, Virginia*

**Daniel D. Hollenbaugh**  
*Applied Technology Laboratory*  
*USARTL (AVRADCOM)*  
*Fort Eustis, Virginia*



National Aeronautics  
and Space Administration

**Scientific and Technical  
Information Branch**





## SUMMARY

This paper presents physical measurements of the interior noise and vibration obtained within eight operational military helicopters. The data were analyzed and are presented in the following forms: noise and vibration spectra, overall root-mean-square acceleration levels in three linear axes, peak accelerations at dominant blade passage frequencies, acceleration exceedance data, and overall and "A"-weighted sound pressure levels. Peak acceleration levels were compared to the ISO 1-hr reduced comfort boundary, the fatigue decreased proficiency boundary, and the NASA discomfort criteria. The "A"-weighted noise levels were compared to the NASA annoyance criteria, and the overall noise spectra were compared to MIL-STD-1294 ("Acoustical Noise Limits in Helicopters"). It is shown that specific vibration components at blade passage frequencies for several aircraft exceeded both the ISO reduced comfort boundary and the NASA passenger discomfort criteria. The "A"-weighted noise levels, corrected for SPH-4 helmet attenuation characteristics, exceeded the NASA annoyance threshold for several aircraft. The spectral components of the noise at cruise, corrected for helmet attenuation, fell within the limits of MIL-STD-1294 for all aircraft.

## INTRODUCTION

The specification of internal noise and vibration criteria for passenger/crew comfort is becoming increasingly important as the helicopter industry strives to achieve an improved quality ride in rotary wing aircraft. In a recent paper (ref. 1), the attainment of a "jet-smooth" ride was identified as a primary goal of the helicopter industry for commercial and certain military helicopters. It was noted that criteria accounting for both multiple axis vibration and interior noise are needed. A key element in the development of such criteria, as well as the development of improved vibration and noise control technology, is knowledge of the interior noise and vibration environments experienced by the occupants of current helicopters.

Although a substantial amount of helicopter vibration and interior noise data exists in the literature (refs. 2 to 7), it is generally not presented in a context or format directed toward the assessment of vehicle ride quality. The purposes of this paper are (1) to present a vibration and interior noise data base in a format suitable for direct evaluation of aircraft ride quality and (2) to assess the measured environment against available criteria as an indication of the state of the art for current machines. These data were obtained within the crew/passenger compartment during operational flights of both Army and Navy helicopters. To accomplish these purposes, a joint effort was conducted between the NASA Langley Research Center at Hampton, Virginia, and the U.S. Army Applied Technology Laboratory, AVRADCOM Research and Technology Laboratories at Ft. Eustis, Virginia. With further cooperation of the Aviation Material Management Division of the U.S. Army Transportation School at Ft. Eustis, Virginia, and NAVAIRLANT located at the Naval Air Station at Norfolk, Virginia, a total of eight helicopters (five Army and three Navy) were used to obtain cabin/cockpit vibration and noise measurements during routine flights over a range of airspeeds. It should be emphasized that the measurements were made on operational vehicles during scheduled mission flights with no attempt at tuning the systems to achieve minimum levels or to select vehicles known to have high vibration and/or

noise levels. The resulting data were extensively analyzed and are presented in this paper in a format suitable for use in the evaluation of helicopter ride quality. The results include the following basic parameters: cabin interior noise and vibration spectra, overall root-mean-square acceleration levels in the three linear axes, peak accelerations at dominant frequencies, overall sound pressure level, and "A"-weighted sound pressure level. The dominant vibration components (1P, 2P, 3P, etc.) for each helicopter are compared to the ISO reduced comfort boundary, the fatigue decreased proficiency boundary, and the recently developed NASA discomfort criteria. Noise-level comparisons are made to the current military interior noise specification and to possible criteria levels obtained from other investigations. The problems involved in achieving acceptable ride quality are discussed, and suggestions are made for a follow-on study to directly obtain crew subjective reactions to helicopter noise and vibration environments.

#### SYMBOLS AND ABBREVIATIONS

"A"	specific weighting of each octave or one-third octave of noise spectra
g	acceleration due to gravity, g units
$g_p$	peak acceleration, g units
$g_{rms}$	root-mean-square acceleration, g units
$L_A$	"A"-weighted overall sound pressure level, dB
P	rotor rotational speed, rps

#### Abbreviations:

dB	decibel
FDPB	fatigue decreased proficiency boundary
H-1 to H-8	helicopter (aircraft) designations
IGE	in ground effect
ISO	International Standards Organization
NASA	National Aeronautics and Space Administration
NP	rotor blade passage frequency, where N is number of main rotor blades, Hz; 1P, 2P, etc., rotor vibrational frequencies
OASPL	overall sound pressure level, dB
OGE	out of ground effect
RCB	reduced comfort boundary
rms	root mean square
rpm	revolutions per minute

SPL        sound pressure level,  $20 \log \frac{\text{Pressure}}{0.00002}$ , dB (re 20  $\mu$ Pa)  
TSA        Time Series Analysis Program

## EXPERIMENTAL METHOD

Interior noise and vibration measurements were obtained on eight military helicopters during routine operational flights. The following sections discuss details of the helicopters, instrumentation, measurements, and data reduction.

### Details of Helicopters (Aircraft)

Various descriptive characteristics of the eight helicopters are given in table I. These include the aircraft and corresponding designation used in this report, branch of military service, design gross weight and actual flight weight, main-rotor and tail-rotor revolutions per minute (rpm), number of rotor blades, and rotor frequencies in hertz. Throughout this report, the aircraft are referred to by the designations listed in table I (H-1 for the OH-58C, H-2 for the UH-1H, H-3 for the AH-1S, H-4 for the SH-2F, H-5 for the UH-60A, H-6 for the UH-46D, H-7 for the CH-47C, and H-8 for the RH-53D). Photographs of these aircraft are shown in figures 1(a) to 1(h).

### Instrumentation

The instrumentation consisted of devices for recording both vibration and noise. The vibration instrumentation consisted of a portable triaxial accelerometer package and a seven-channel analog frequency-modulated (FM) tape recorder. The accelerometers had a flat frequency response from 0 to 20 Hz, and the response was down 3 dB at 30 Hz, 4.5 dB at 50 Hz, and 13 dB at 100 Hz. The reason for the roll-off was that the accelerometer package was designed for ride quality purposes which required high sensitivity to low-frequency vibrations. Vibration at higher frequencies (above about 30 Hz) is less important to ride quality and, in fact, is usually obscured by the noise environment. (See ref. 8.) The seven-channel FM tape recorder used to record vibration had flat response from 0 to 500 Hz. Prior to each flight a calibration signal was recorded. The vibration calibration was 1g in each axis, accomplished by rotating the accelerometer box. In addition, a 1-volt direct-current signal was used on a separate channel as a data marker. The signal was turned on when the tape was up to speed and turned off at the end of each data segment.

The sound recording instrumentation consisted of a dual-track tape recorder and dual microphones usually semisoft mounted near the pilot's and co-pilot's heads. Other times the microphones were located in the cabin. (See "Measurements.") The microphones had flat response from 2 Hz to 15 000 Hz. The audio tape recorder had flat response from 16 Hz to 15 000 Hz and was down 4 dB at 12.5 Hz and 9 dB at 10 Hz. Prior to each flight, a noise calibration signal of 114 dB at 1000 Hz (from a pistonphone) was recorded on each track of the audio recorder. A separate voice track on each recorder was used to record point number and flight conditions. The accelerometer system, microphones, and both tape recorders were powered by internal batteries. This required no aircraft power connection and allowed for quick instrumentation installation and removal.

## Measurements

The accelerometer package was generally placed on the floor near the pilot's seat. The actual locations of the accelerometer package and microphones within each aircraft are shown in figure 2. The use of floor measurements, as opposed to seat measurements, was based on the results of NASA research which demonstrated that floor acceleration correlated as well as seat acceleration with passenger comfort ratings (ref. 9).

This location of accelerometers was suitable for the smaller aircraft but proved unworkable in the larger aircraft (H-6, H-7, and H-8) because of insufficient cord lengths and the fact that this would have placed the measuring instruments out of sight and reach of the test engineer. Therefore, in these aircraft the accelerometer box and microphones were placed in the cabin rather than the cockpit. In aircraft H-7 the accelerometer was mounted in the passageway between cabin and cockpit, as shown in figure 1(i). In aircraft H-6 and H-8 the accelerometers were "semisoft" mounted along the bulkhead separating cabin and cockpit. In each of these aircraft the microphones were mounted above the troop seats in the cabin, one on the port side and one starboard. The unique interior layout of aircraft H-4 prompted a similar microphone installation. A typical microphone installation for the smaller aircraft is shown in figure 1(j). Both recorders and the accelerometer box in aircraft H-8 are shown in figure 1(k).

Recordings of sound and vibration were made for a wide range of flight conditions on each aircraft, including hover in ground effect (IGE), hover out of ground effect (OGE), left and right sideward flight, rearward flight IGE at approximately 10 knots, and forward level flight at speeds up to aircraft maximum. At each data condition the aircraft velocity and altitude were recorded from the aircraft instruments. Aircraft speed data below 30 knots must be considered approximate since rotor downwash in this region rendered the internal airspeed measuring devices inaccurate. Prior to each flight, aircraft take-off gross weight, airfield temperature, and altimeter settings were recorded.

## Data Reduction

The interior noise and vibration recordings made in the field were subjected to "quick-look" analyses for obtaining overall levels and to detailed analyses for obtaining spectrum content. The results of these analyses are presented in both tabular and graphical form in this report. Details of the analyses are given in the following sections.

Vibration analyses.— The "quick-look" analysis of the vibration acceleration recordings consisted of playing the recorded signals into a strip chart recorder and simultaneously into a frequency analyzer which provided real-time narrow-band (0.125 Hz) analyses of the rms acceleration level as a function of frequency for each axis and flight condition. These levels were subsequently verified by more detailed spectral analyses using the computer software available at NASA Langley Research Center for the analysis of digital time series data (TSA program, ref. 10). The output of the TSA program consisted of acceleration power spectral density in  $g^2/Hz$ , summary statistics (such as maximum, minimum, overall rms, standard deviation), and exceedance values. Approximate peak acceleration levels at specific frequencies of interest and associated harmonics were determined by integration of the acceleration power spectral density data. To obtain these values, it was assumed that the

acceleration waveforms were made up of basically sinusoidal components. This assumption was verified by examination of the acceleration time histories and the rms power spectra.

Interior noise.- The "quick-look" analysis of the noise signals was accomplished by playing the signals into graphic level recorders which produced time histories of OASPL (overall sound pressure levels) and  $L_A$  ("A"-weighted sound pressure levels). One-minute recordings of interior cabin/cockpit noise for each flight condition were also analyzed with a real-time one-third octave analyzer and graphic level recorders to obtain one-third octave band noise spectra (OASPL) and  $L_A$ . To obtain representative noise levels during each flight condition, the arithmetic average of the overall SPL's from the two microphones was used.

## RESULTS AND DISCUSSION

The results of this investigation are presented in both tabular and graphical form (tables II to VI and figs. 3 to 13). The first part of this section discusses the various parameters used to define the helicopter vibration environment for each of the flight conditions, and the second part describes the interior-noise-measurement results. This section concludes with a comparison of noise and vibration data to existing criteria and a discussion of the problems and possibilities of achieving acceptable ride quality.

### Vibration

Peak acceleration levels at predominant frequencies.- Peak acceleration levels at predominant frequencies are presented in table II for each aircraft flight condition and axis of vibration (i.e., vertical, lateral, longitudinal). These data are shown graphically in figures 3(a) to 3(h). The frequencies shown in both table II and the graphs of figure 3 are those at which the largest vibration levels were observed. The data in figures 3(a) to 3(h) correspond to aircraft having two-bladed rotors (figs. 3(a) to 3(c)), four-bladed rotors (figs. 3(d) and 3(e)), tandem three-bladed rotors (figs. 3(f) and 3(g)), and a six-bladed rotor (fig. 3(h)). Examination of these figures shows that the peak floor acceleration levels due to individual predominant frequencies reached relatively high levels within several aircraft (e.g., H-5 and H-7) and moderate levels in all of the aircraft. No systematic variation of peak acceleration levels as a function of flight condition or axis of vibration is apparent. The range of peak accelerations, however, does include levels which could compromise ride quality.

It is generally expected that the highest accelerations will occur at the blade passage frequency NP; this did occur for most of the aircraft measured in the present study. In certain cases, however, the highest accelerations were experienced at a multiple of NP; this occurred in the lateral direction at 2NP (or 4P) for aircraft H-3. (See fig. 3(c).) For aircraft H-7 with tandem three-bladed rotors, the 6P accelerations were largest (table II (g)); this was due to the reduction of the 3P accelerations by use of cockpit vibration absorbers (used only on aircraft H-7) tuned to the 3P frequency.

Acceleration spectra.- Figures 4(a) to 4(h) show vertical rms acceleration spectra for the normal cruise condition of each aircraft. The acceleration levels are shown in  $g_{rms}$  units. The predominant frequencies are indicated on each figure. These figures clearly demonstrate the discrete frequency character of the measured

vibration data for each aircraft and thereby support the assumption made in the procedure (see "Vibrational Analysis") for determining peak acceleration level at the rotational frequencies and associated harmonics. It should be noted that values of rms acceleration taken from these figures and converted to peak acceleration may vary slightly from the values listed in table II. This is because the values in table II were derived from power spectral density data provided as output of the TSA program whereas the spectra of figure 4 were obtained from real-time narrow-band analysis using a frequency analyzer. (See section "Data Reduction.") These differences, however, are small. The data of figure 4 show that significant vibrations are present within each helicopter at frequencies well within the range known to adversely affect ride quality, namely in the range below 30 Hz. The vibration spectra for the lateral and longitudinal axes are not shown in this report since they exhibit spectral characteristics similar to those shown for the vertical axis but with generally lower levels. However, accurate assessment of helicopter ride quality will also have to account for the additional effects of the combined axes.

Exceedance data.- An optional output available from the TSA program is the computation of a parameter similar to a frequency count in grouped frequency distribution. This parameter is called percent exceedance and is defined as follows: for a signal time history of finite length, percent exceedance is the percent of time (relative to the total signal record length) that the signal takes on values between given upper and lower limits. The usefulness of the exceedance data, particularly for random signals, lies in the fact that it provides information with regard to the relative frequency of occurrence of extreme values of the signal. The exceedance data for the present study are presented in table IV for vertical vibration at the cruise condition for each aircraft. The data in table IV indicate that peak acceleration levels in excess of  $\pm 0.60g$  occurred on two aircraft (H-6 and H-8), that levels of  $\pm 0.50g$  or greater occurred on five aircraft (H-4, H-5, H-6, H-7, and H-8), and that all aircraft experienced peak levels up to  $\pm 0.20g$ . These levels occurred, however, relatively infrequently, as indicated by the low percent exceedance values for the extreme levels measured for each aircraft.

Overall root-mean-square acceleration.- Overall vibration levels over the frequency range of 0.1 Hz to 30 Hz are listed in table III in terms of rms (root-mean-square) acceleration levels in each axis and shown in figures 5(a) to 5(c) as a function of airspeed for each aircraft. It should be recalled that these levels reflect vibrations predominantly at frequencies below 30 Hz because of the instrumentation roll-off characteristics. Inspection of figures 5(a) to 5(c) shows that the overall rms acceleration levels in each axis vary substantially with flight speed and that these variations do not appear to be very systematic in nature. Also evident is a considerable variation in overall acceleration level from aircraft to aircraft. These data are summarized in a more convenient form in figure 6, which shows the range over flight conditions of overall rms acceleration level for each axis and aircraft. In most cases the vertical vibration levels were highest and longitudinal vibrations were lowest. Exceptions to this were aircraft H-2 and H-6. From the standpoint of the ride quality of these eight aircraft, the range of acceleration depicted in figure 6 exceeds existing ride quality vibration criteria.

## Interior Noise

One-third octave spectra.- One-third octave spectra for each aircraft in the cruise condition are shown in figures 7(a) to 7(i). These figures present the sound pressure levels within each one-third octave band for center frequencies between 4 Hz and 16 000 Hz. The levels are in decibels, referenced to 20  $\mu Pa$ . Also indicated on

each figure is the overall sound pressure level (OASPL). Both OASPL and "A"-weighted sound pressure levels  $L_A$  are given in table V for all measured flight conditions.

Figures 7(b) to 7(i) show that both the interior noise levels and frequency content vary significantly from aircraft to aircraft. Overall noise levels (OASPL) ranged from 107 dB (aircraft H-1) to 121 dB (aircraft H-6); the corresponding values of  $L_A$  were 94 dB and 106 dB, respectively. For all of the aircraft the highest one-third octave level occurred within the one-third octave band containing the blade passage frequency. However, figures 7(d) and 7(h) indicate that the maximum noise level was in the band containing the second harmonic of the blade passage frequency. This indication is due to the fact that the tape-recorder response rolled off at the lower frequencies (9 dB down at 10 Hz and 4 dB down at 12.5 Hz). When the noise levels are corrected for tape recorder roll-off, it is noted that the highest one-third octave noise levels for aircraft H-3 and H-7 also occur in the one-third octave containing NP. (Note: The low-frequency roll-off shown on each chart of figure 7 is due to the tape-recorder frequency response characteristics.) Higher harmonics of the blade passage frequency are evident in most of the spectra, and it is the higher harmonics that would most likely influence passenger annoyance and, hence, affect overall ride quality.

Noise levels.— The variations of overall sound pressure level (OASPL) and "A"-weighted sound pressure level  $L_A$  with flight condition are shown in figures 8 and 9. For both noise metrics the levels remain relatively constant over most of the flight speed range although several aircraft (H-1, H-3, H-5, and H-8) indicated increased interior "A"-weighted noise levels at the higher speeds. Generally, however, the noise levels remained within 3 dB relative to the IGE hover condition. Several additional points of interest with regard to the data presented in figures 8 and 9 include the following: First, the range of values of OASPL between aircraft is much less than the range of values of  $L_A$ . This results from the fact that the "A"-weighted sound pressure level is the sound pressure level modified to attenuate the effects of sound at frequencies less than 1000 Hz and greater than 5000 Hz. Sound at frequencies between 1000 Hz and 5000 Hz is slightly emphasized (ref. 11). Hence, aircraft with two-bladed rotors will usually show the greatest reduction in level due to "A"-weighting; this is evident in figures 8 and 9 since aircraft H-1, H-2, and H-3 have two-bladed rotors and generate significant acoustic energy at low frequencies. The noise level of aircraft H-5 was also significantly lowered by "A"-weighting, because it has a four-bladed rotor and its dominant noise band is at the 4P frequency (17.5 Hz). Another point of interest is that the relative ranking of the aircraft in terms of OASPL and  $L_A$  differ substantially. Since  $L_A$  is usually considered to be a metric that correlates well with human annoyance response, the relative levels shown in figure 8 may be useful in roughly assessing relative subjective acceptance of the measured environments. This interpretation must be used with caution, however, since  $L_A$  does not account for tonal effects or for the effects of noise duration. Thus,  $L_A$  may not be the best available metric for the assessment of helicopter noise since a large part of the aircraft's acoustic energy is of a low-frequency tonal character. It is reasonable to conclude, however, that OASPL may not be useful as an indicator of relative ride quality and that  $L_A$  provides a better indicator of the impact of noise on ride quality of these aircraft.

#### Comparison With Available Criteria

This section discusses the relationship of the noise and vibration data presented in the previous sections to existing standards and/or criteria. The vibration data are compared to the 1-hour reduced comfort boundary (RCB) and the 1-hour fatigue

decreased proficiency boundary (FDPB) defined by the International Standards Organization (ISO) in reference 12. Comparisons are also made with the discomfort threshold contour developed in research conducted by the National Aeronautics and Space Administration (NASA) and reported in reference 13. The noise data are compared to the recent military standard MIL-STD-1294 (ref. 14), for interior noise limits in helicopters, and to an "A"-weighted level corresponding to the threshold of annoyance for simulated turboprop interior noise (ref. 15). It should be kept in mind, however, that the most meaningful comparison should be to criteria that reflect the combined effects of vibration and noise. Such criteria are not currently available although the NASA ride comfort model approach of reference 13 offers a possible approach to defining combined criteria.

Comparison with vibration criteria.- Comparisons of measured peak acceleration levels at various blade passage frequencies to the ISO 1-hour RCB and FDPB and to the NASA discomfort threshold curve are shown in figures 10(a), 10(b), and 10(c) for the vertical, lateral, and longitudinal directions, respectively. Each aircraft (except H-7) is designated with a symbol and is plotted at its blade passage frequency. The data for aircraft H-7 are plotted at the frequency of the 2NP (6P) component of vibration since 6P was the dominant component for this aircraft. The upper and lower symbols on each vertical line represent the highest and lowest acceleration levels measured over the aircraft's airspeed range. These data indicate that six of the eight aircraft experienced vertical vibration levels which exceeded either the ISO 1-hour RCB or the NASA discomfort threshold limits. Three of these aircraft (H-3, H-5, and H-7) exceeded the vertical acceleration limits by substantial margins, indicating significant reduction in ride quality. None of these aircraft exceeded the vibration criteria for the lateral and longitudinal axes of vibration. (See figs. 10(b) and 10(c).) It is possible, however, that the combined effects of the individual vibrations could act to produce uncomfortable levels.

Comparison with noise criteria.- The ranges of the "A"-weighted noise levels for the military aircraft of this paper are compared to the "A"-weighted annoyance threshold value (ref. 15) in figure 11(a). It is seen that the interior noise measured within each aircraft exceeds the annoyance threshold by a considerable margin and would be totally unacceptable without ear protection. The SPH-4 helmet (ref. 16 and table VI) worn by Army helicopter crew members affords 19 to 24 dB overall attenuation of the interior noise "A"-weighted spectrum in the range of 63 Hz to 2000 Hz. The "A"-weighted noise levels corrected for helmet attenuation are shown in figure 11(b). This figure indicates that only four aircraft (H-4, H-6, H-7, and H-8) definitely exceed the annoyance threshold over the total range of flight conditions. Whether these levels would be sufficient to adversely affect military mission performance is not known.

Comparisons of the interior octave band noise spectra at cruise with the most recent military limit design criteria (ref. 14) are shown in figures 12(a) and 12(b). Figure 12(a) presents comparisons for helicopters having gross weights under 20 000 lb, and figure 12(b), for helicopters with gross weights in excess of 20 000 lb. The levels shown in figures 12(a) and 12(b) have been corrected for helmet attenuation; this was done since MIL-STD-1294 represents design limit levels for crew members wearing helmets (SPH-4 for Army crew members and helmets with similar attenuation characteristics for Navy crew members) and for passengers using approved hearing protection. This comparison indicates that the helmets effectively reduce the levels such that they fall well below the design limit curves; this does not mean that the levels would not be annoying. For example, recall the results of figure 11(b), which showed that several aircraft produced annoyance levels in excess of the annoyance threshold. The levels probably are not sufficient to adversely affect



mission performance, but, when combined with the vibration environment, they usually produce additional degradation of passenger ride quality. Occasionally, passengers may not have or use hearing protection. In this case, it is appropriate to compare the noise spectra without helmet corrections to MIL-STD-1294. The comparison is shown in figures 13(a) and 13(b) from which it is seen that some octave band noise levels for each aircraft exceed specified limits. The results indicate the importance of providing and insisting upon the use of approved hearing protection devices when flying in these aircraft.

### Passenger Ride Quality Considerations

This section discusses the implication of the results presented earlier in the paper with regard to the achievement of helicopter passenger ride quality comparable to that of commercial jet transports. It should be understood that levels of noise and/or vibration consistent with a "jet-smooth" ride are much less than those required to assure acceptable mission performance. Consequently, attainment of such levels will entail additional costs for vibration and noise suppression systems.

Comparisons of vibrations (fig. 10) and interior noise (fig. 11) to several ride quality criteria indicated the extent to which reductions in noise and vibration may be required in order to achieve acceptable passenger ride quality. For vibration, it was observed that substantial reduction in vibration levels associated with specific blade passage frequencies would be necessary to bring the levels within the ISO and NASA criteria limits for most of the aircraft discussed in this paper. This would require improvements in the existing vibration reduction systems or implementation of additional vibration control systems.

For the noise environment, it was seen that  $L_A$  (corrected for helmet attenuation) exceeded the annoyance threshold on four of the eight aircraft. All of the aircraft data corrected for helmet attenuation met the requirements of MIL-STD-1294. To bring all of the aircraft below the annoyance threshold limits would require adding noise control treatment to those aircraft which exceeded the limit. An example of a current noise control treatment that was effective in quieting a large civil helicopter (similar to aircraft H-8) is described in reference 6. That particular treatment resulted in an average reduction in  $L_A$  of about 28 dB with a weight penalty of approximately 1 percent of mission gross weight. Certainly there are many missions for which passenger ride comfort is relatively unimportant as long as crew performance and mission objectives are not compromised. There remains, however, a large number of missions (i.e., civil transports, military gunships, and military executive aircraft) for which improved ride quality offers distinct benefits.

Another question that should be considered is the effect of the combined noise and vibration environment upon passenger acceptance and the development of realistic criteria that account for the combined effects. The only method known to exist that accounts for both noise and vibration is the NASA ride comfort model approach given in reference 13. This method produces a single number index of discomfort that is a direct correlate of passenger comfort within the combined environment. Additional studies, using a ground-based simulator, should be conducted to directly obtain crew members' subjective reactions to the combined environments. These results could then be used to validate the NASA model for the helicopter environment.

## CONCLUDING REMARKS

Physical measurements of helicopter interior noise and vibration have been obtained on eight operational military aircraft. The data were extensively analyzed and presented in the form of the following basic physical parameters: cabin interior noise and vibration spectra, overall root-mean-square acceleration levels in three linear axes, peak acceleration at dominant blade passage frequencies, acceleration exceedance data, and overall and "A"-weighted sound pressure levels. Where appropriate, the data were compared with various ride quality criteria. The acceleration levels at dominant vibration frequencies were compared to (1) the ISO reduced comfort boundary, (2) the ISO fatigue decreased proficiency boundary, and (3) the NASA discomfort criteria. The "A"-weighted noise levels were compared to simple annoyance criteria developed during NASA interior noise research, and the overall noise spectra were compared to the MIL-STD-1294 ("Acoustical Noise Limits in Helicopters"). It is shown that specific vibration components at certain harmonics of the blade passage frequency for several aircraft exceeded both the ISO reduced comfort boundary and the NASA passenger discomfort criteria. Further, "A"-weighted noise levels, corrected for SPH-4 helmet attenuation characteristics, exceeded the NASA annoyance threshold for several aircraft. The overall noise levels for all aircraft, when corrected for helmet attenuation, fell within the limits of MIL-STD-1294.

Specific comments and implications of these results relative to the goal of achieving passenger ride quality comparable to commercial jet transport include the following:

1. The fact that a number of vibration components exceeded both ISO and NASA criteria indicates that additional effort is required to reduce the vibration environment experienced by passengers and crew.
2. The interior noise levels within all of the aircraft measured in this study would be totally unacceptable to passengers without hearing protection. Even with helmets, the levels were unacceptable in four of the eight aircraft. Thus, for aircraft in which passenger ride quality is an important consideration, additional acoustic treatment will be required.
3. The interior noise levels were not sufficient to impair mission performance for crew members wearing the SPH-4 or similar helmets. Thus, for aircraft in which military mission performance is the primary objective and passenger/crew comfort is secondary, it would be unnecessary to reduce either vibration or noise levels.
4. The effects of the combined noise and vibration environments on passenger acceptance should be considered. NASA research has indicated that the two parameters interact to produce a total passenger discomfort response greater than either individual component. Criteria are needed which would effectively and realistically account for the combined effects.

Langley Research Center  
National Aeronautics and Space Administration  
Hampton, VA 23665  
June 13, 1983

## REFERENCES

1. Balke, R. W.: The Helicopter Ride Revolution. Technology for the Jet Smooth Ride - A National Specialists' Meeting on Helicopter Vibration, American Helicopter Soc., Nov. 1981, pp. 81-4-1 - 81-4-14.
2. Rita, A. D.; McGarvey, J. H.; and Jones, R.: Helicopter Rotor Isolation Evaluation Utilizing the Dynamic Antiresonant Vibration Isolator. J. American Helicopter Soc., vol. 23, no. 1, Jan. 1978, pp. 22-29.
3. Spring, Sherwood C.; Burch, Thomas E.; Buckanin, Robert M.; and Niemann, John R.: Airworthiness and Flight Characteristics Evaluation - OH-58C Interim Scout Helicopter. USAAEFA Proj. No. 76-11-2, U.S. Army, Apr. 1979. (Available from DTIC as AD A080 138.)
4. Sternfeld, Harry, Jr.; and Doyle, Linda Bukowski: A Method for Determining Internal Noise Criteria Based on Practical Speech Communication Applied to Helicopters. Helicopter Acoustics, NASA CP-2052, Pt. II, 1978, pp. 493-511.
5. Murray, Bruce S.; and Wilby, John F.: Helicopter Cabin Noise - Methods of Source and Path Identification and Characterization. Helicopter Acoustics, NASA CP-2052, Pt. II, 1978, pp. 583-594.
6. Howlett, James T.; Clevenson, Sherman A.; Rupf, John A.; and Snyder, William J.: Interior Noise Reduction in a Large Civil Helicopter. NASA TN D-8477, 1977.
7. Hammond, C. E.; Hollenbaugh, D. D.; Clevenson, S. A.; and Leatherwood, J. D.: An Evaluation of Helicopter Noise and Vibration Ride Qualities Criteria. NASA TM-83251, 1981.
8. Clevenson, Sherman A.: Effect of Synthesized Propeller Vibration on Passenger Annoyance in a Turboprop Interior Noise Environment. NASA TM-84515, 1982.
9. Dempsey, Thomas K.; and Leatherwood, Jack D.: Experimental Studies for Determining Human Discomfort Response to Vertical Sinusoidal Vibration. NASA TN D-8041, 1975.
10. Gridley, Doreen: An Introduction to Time Series Analysis and Data Reduction Programming Capabilities. NASA CR-165782, 1981.
11. Bennett, Ricarda L.; and Pearsons, Karl S.: Handbook of Aircraft Noise Metrics. NASA CR-3406, 1981.
12. Guide for the Evaluation of Human Exposure to Whole-Body Vibration. ISO 2631-1974 (E), Int. Organ. Stand., July 1, 1974.
13. Leatherwood, Jack D.; Dempsey, Thomas K.; and Clevenson, Sherman A.: A Design Tool for Estimating Passenger Ride Discomfort Within Complex Ride Environments. Hum. Factors, vol. 22, no. 3, June 1980, pp. 291-312.
14. Military Standard - Acoustical Noise Limits in Helicopters. MIL-STD-1294, Mar. 9, 1981.

15. Mixson, J. S.; Farassat, F.; Leatherwood, J. D.; Prydz, R.; and Revell, J. D.: Interior Noise Considerations for Advanced High-Speed Turboprop Aircraft. AIAA-82-1121, June 1982.
16. Military Specification - Helmet, Flyer's, Protective, SPH-4. MIL-H-43925A, Feb. 4, 1980. (Supersedes MIL-H-43925, Mar. 31, 1975.)

TABLE I.- HELICOPTER CHARACTERISTICS

Aircraft	Designation	Service	Design gross weight, lb	Flight weight, lb	Main rotor								Tail rotor				
					rpm	Number of blades	Frequency, Hz						rpm	Number of blades	Frequency, Hz		
							1P	2P	3P	4P	6P	8P			1P	2P	4P
OH-58C	H-1	Army	3 200	3 000	354	2	5.9	11.8		23.6	35.4	47.2	2290	2	38.2	76.3	152.7
UH-1H	H-2	Army	7 300	7 500	324	2	5.4	10.8		21.6	32.4	43.2	1655	2	27.6	55.2	110.3
AH-1S	H-3	Army	10 000	8 500	324	2	5.4	10.8		21.6	35.4	43.2	1655	2	27.6	55.2	110.3
SH-2F	H-4	Navy	12 800	11 100	298	4	4.97			19.9		39.7	1708	4	28.5		113.9
UH-60A	H-5	Army	16 835	13 700	262	4	4.4			17.5		35.0	1190	4	19.8		79.3
UH-46D	H-6	Navy	20 800	18 000	264	3	4.4		13.2		26.4		NA	NA	NA	NA	NA
CH-47C	H-7	Army	33 000	32 000	235	3	3.9		11.8		23.5		NA	NA	NA	NA	NA
RH-53D	H-8	Navy	33 500	42 000	185	6	3.1				18.5		790	4	13.2		52.7

TABLE II.- PEAK ACCELERATION LEVELS FOR AIRCRAFT H-1 TO H-8

## (a) Aircraft H-1

Flight condition	1P = 5.9 Hz			2P = 11.8 Hz			4P = 23.6 Hz		
	Peak acceleration, $g_p$ , g units								
	Vertical	Lateral	Longitudinal	Vertical	Lateral	Longitudinal	Vertical	Lateral	Longitudinal
Ground runup	0.0598	0.0098	0.0189	0.0178	0.0098	0.0206	0.0008	0.0014	0.0112
OGE hover	.0086	.0082	.0074	.0544	.0150	.0223	.0116	.0037	.0205
IGE hover	.0096	.0051	.0049	.0141	.0079	.0174	.0059	.0033	.0045
≈20 knots	.0037	.0057	.0038	.0242	.0144	.0134	.0106	.0059	.0191
60 knots	.0071	.0049	.0042	.0335	.0238	.0116	.0133	.0037	.0109
*80 knots	.0129	.0048	.0044	.0626	.0288	.0100	.0090	.0092	.0144
100 knots	.0185	.0072	.0066	.0978	.0297	.0103	.0055	.0076	.0215

\*Cruise speed.

## (b) Aircraft H-2

Flight condition	1P = 5.4 Hz			2P = 10.8 Hz			4P = 21.6 Hz		
	Peak acceleration, $g_p$ , g units								
	Vertical	Lateral	Longitudinal	Vertical	Lateral	Longitudinal	Vertical	Lateral	Longitudinal
OGE hover	0.0134	0.0120	0.0052	0.0362	0.0431	0.0522	0.0274	0.0450	0.0041
IGE hover	.0074	.0058	.0030	.0239	.0180	.0132	.0188	.0167	.0100
≈20 knots	.0130	.0089	.0059	.0156	.0194	.0126	.0274	.0175	.0037
40 knots	.0049	.0133	.0033	.0215	.0304	.0273	.0170	.0260	.0027
60 knots	.0061	.0156	.0045	.0242	.0314	.0287	.0085	.0185	.0088
80 knots	.0059	.0147	.0033	.0270	.0359	.0304	.0218	.0188	.0093
*90 knots	.0147	.0132	.0041	.0352	.0451	.0493	.0351	.0447	.0068
100 knots	.0100	.0174	.0037	.0342	.0409	.0365	.0296	.0305	.0083
120 knots	.0160	.0132	.0112	.0307	.0556	.0547	.0296	.0404	.0041

\*Cruise speed.

TABLE II.- Continued

## (c) Aircraft H-3

Flight condition	1P = 5.4 Hz			2P = 10.8 Hz			4P = 21.6 Hz		
	Peak acceleration, $g_p$ , g units								
	Vertical	Lateral	Longitudinal	Vertical	Lateral	Longitudinal	Vertical	Lateral	Longitudinal
OGE hover	0.0064	0.0099	0.0049	0.0334	0.0570	0.0099	0.0209	0.0404	0.0112
IGE hover	.0061	.0192	.0040	.0376	.0434	.0096	.0173	.0225	.0076
≈20 knots	.0189	.0163	.0078	.0315	.0354	.0204	.0259	.0293	.0170
40 knots	.0153	.0103	.0054	.0283	.0382	.0206	.0236	.0238	.0178
60 knots	.0211	.0079	.0078	.0329	.0537	.0120	.0382	.0461	.0211
80 knots	.0363	.0202	.0116	.0916	.0527	.0161	.0778	.0962	.0387
100 knots	.0098	.0165	.0096	.1070	.0462	.0151	.0617	.0902	.0296
120 knots	.0349	.0168	.0109	.1285	.0281	.0168	.0696	.0953	.0378
*135 knots	.0161	.0130	.0058	.0646	.0454	.0315	.0154	.0990	.0151
140 knots	.0448	.0235	.0130	.1584	.0619	.0262	.0935	.1168	.0421
148 knots	.0293	.0151	.0100	.1048	.0560	.0137	.0656	.0908	.0270

\*Cruise speed.

## (d) Aircraft H-4

Flight condition	1P = 4.97 Hz			4P = 19.9 Hz		
	Peak acceleration, $g_p$ , g units					
	Vertical	Lateral	Longitudinal	Vertical	Lateral	Longitudinal
Ground runup	0.0409	0.0164		0.0252	0.0112	
OGE hover	.0264	.0267		.0124	.0243	
IGE hover	.0204	.0240		.0250	.0341	
≈20 knots	.0219	.0206		.0766	.0773	
40 knots	.0854	.0771		.0812	.1092	
60 knots	.0173	.0124		.1015	.1740	
80 knots	.0134	.0103		.0674	.1314	
100 knots	.0133	.0074		.0130	.0404	
*120 knots	.0151	.0089		.0170	.0376	
130 knots	.0222	.0096		.0433	.0925	

\*Cruise speed.

TABLE II.- Continued

(e) Aircraft H-5

Flight condition	1P = 4.4 Hz			4P = 17.6 Hz		
	Peak acceleration, $g_p$ , g units					
	Vertical	Lateral	Longitudinal	Vertical	Lateral	Longitudinal
Ground runup	0.0095	0.0252	0.0082	0.1527	0.0532	0.399
OGE hover	.0177	.0161	.0161	.2687	.0536	.0700
IGE hover	.0055	.0065	.0034	.0536	.0327	.0188
40 knots	.0059	.0051	.0030	.2124	.1184	.0638
60 knots	.0076	.0064	.0052	.0827	.0597	.0124
80 knots	.0141	.0088	.0034	.0116	.0557	.0188
100 knots	.0119	.0081	.0035	.0662	.0452	.0472
120 knots	.0164	.0072	.0027	.1509	.0419	.0813
*145 knots	.0335	.0098	.0051	.1951	.1489	.0827
165 knots	.0255	.0161	.0076	.2240	.0748	.0752

\*Cruise speed.

(f) Aircraft H-6

Flight condition	1P = 4.4 Hz			3P = 13.2 Hz			6P = 26.4 Hz		
	Peak acceleration, $g_p$ , g units								
	Vertical	Lateral	Longitudinal	Vertical	Lateral	Longitudinal	Vertical	Lateral	Longitudinal
Ground runup	0.0175	0.0137	0.0530	0.0790		0.0607	0.0250	0.0228	0.0328
OGE hover	.0205	.0199	.0427	.0660	0.0436	.0458	.0433	.0017	.0502
IGE hover	.0113	.0146	.0294	.0588	.0525	.0519	.0503	.0175	.0358
≈10 knots	.0233	.0208	.0460	.0683	.0465	.0601	.0525	.0335	.0188
≈20 knots	.0215	.0156	.0352	.0946	.0874	.0830	.0942	.0946	.0156
40 knots	.0088	.0171	.0290	.0600	.0742	.0966	.0468	.0700	.0208
60 knots	.0110	.0156	.0212	.1403	.0554	.0974	.0294	.0778	.1052
80 knots	.0187	.0157	.0215	.1356	.0462	.0810	.0352	.0868	.0942
100 knots	.0328	.0154	.0223	.0741	.0395	.0509	.0221	.0711	.0807
*120 knots	.0502	.0197	.0260	.0622	.0602	.0881	.0430	.0707	.0744
125 knots	.0475	.0184	.0253	.0560	.0546	.0908	.0351	.0564	.0656

\*Cruise speed.



TABLE II.- Concluded

## (g) Aircraft H-7

Flight condition	1P = 3.9 Hz			3P = 11.7 Hz			6P = 23.4 Hz		
	Peak acceleration, $g_p$ , g units								
	Vertical	Lateral	Longitudinal	Vertical	Lateral	Longitudinal	Vertical	Lateral	Longitudinal
Ground runup									
OGE hover	0.0201	0.0177	0.0157	0.0510	0.0134	0.0297	0.4012	0.1250	0.0807
IGE hover	.0214	.0161	.0154	.0667	.0219	.0322	.3579	.0846	.0475
≈20 knots	.0177	.0208	.0198	.0697	.0322	.0663	.2294	.1854	.0655
40 knots	.0157	.0208	.0202	.0400	.0366	.0512	.1858	.1579	.0546
60 knots	.0156	.0216	.0215	.0112	.0338	.0544	.0976	.1004	.0253
80 knots	.0170	.0201	.0198	.0195	.0221	.0462	.1811	.0971	.0208
100 knots	.0139	.0242	.0219	.0354	.0185	.0297	.3169	.0885	.0240
*120 knots	.0122	.0271	.0216	.0450	.0208	.0362	.2927	.0370	.0621
140 knots	.0276	.0274	.0202	.0560	.0641	.0713	.2115	.0366	.0793

\*Cruise speed.

## (h) Aircraft H-8

Flight condition	1P = 3.08 Hz			6P = 18.5 Hz		
	Peak acceleration, $g_p$ , g units					
	Vertical	Lateral	Longitudinal	Vertical	Lateral	Longitudinal
OGE hover	0.0123	0.0404	0.0010	0.0492	0.0069	0.0001
IGE hover	.0136	.0018	.0011	.0602	.0188	.0003
≈20 knots	.0092	.0065	.0010	.0202	.0192	.0003
40 knots	.0255	.0283	.0011	.0148	.0655	.0003
60 nots	.0048	.0058	.0010	.0789	.0393	.0003
80 knots	.0058	.0047	.0008	.0515	.0341	.0003
100 knots	.0081	.0058	.0010	.0547	.0566	.0003
*120 knots	.0105	.0064	.0010	.0594	.0191	.0003
140 knots	.0192	.0132	.0010	.0865	.0168	.0003
155 knots	.0875	.0814	.0008	.1338	.0214	.0001

\*Cruise speed.

TABLE III.- OVERALL ROOT-MEAN-SQUARE ACCELERATION LEVELS

Flight condition	H-1			H-2			H-3		
	rms acceleration, $g_{rms}$ , g units								
	Vertical	Lateral	Longitudinal	Vertical	Lateral	Longitudinal	Vertical	Lateral	Longitudinal
Left				0.046	0.054	0.047			
Right	0.260	0.242	0.254	.045	.136	.082	0.047	0.071	0.026
Rear	.047	.025	.029	.041	.047	.041	.048	.055	.029
Ground runup	.081	.024	.039						
OGE hover	.070	.030	.041	.048	.066	.062	.039	.049	.019
IGE hover	.037	.021	.030	.055	.048	.052	.041	.062	.025
≈20 knots	.050	.021	.039	.042	.038	.029	.055	.051	.040
40 knots				.033	.070	.064	.044	.044	.033
60 knots	.080		.042	.043	.063	.048	.066	.068	.037
80 knots	.063*	.030*	.033*	.040	.056	.041	.084	.074	.034
90 knots				.051*	.066*	.065*			
100 knots	.097	.049	.045	.047	.059	.043	.117	.092	.039
120 knots				.118	.129	.125	.132	.100	.055
135 knots							.075*	.054*	.043*
140 knots							.165	.124	.056
148 knots							.109	.093	.034

\*At cruise speed.

TABLE III.- Continued

Flight condition	H-4		H-5			H-6		
	rms acceleration, $g_{rms}$ , g units							
	Vertical	Lateral	Vertical	Lateral	Longitudinal	Vertical	Lateral	Longitudinal
Left			0.082	0.053	0.033			
Right			.133	.058	.045			
Rear			.116	.091	.041			
Ground runup	0.098	0.048	.124	.055	.039	0.085	0.033	0.087
OGE hover	.056	.063	.218	.053	.069	.068	.075	.087
IGE hover	.059	.066	.050	.034	.022	.089	.075	.087
≈10 knots						.103	.069	.092
≈20 knots	.090	.079				.114	.132	.154
40 knots			.170	.091	.058	.081	.104	.104
60 knots	.109	.162	.081	.054	.021	.145	.092	.101
80 knots	.081	.124	.049	.048	.026	.144	.093	.098
100 knots	.057	.073	.062	.041	.040	.104	.082	.094
120 knots	.055*	.066*	.128	.049	.070	.121*	.103*	.106*
125 knots						.109	.096	.105
130 knots	.097	.163						
145 knots			.169*	.058*	.078*			
165 knots			.205	.091	.082			

\*At cruise speed.

TABLE III.- Concluded

Flight condition	H-7			H-8		
	rms acceleration, $g_{rms}$ , g units					
	Vertical	Lateral	Longitudinal	Vertical	Lateral	Longitudinal
Left	0.284	0.088	0.082			
Right	.165	.052	.084			
Rear	.282	.066	.063			
Ground runup						
OGE hover	.320	.127	.086	0.074	0.008	
IGE hover	.297	.067	.110	.066	.032	0.008
≈10 knots	.238	.195	.099			
≈20 knots	.192	.151	.079	.039	.025	.007
40 knots	.165	.136	.067	.138	.072	.007
60 knots	.089	.092	.055	.072	.038	.007
80 knots	.148	.092	.047	.050	.034	.007
100 knots	.254	.086	.046	.054	.053	.007
120 knots	.238*	.086*	.064*	.058*	.023*	.007*
140 knots	.199	.110	.119	.119	.032	.007
155 knots				.188	.099	.007

\*At cruise speed.

TABLE IV.- ACCELERATION EXCEEDANCE FOR VERTICAL DIRECTION  
AT CRUISE CONDITION FOR EACH AIRCRAFT

Peak acceleration, $g_p$ , g units	Acceleration exceedance, percent							
	H-1	H-2	H-3	H-4	H-5	H-6	H-7	H-8
<-0.60						1.64		0.01
-0.60 to -0.55						.70	0.03	.00
-.55 to -.50				0.01		1.06	.69	.05
-.50 to -.45				.04	0.01	1.34	2.82	.23
-.45 to -.40				.15	.19	1.69	6.08	.52
-.40 to -.35				.35	.83	2.41	7.64	1.14
-.35 to -.30				1.07	2.84	3.08	7.68	2.05
-.30 to -.25			0.11	2.08	5.23	3.99	6.83	3.08
-.25 to -.20	0.36	0.07	.76	4.25	7.07	5.04	4.89	4.74
-.20 to -.15	2.71	.84	4.05	6.75	8.46	5.92	4.44	6.83
-.15 to -.10	10.23	7.83	9.01	9.72	9.67	7.25	3.95	8.10
-.10 to -.05	17.05	23.58	16.18	11.62	9.58	8.01	3.49	9.84
-.05 to .00	23.28	31.22	20.97	13.37	9.13	8.16	3.46	10.11
.00 to .05	21.61	20.45	23.08	13.33	7.41	8.21	3.42	10.03
.05 to .10	14.91	10.38	16.10	12.03	6.51	8.07	3.24	10.29
.10 to .15	6.78	4.66	7.42	9.95	6.38	7.42	3.78	9.23
.15 to .20	2.29	.94	1.77	6.89	6.66	5.88	3.60	8.31
.20 to .25	.59	.03	.38	4.17	6.55	5.39	5.41	6.96
.25 to .30	.19		.14	2.48	5.47	3.87	8.94	4.30
.30 to .35	.01		.01	1.08	3.98	3.11	10.92	2.34
.35 to .40				.52	2.54	2.26	6.42	1.28
.40 to .45				.13	1.21	1.69	2.04	.40
.45 to .50				.01	.29	1.16	.21	.13
.50 to .55					.02	.81	.01	.03
.55 to .60						.51		
>0.60						1.33		

TABLE V.- NOISE LEVELS FOR MEASURED FLIGHT CONDITIONS

Flight condition	H-1		H-2		H-3		H-4		H-5		H-6		H-7		H-8	
	OASPL	L <sub>A</sub>	OASPL	L <sub>A</sub>	OASPL	L <sub>A</sub>	OASPL	L <sub>A</sub>	OASPL	L <sub>A</sub>	OASPL	L <sub>A</sub>	OASPL	L <sub>A</sub>	OASPL	L <sub>A</sub>
Ground runup	105	98					115	103	115	101	118	104			116	105
Left			119	91	115	95		106	115	95	117	103	114	107		
Right	107	95	119	92	115	95		103	116	95	118	106	117	107		
Rear	106	93	119	91	115	95		105	118	97	121	106	117	107	119	107
IGE	110	95	116	87	114	96	113	104	114	95	120	106	116	109	115	107
OGE	109	94	116	89	113	94	113	103	114	97	119	105	116	107	115	108
10 knots	109	95	117	90	113	96	110	103			121	106	115	107	115	108
20 knots	109	95	117	90	112	94	110	103			120	106	116	107	114	108
30 knots	109	95	117	90			110	102			120	106				
40 knots	107	94	116	90	113	92	112	103	113	95	118	106	116	108	117	107
50 knots																
60 knots	106	95	115	90	114	92	114	103	112	94	121	104	115	108	116	105
80 knots	*107	94	114	93	115	95		104	111	93	121	107	116	109	115	104
90 knots			*113	94			*115	104								
100 knots	107	94	114	95	117	96	114	104	111	94	120	108	117	108	116	103
110 knots																
120 knots			115	98	118	98	117	104	111	93	*121	106	*118	108	*118	105
125 knots											121	106				
130 knots							115	106								
135 knots					*120	97							120	107		
140 knots					120	98										
145 knots									*115	99			120	105	123	109
148 knots					121	99										
155 knots															123	109
165 knots									115	101						

\*At cruise speed.

TABLE VI.- ATTENUATION OF SPH-4 HELMET

Frequency, Hz	Attenuation, dB
75	17
125	16
250	14
500	25
1000	24
2000	30
3000	40
4000	43
6000	44
8000	36



L-81-7326

(a) Aircraft H-1.

Figure 1.- Photographs of aircraft H-1 to H-8 and instrumentation locations.





L-81-7328

(b) Aircraft H-2.

Figure 1.- Continued.



L-81-7329

(c) Aircraft H-3.

Figure 1.- Continued.





L-82-7006

(d) Aircraft H-4.

Figure 1.- Continued.



L-82-7007

(e) Aircraft H-5.

Figure 1.- Continued.





L-82-7008

(f) Aircraft H-6.

Figure 1.- Continued.



L-81-7325

(g) Aircraft H-7.

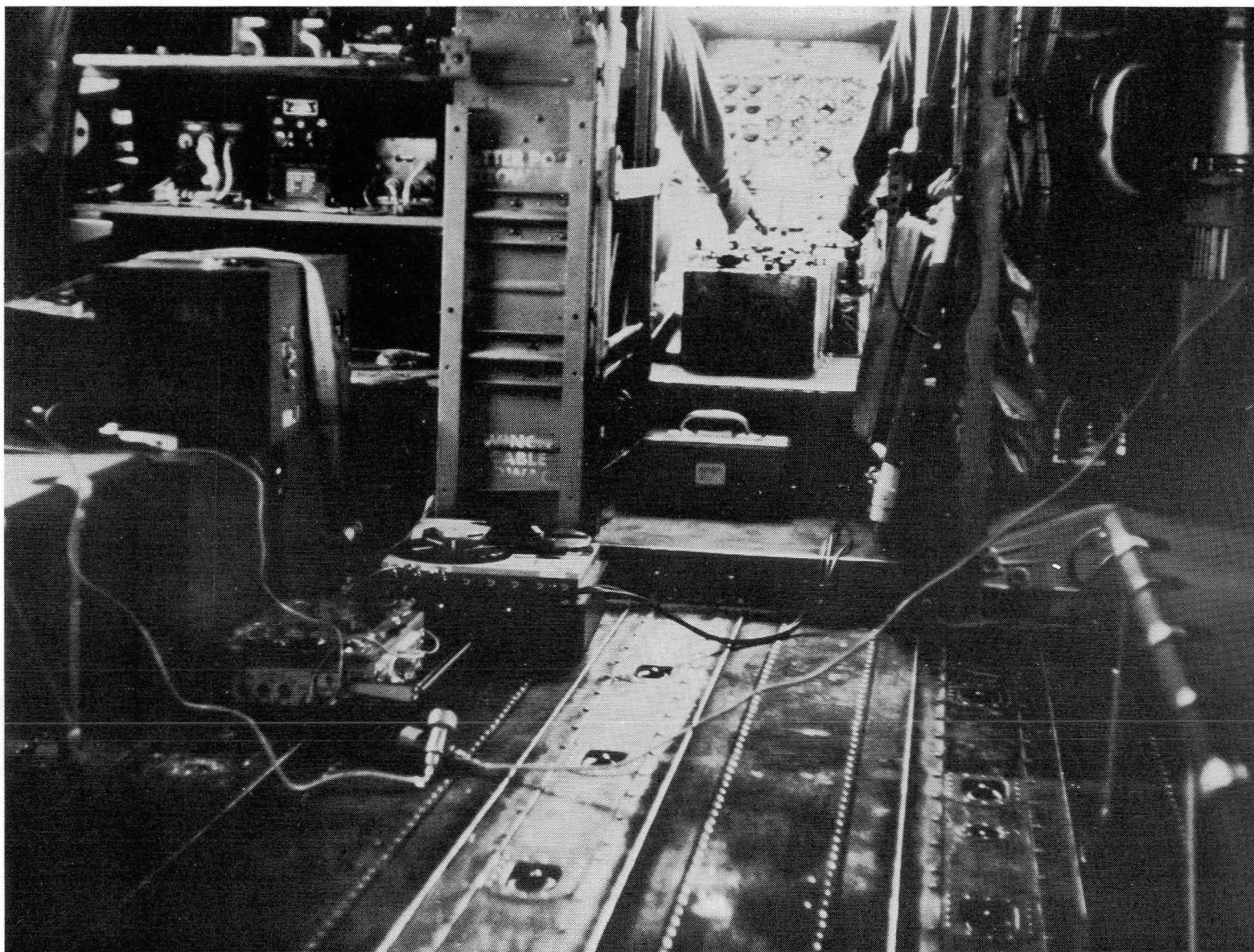
Figure 1.- Continued.





(h) Aircraft H-8.

Figure 1.- Continued.



L-81-8793

(i) Tape recorders located in aircraft H-7.

Figure 1.- Continued.

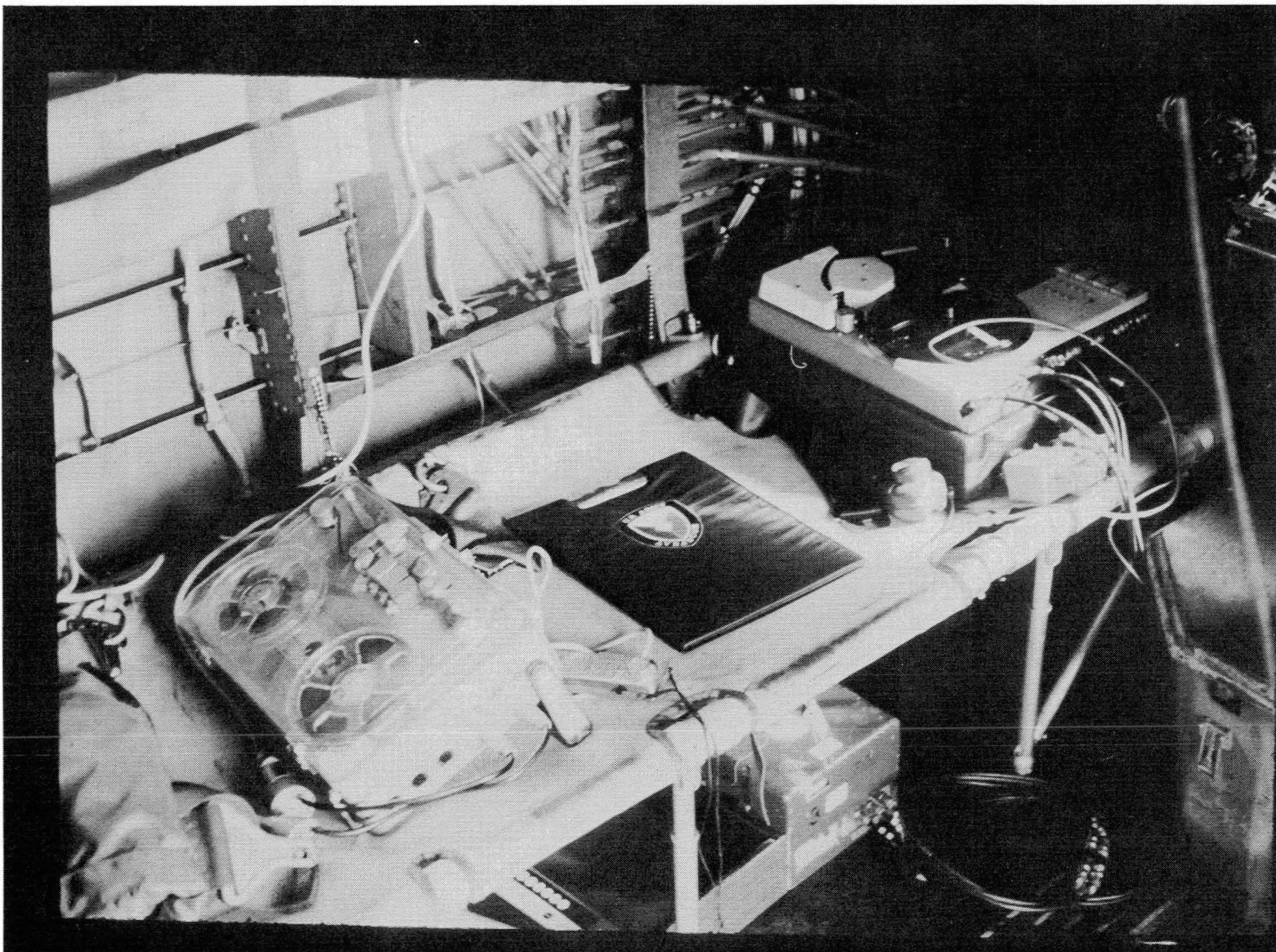




L-81-8794

(j) Microphone and tape recorder located in aircraft H-5.

Figure 1.- Continued.



(k) Acceleration box and tape recorder located in aircraft H-8.

Figure 1.- Concluded.

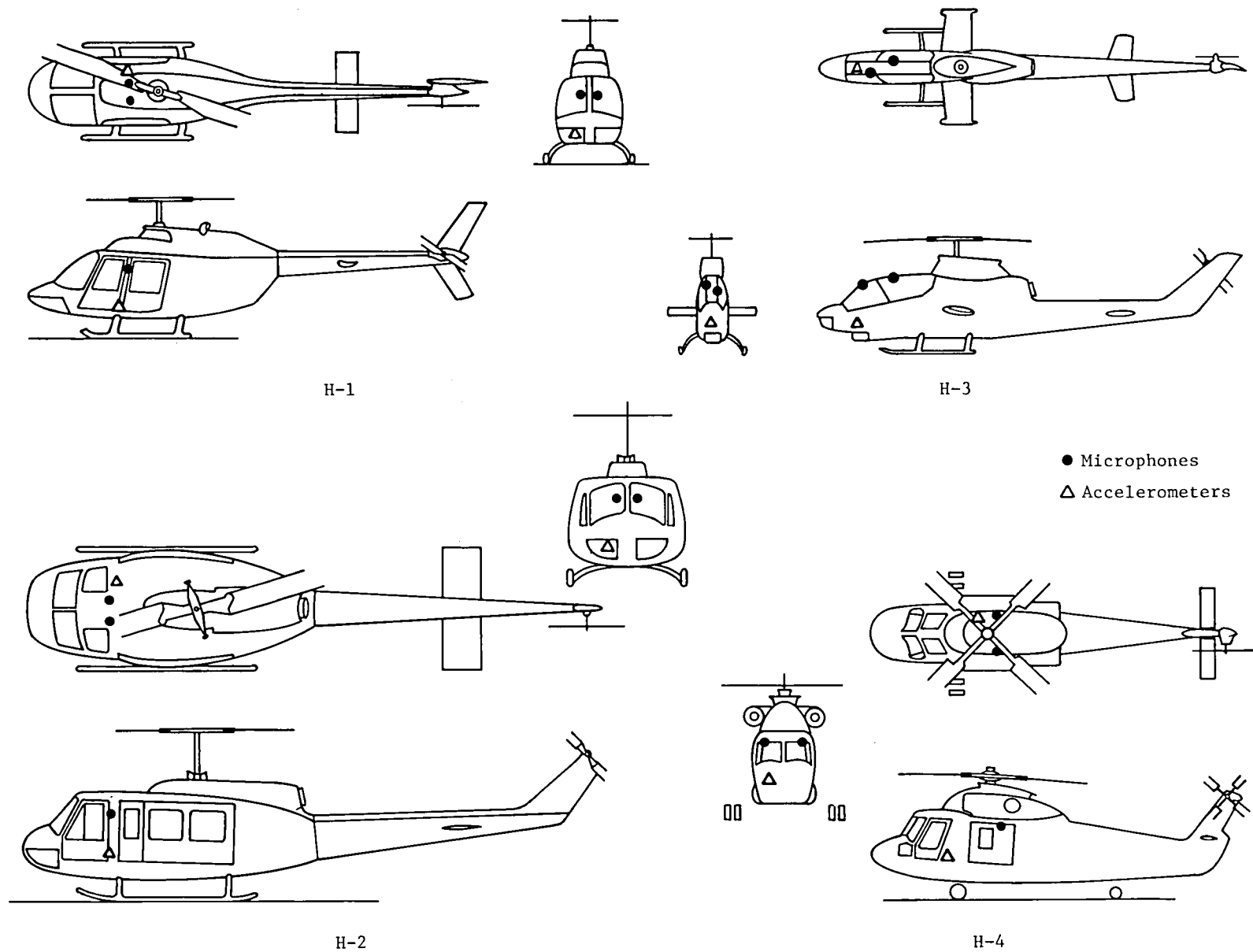
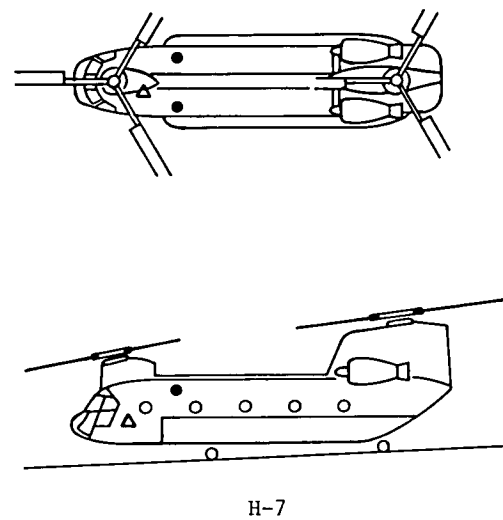
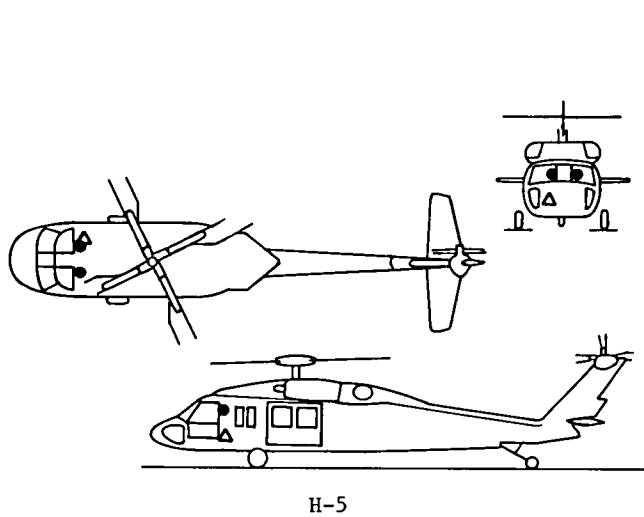


Figure 2.- Locations of microphones and accelerometers. (NB not to scale.)



● Microphones  
Δ Accelerometers

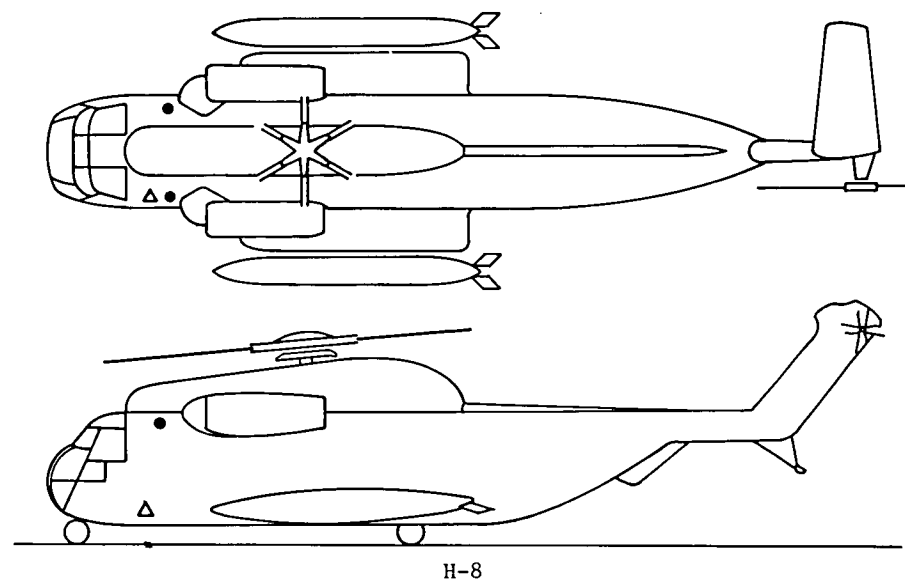
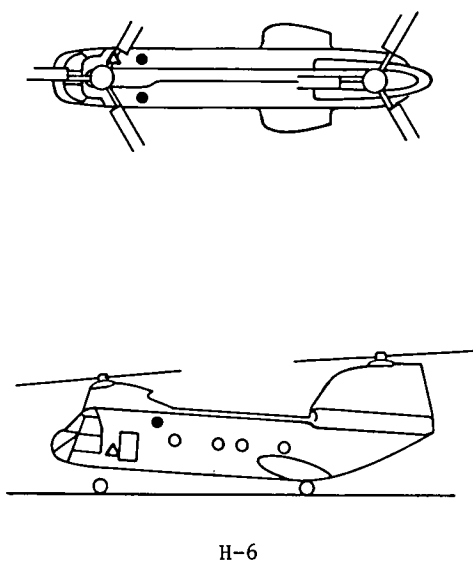
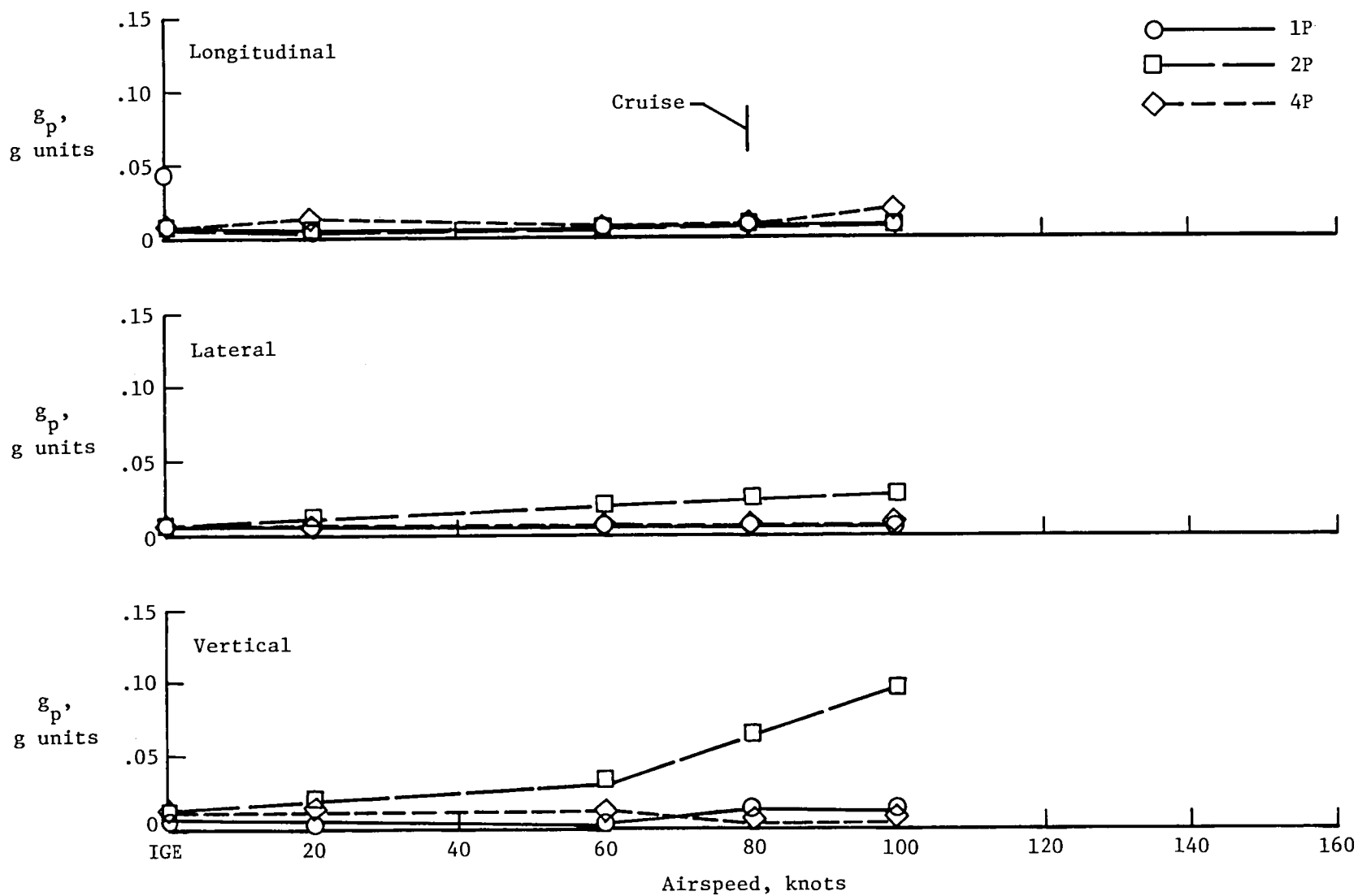
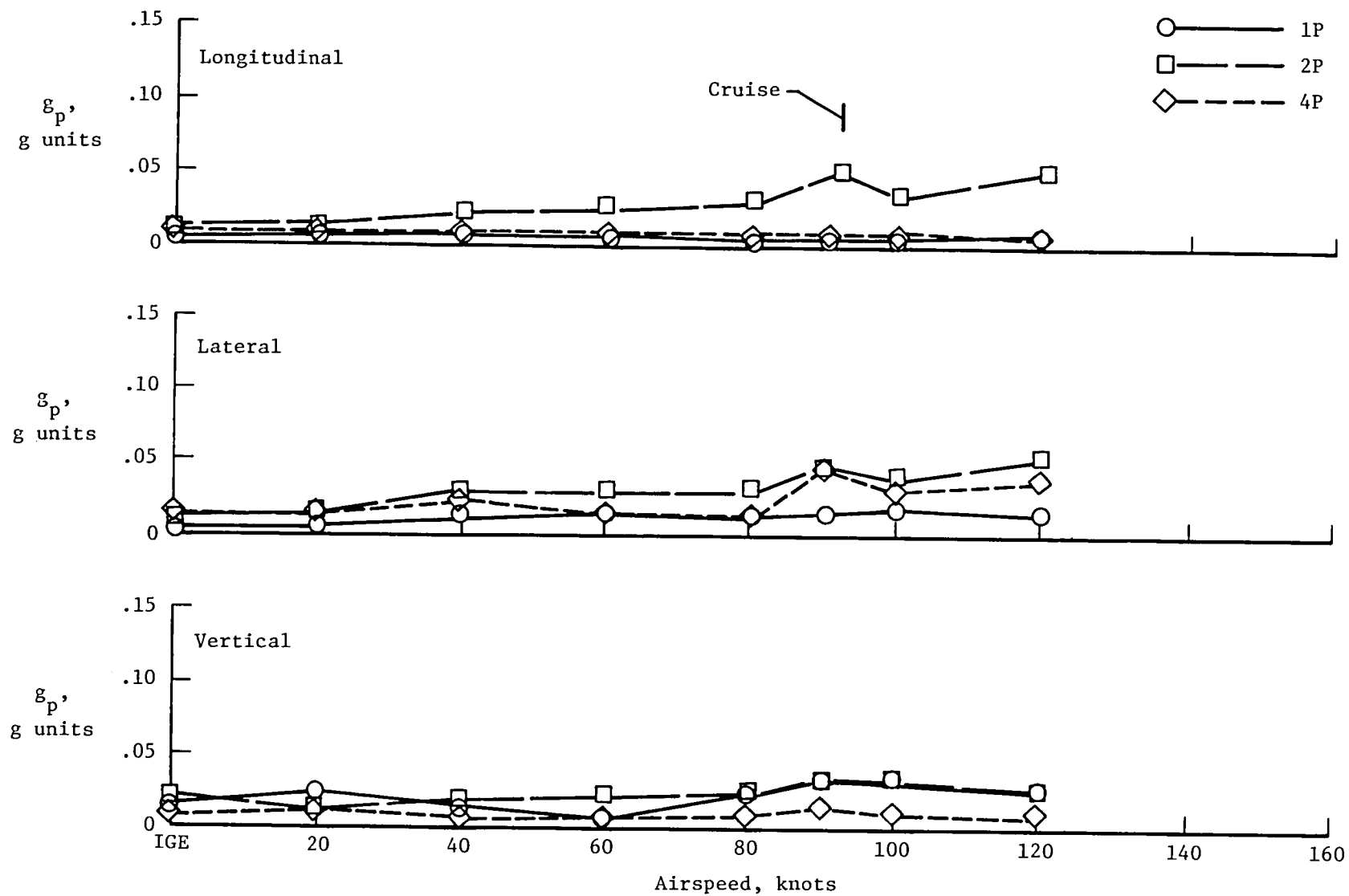


Figure 2.- Concluded.



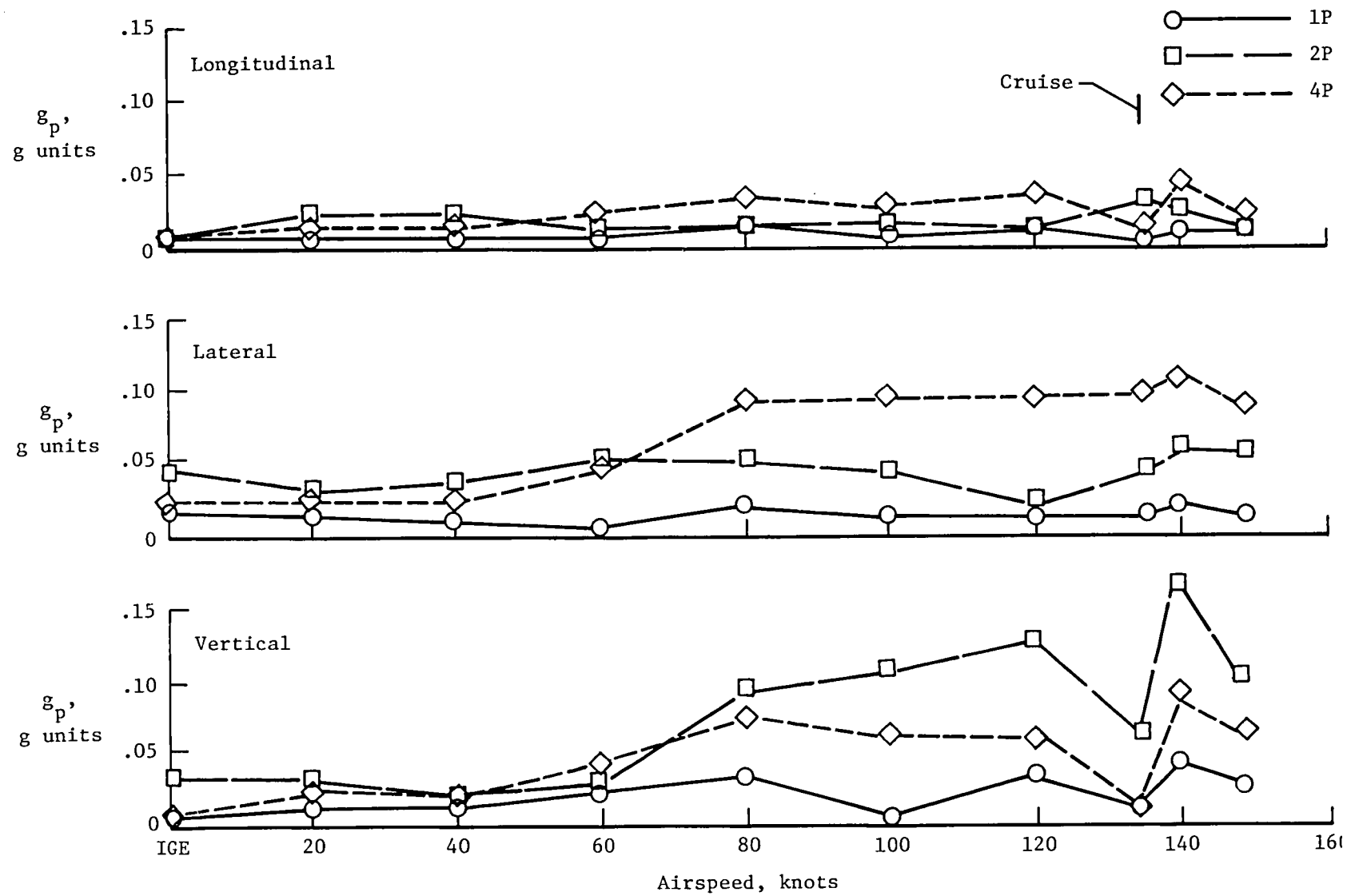
(a) Aircraft H-1.

Figure 3.- Peak accelerations at predominant frequencies as function of airspeed.



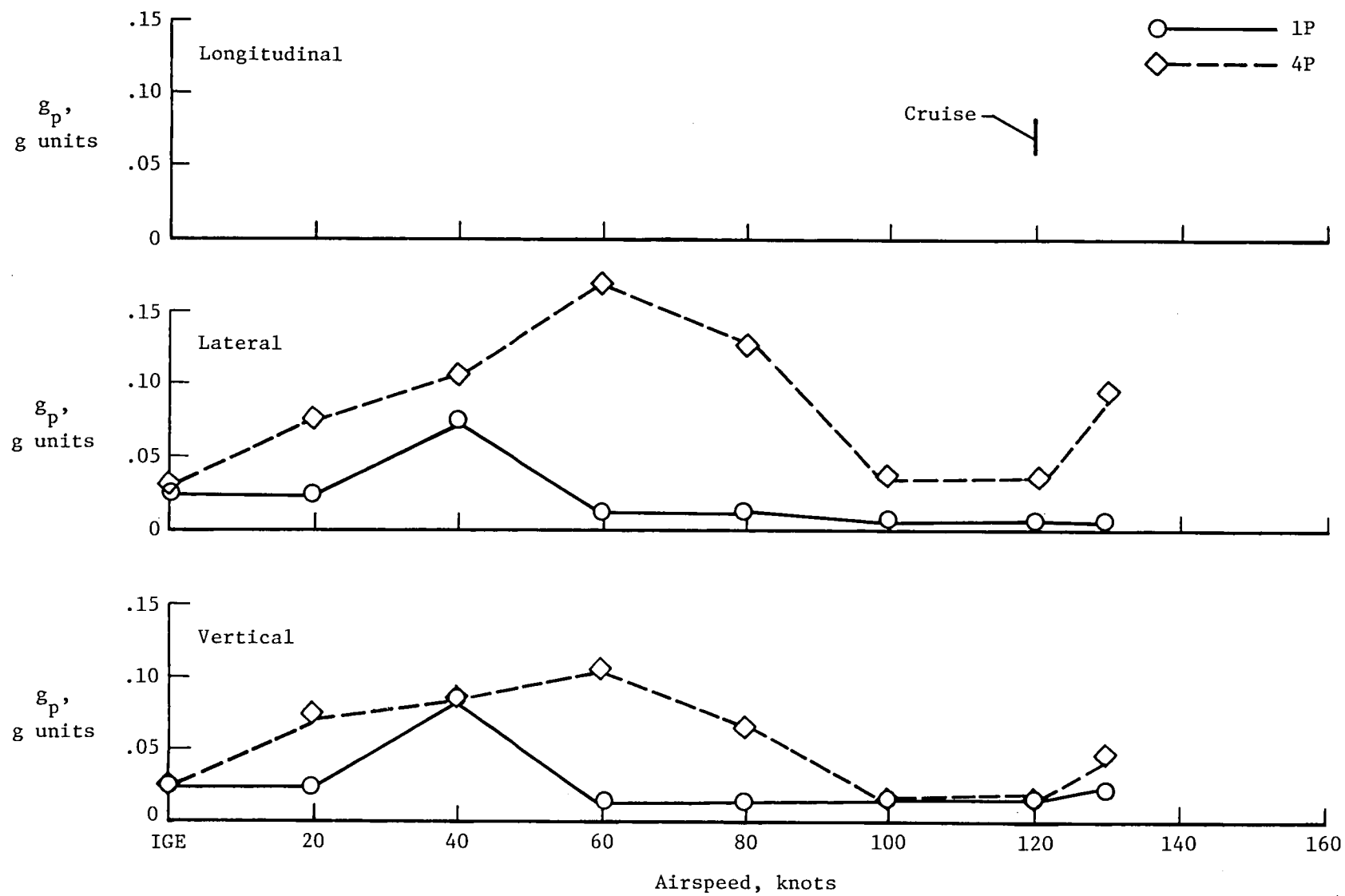
(b) Aircraft H-2.

Figure 3.- Continued.



(c) Aircraft H-3.

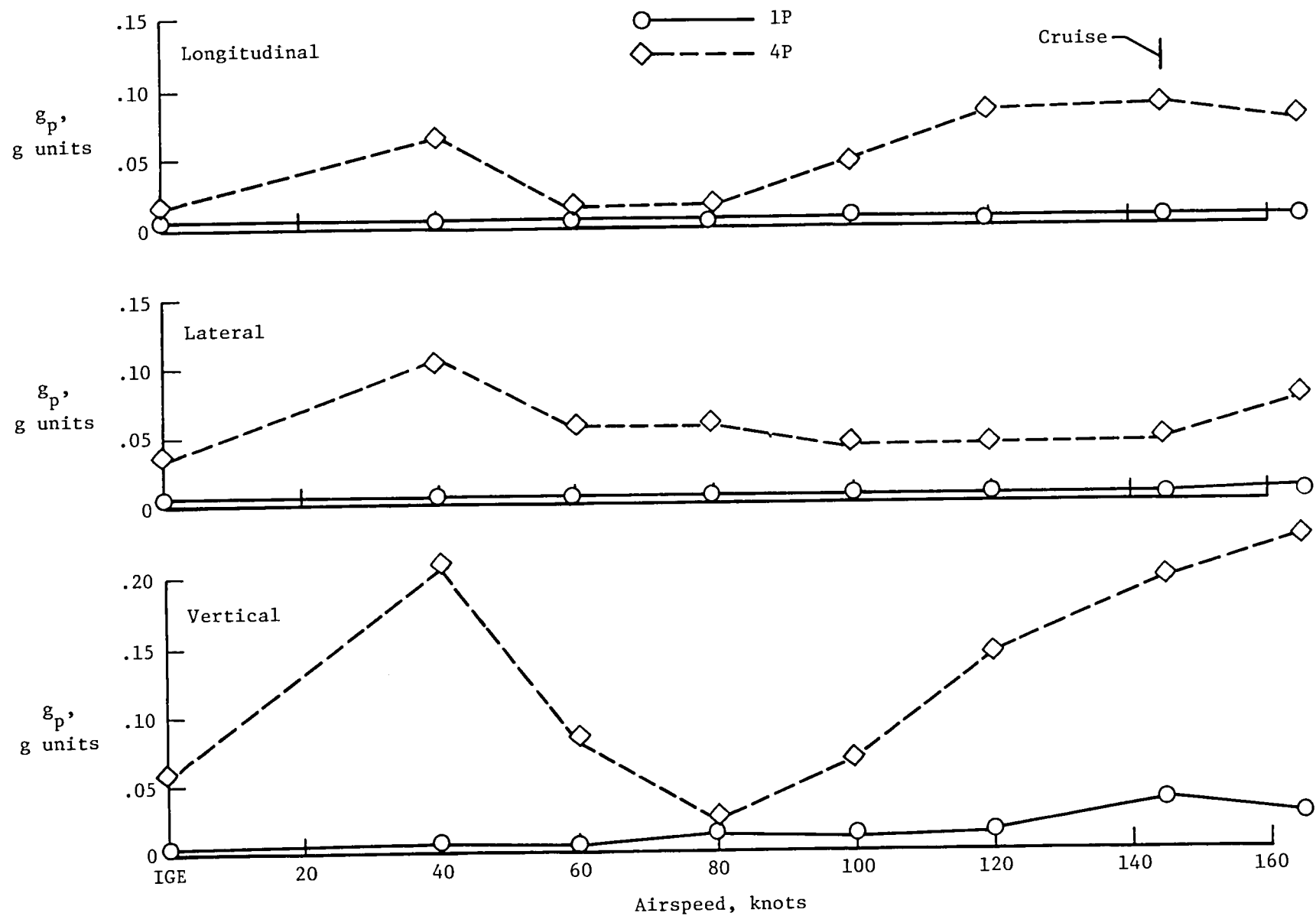
Figure 3.- Continued.



(d) Aircraft H-4.

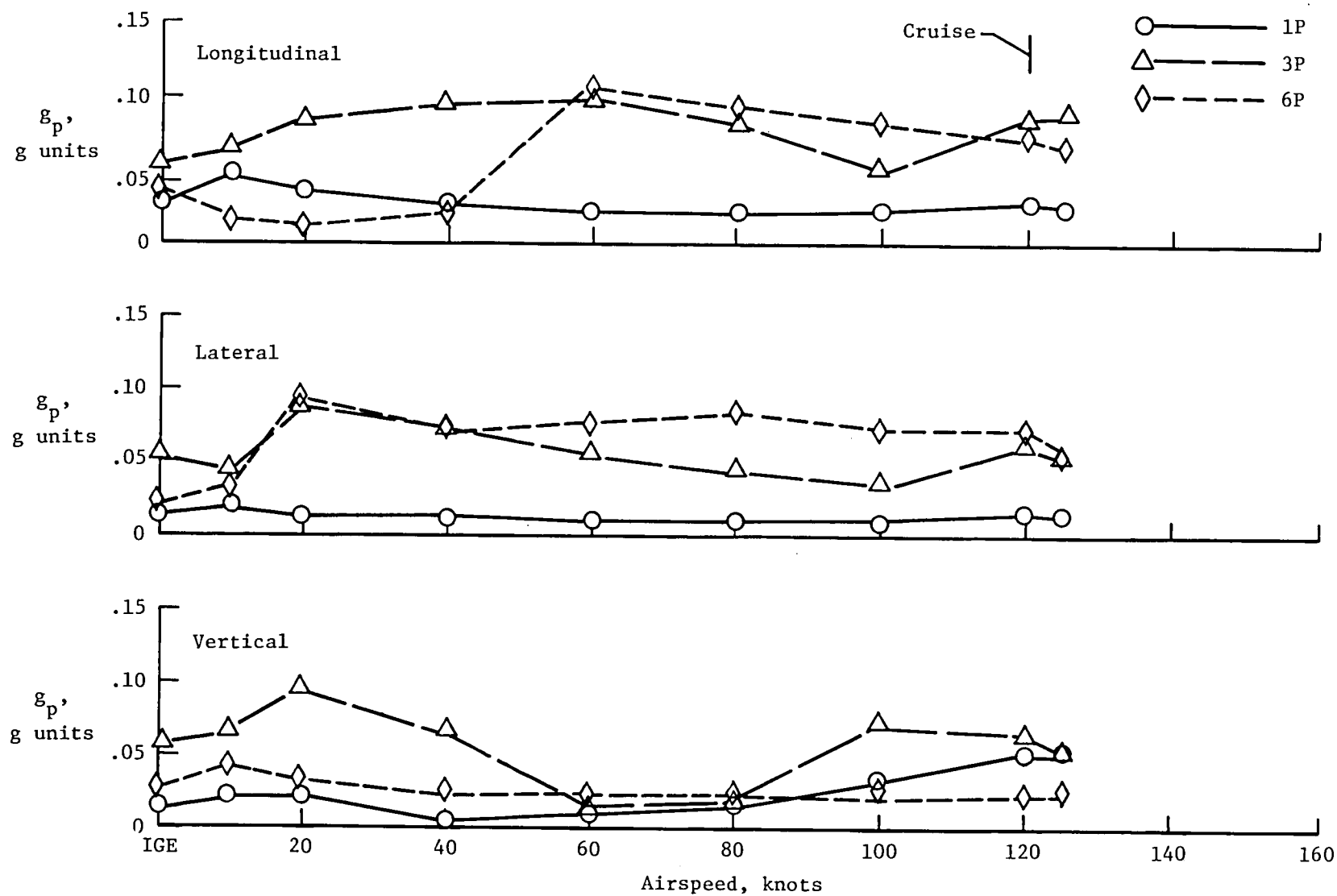
Figure 3.- Continued.





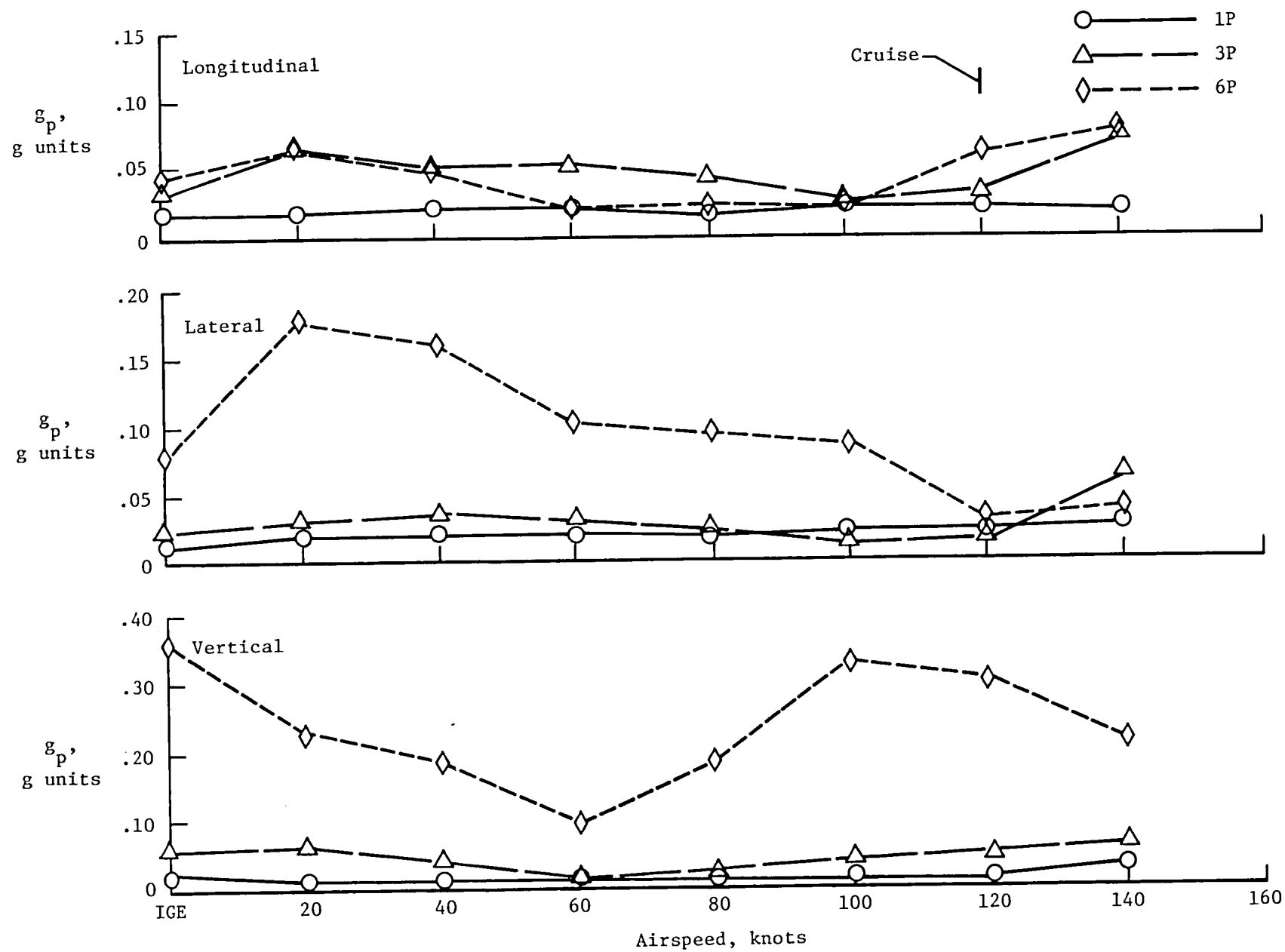
(e) Aircraft H-5.

Figure 3.- Continued.



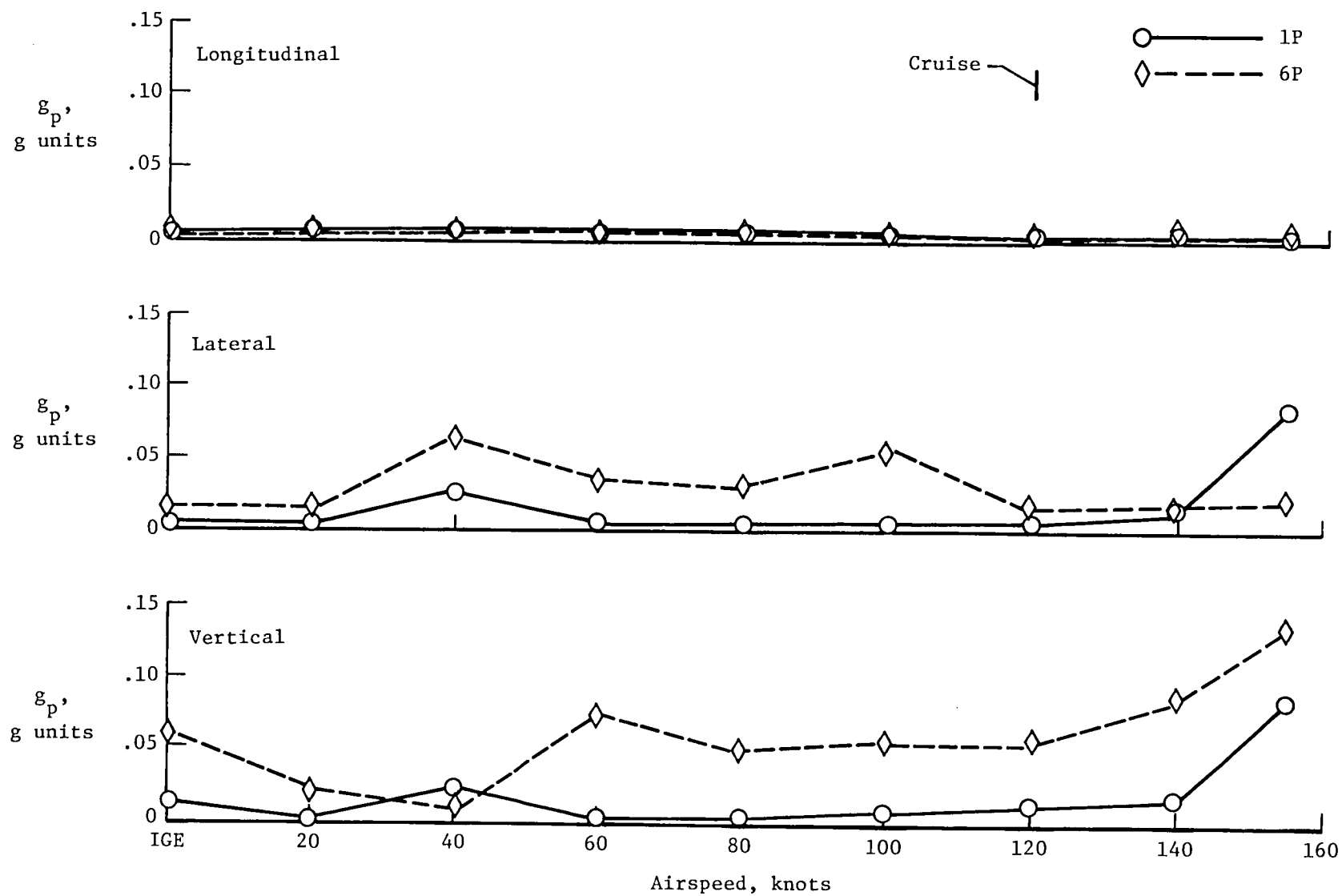
(f) Aircraft H-6.

Figure 3.- Continued.



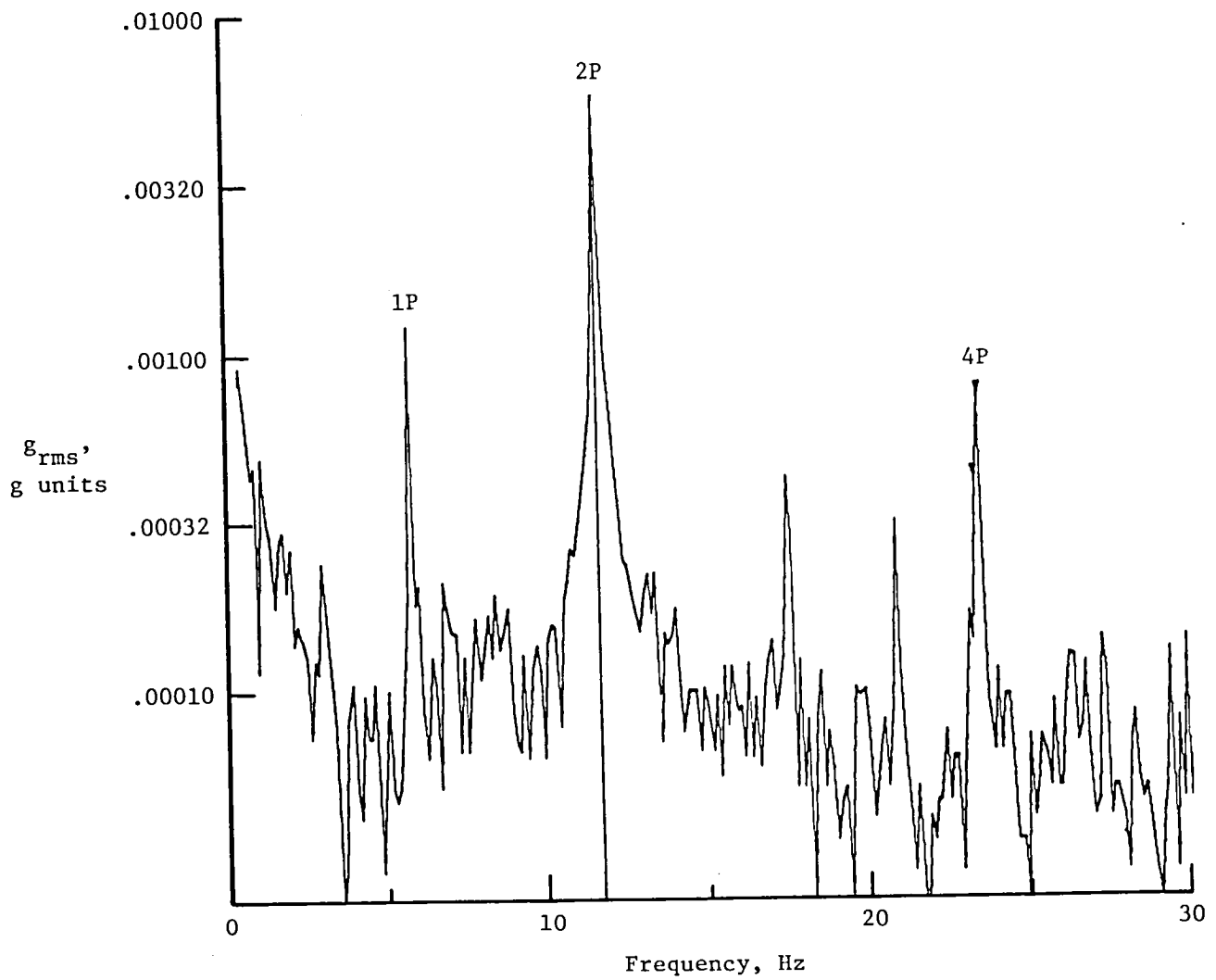
(g) Aircraft H-7.

Figure 3.- Continued.



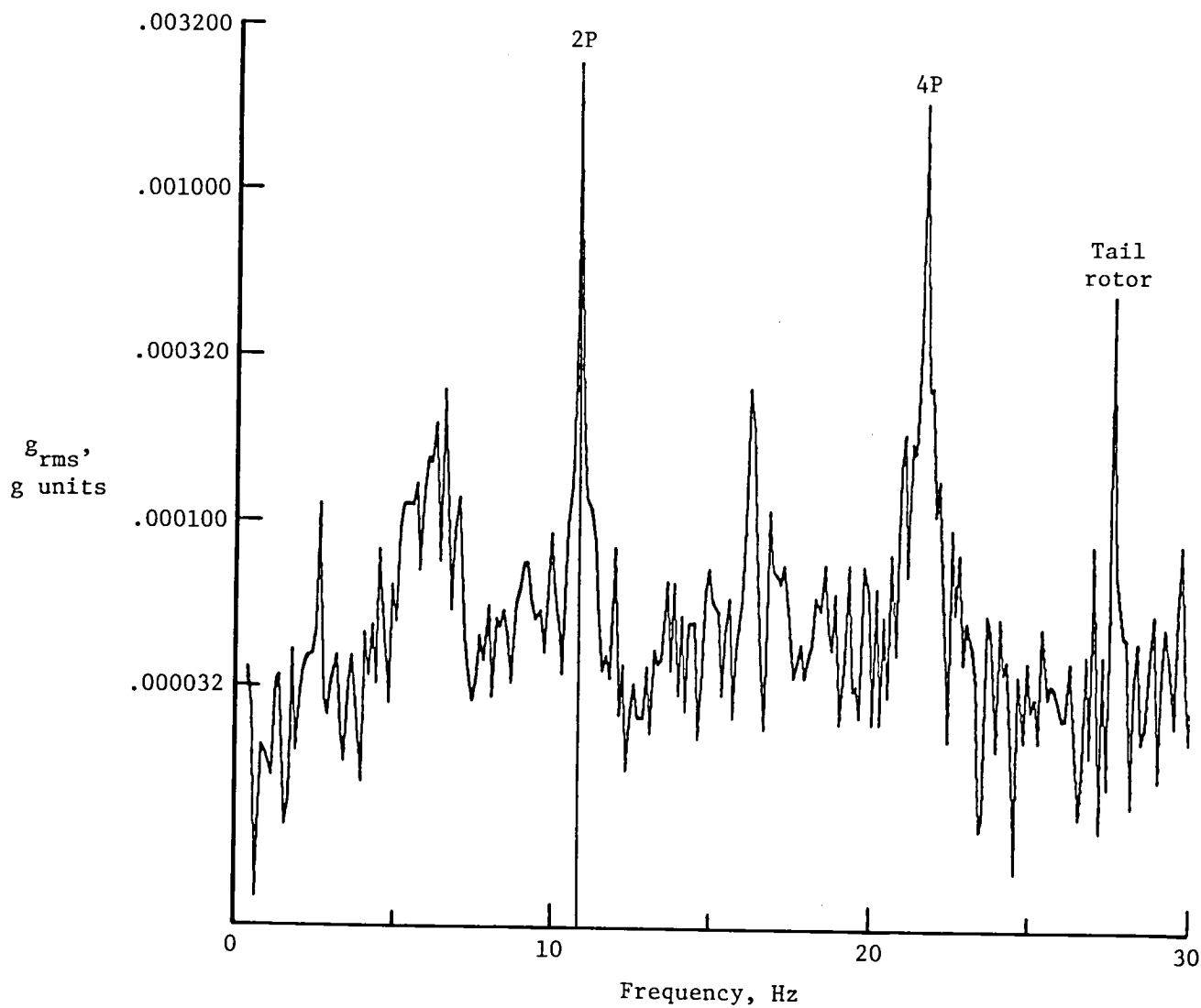
(h) Aircraft H-8.

Figure 3.- Concluded.



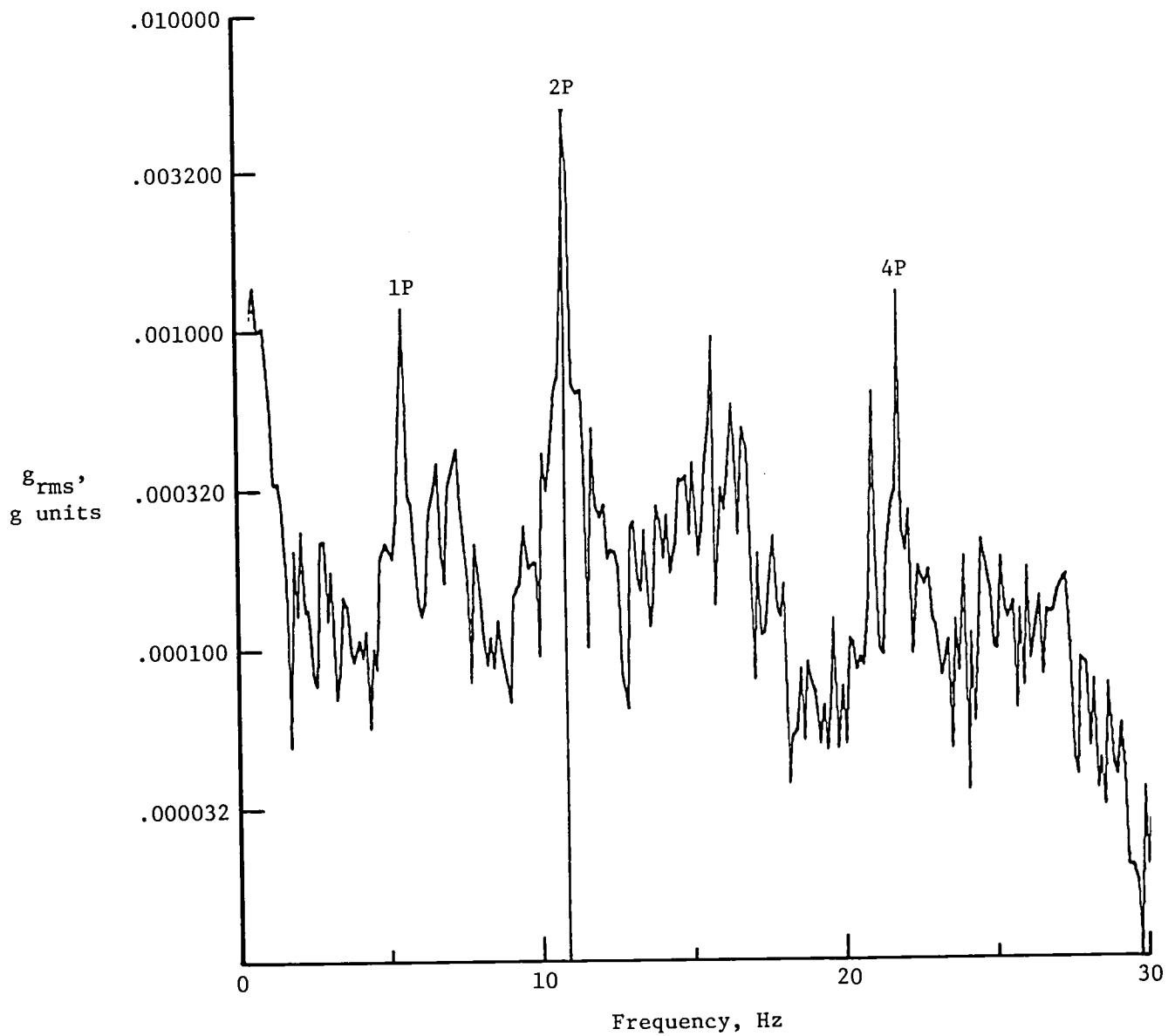
(a) Aircraft H-1.

Figure 4.- Variation of vertical rms acceleration with frequency, cruise condition.



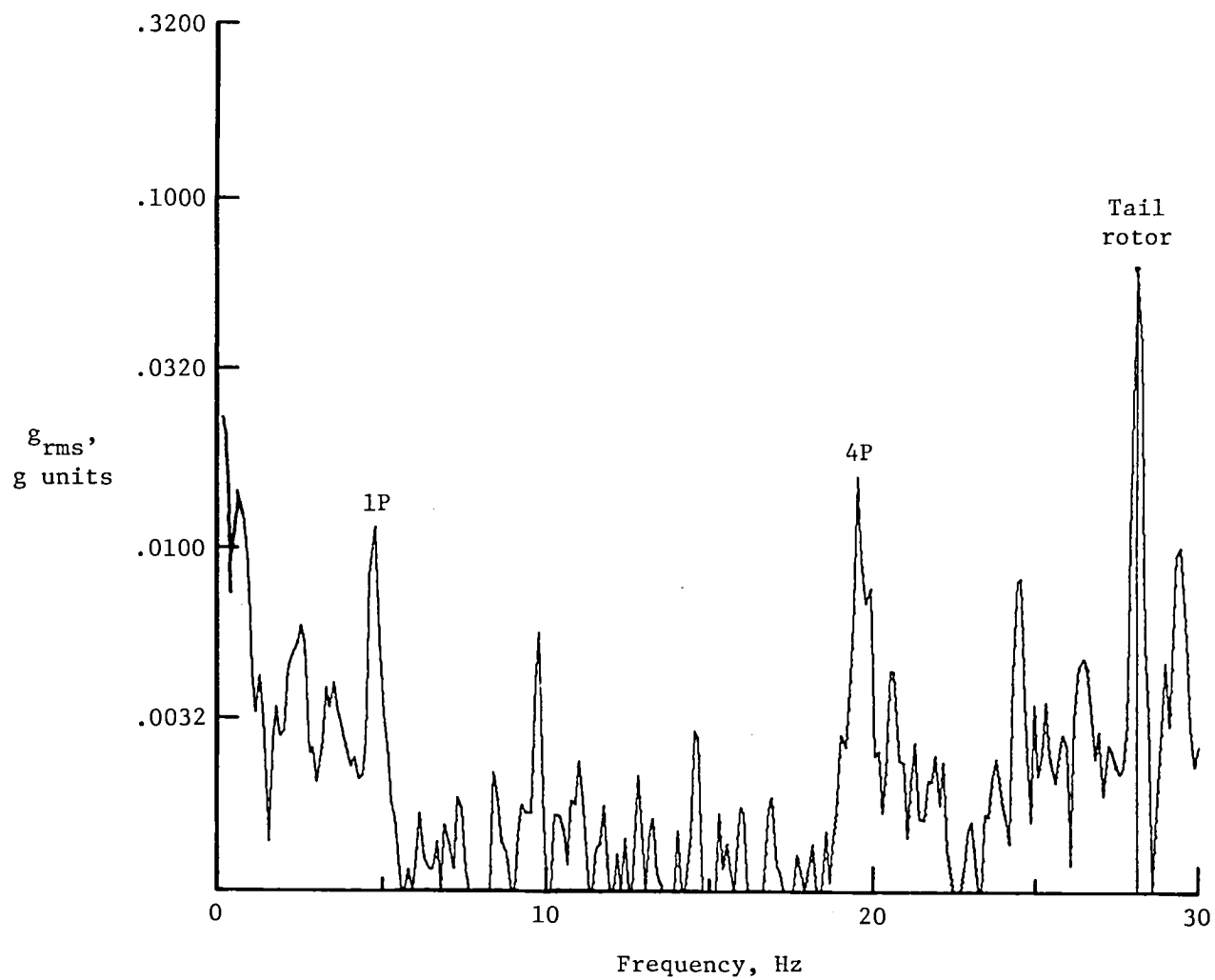
(b) Aircraft H-2.

Figure 4.- Continued.



(c) Aircraft H-3.

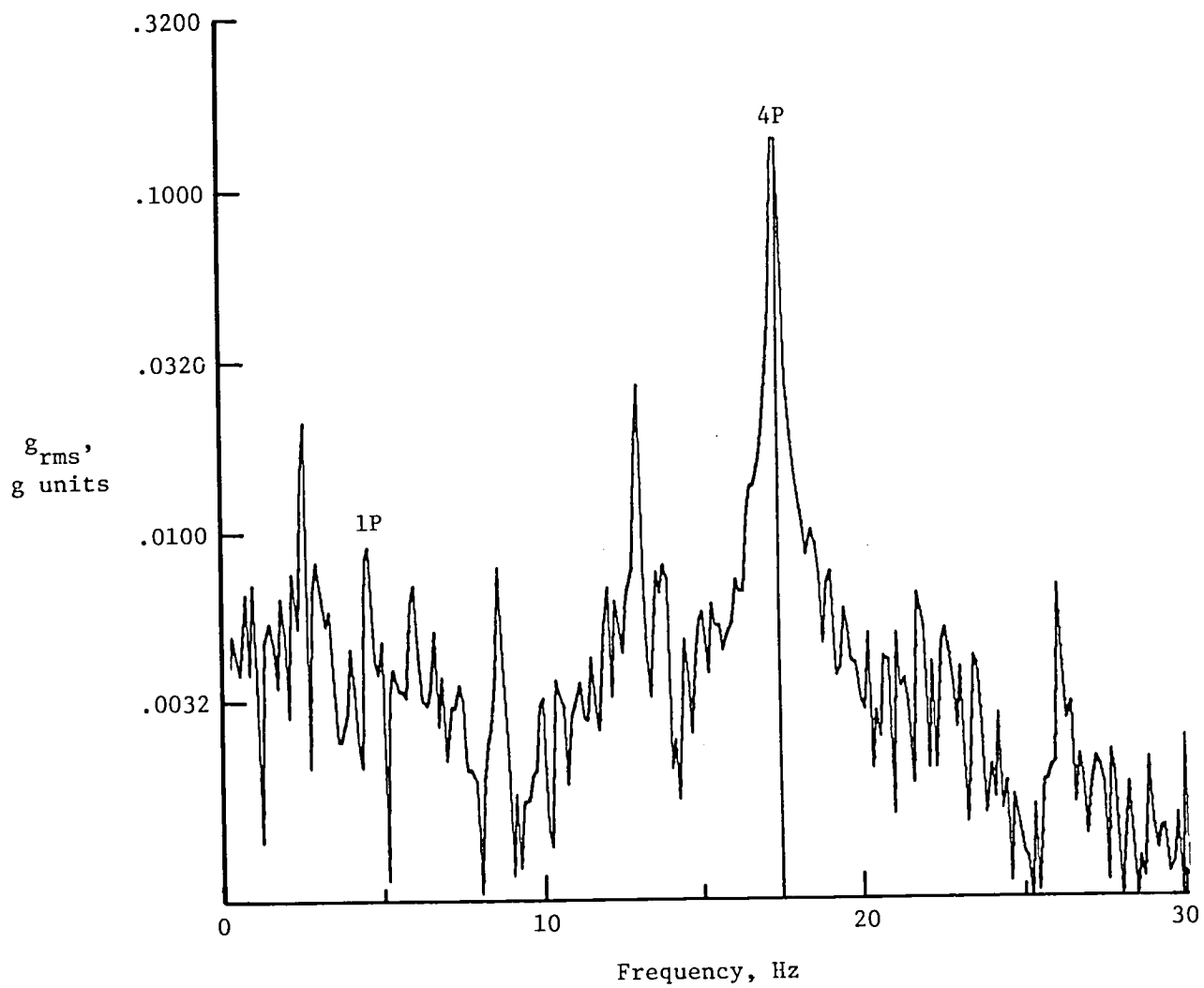
Figure 4.- Continued.



(d) Aircraft H-4.

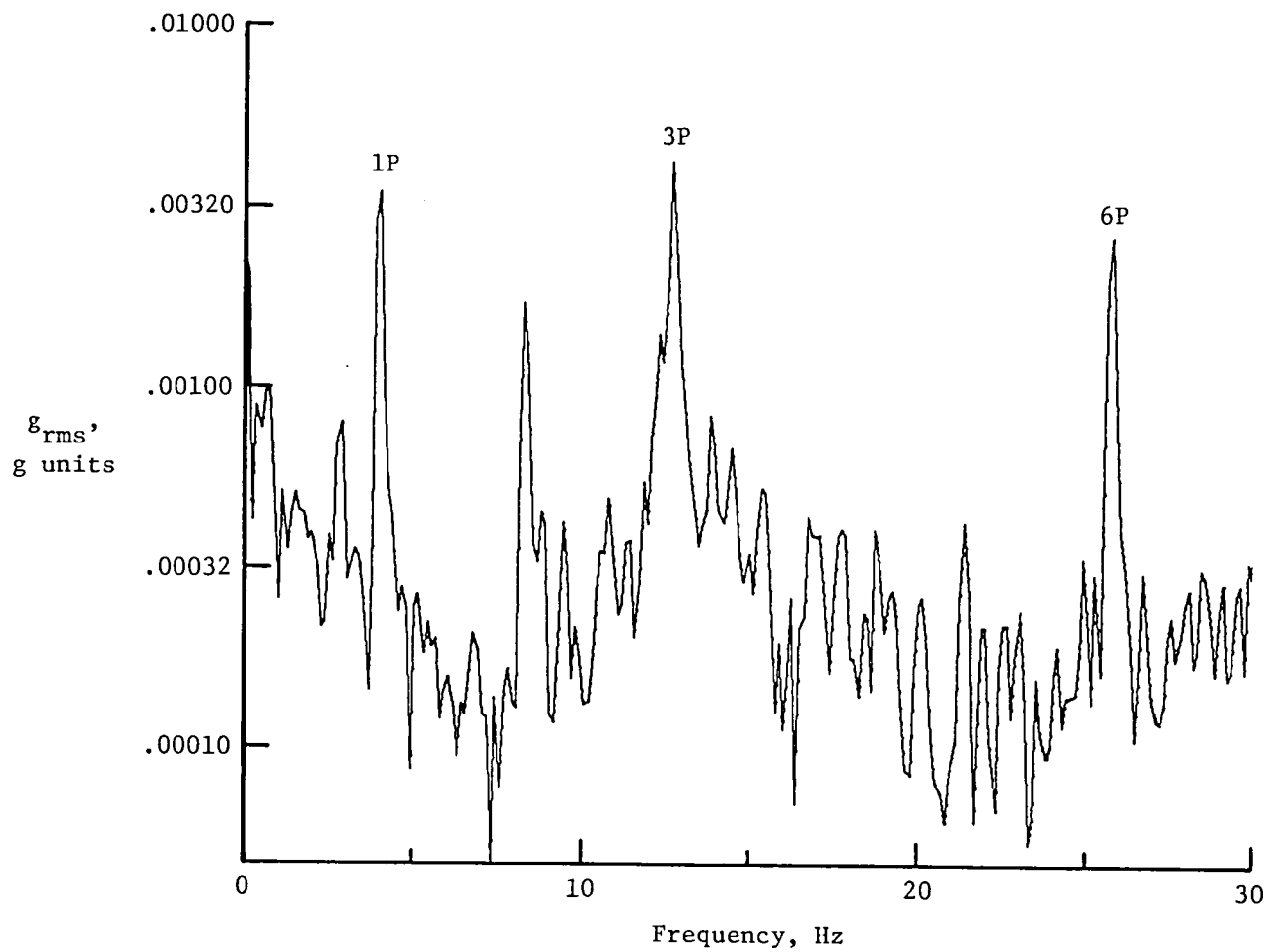
Figure 4.- Continued.





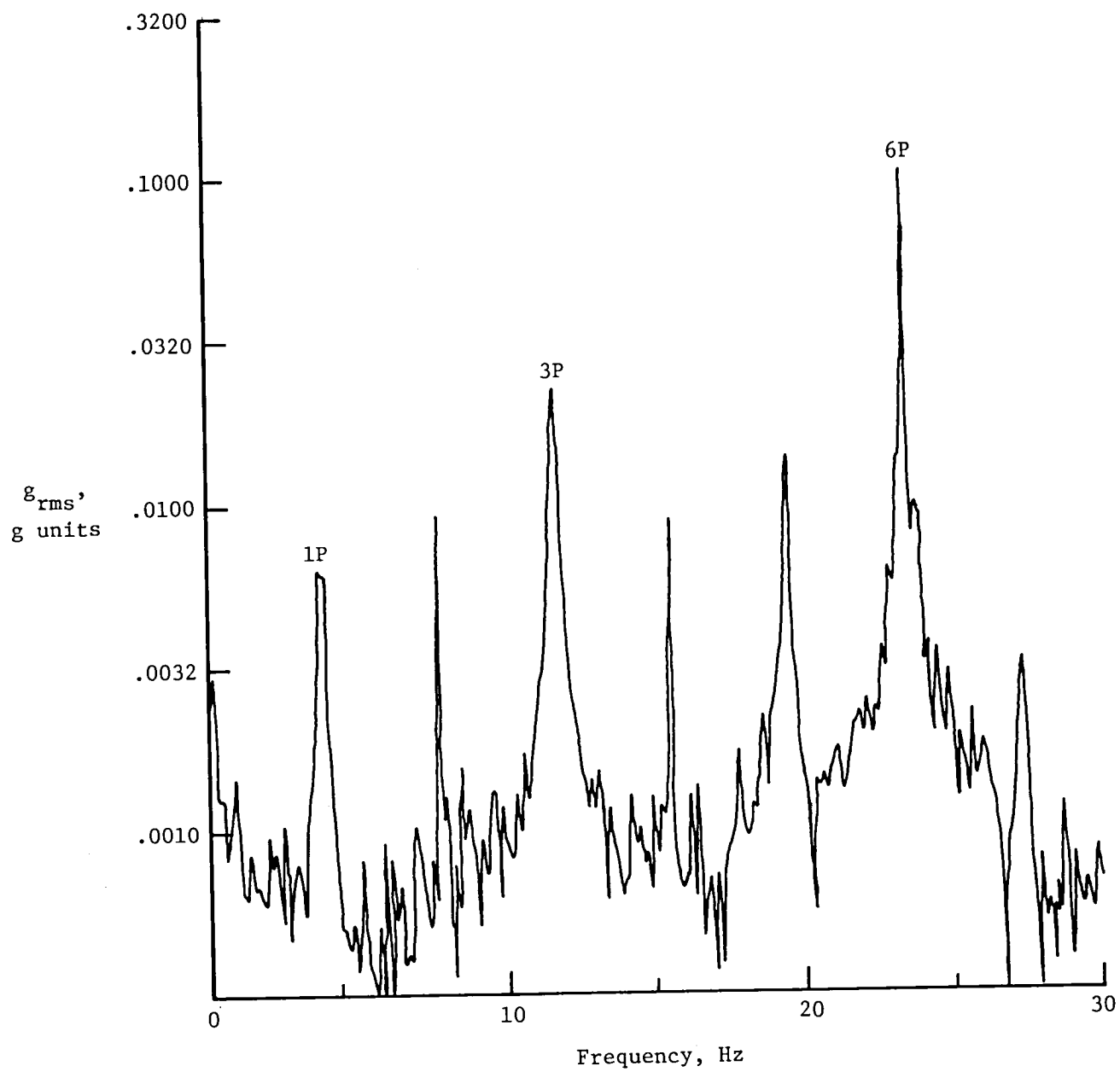
(e) Aircraft H-5.

Figure 4.- Continued.



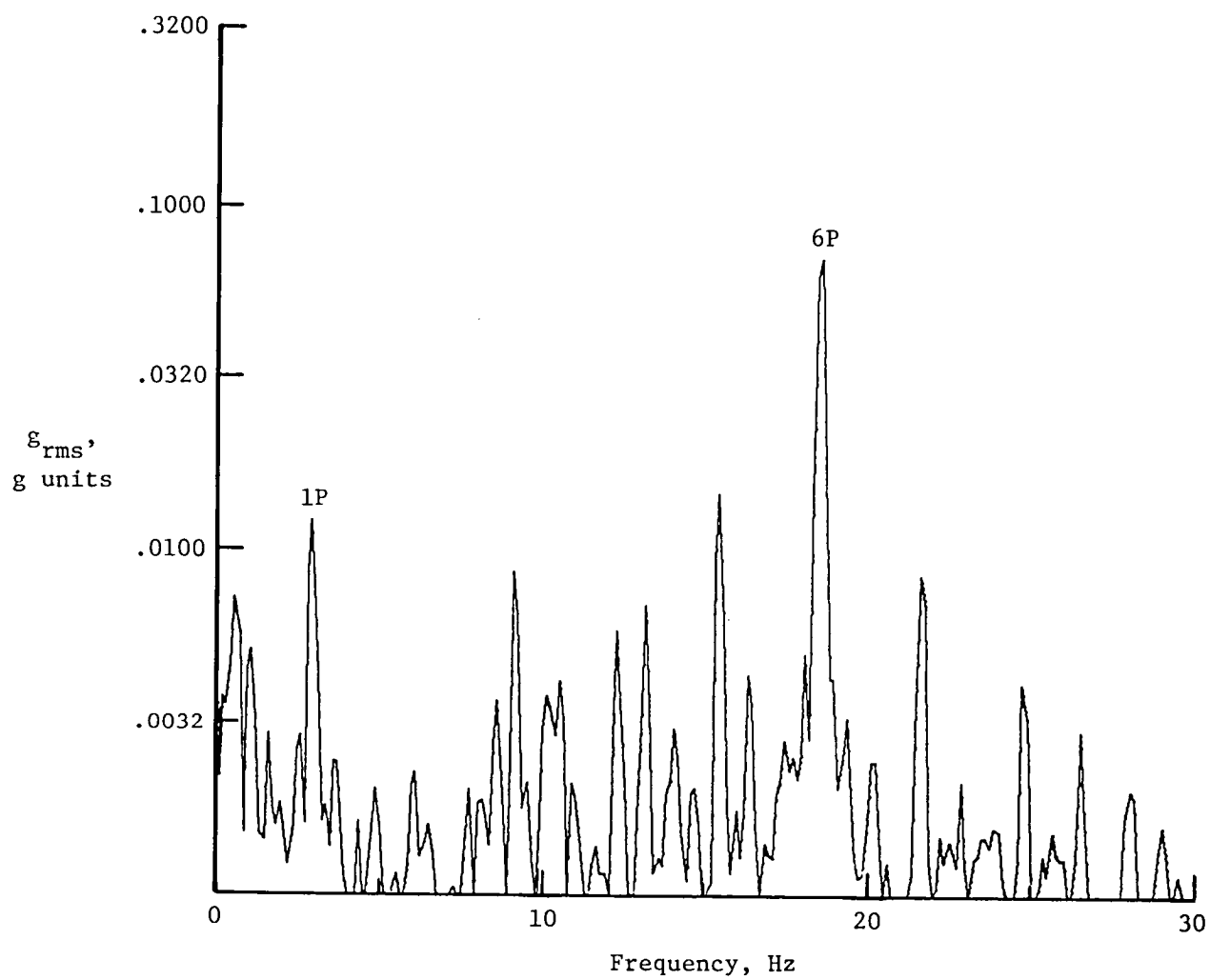
(f) Aircraft H-6.

Figure 4.- Continued.



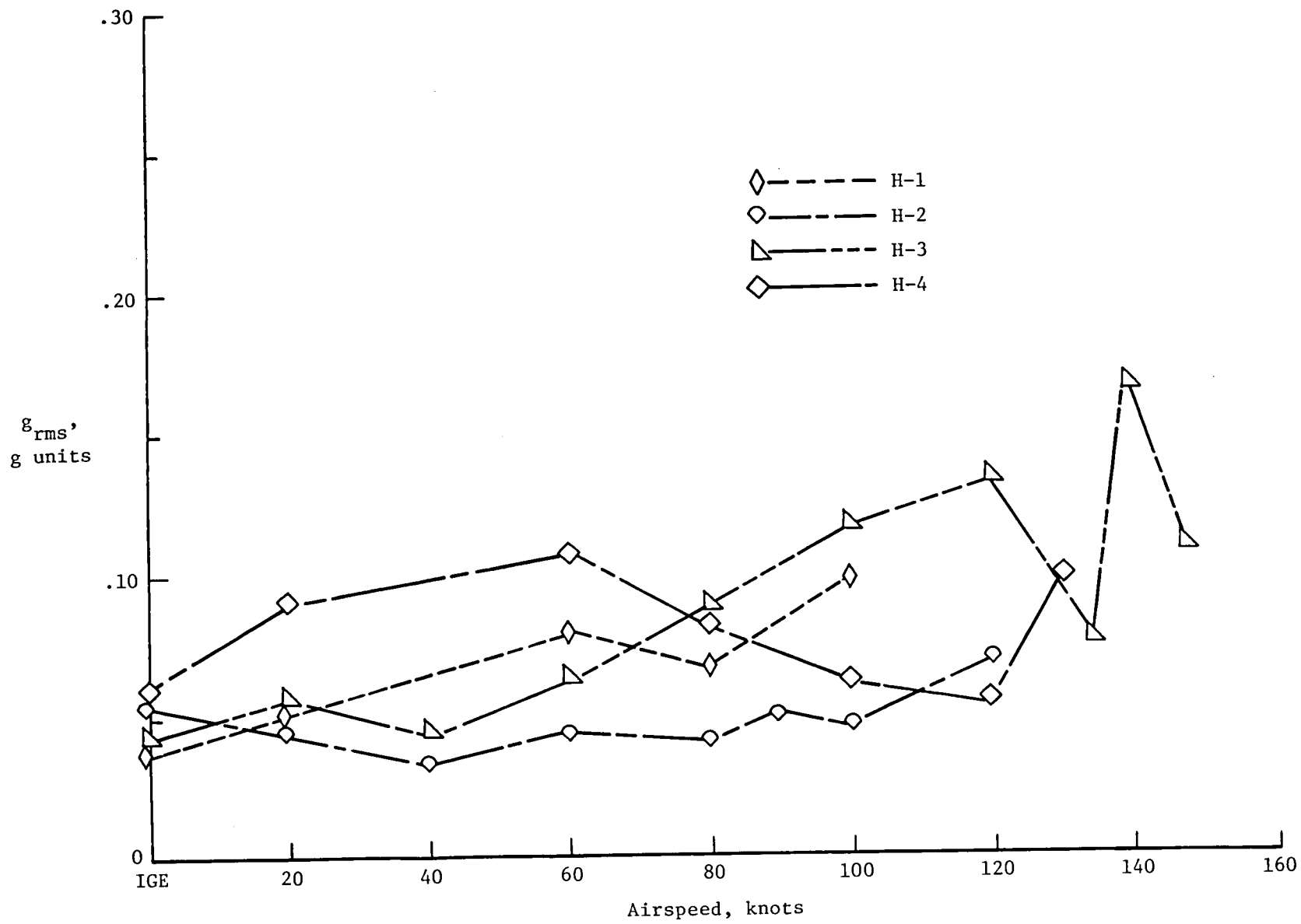
(g) Aircraft H-7.

Figure 4.- Continued.



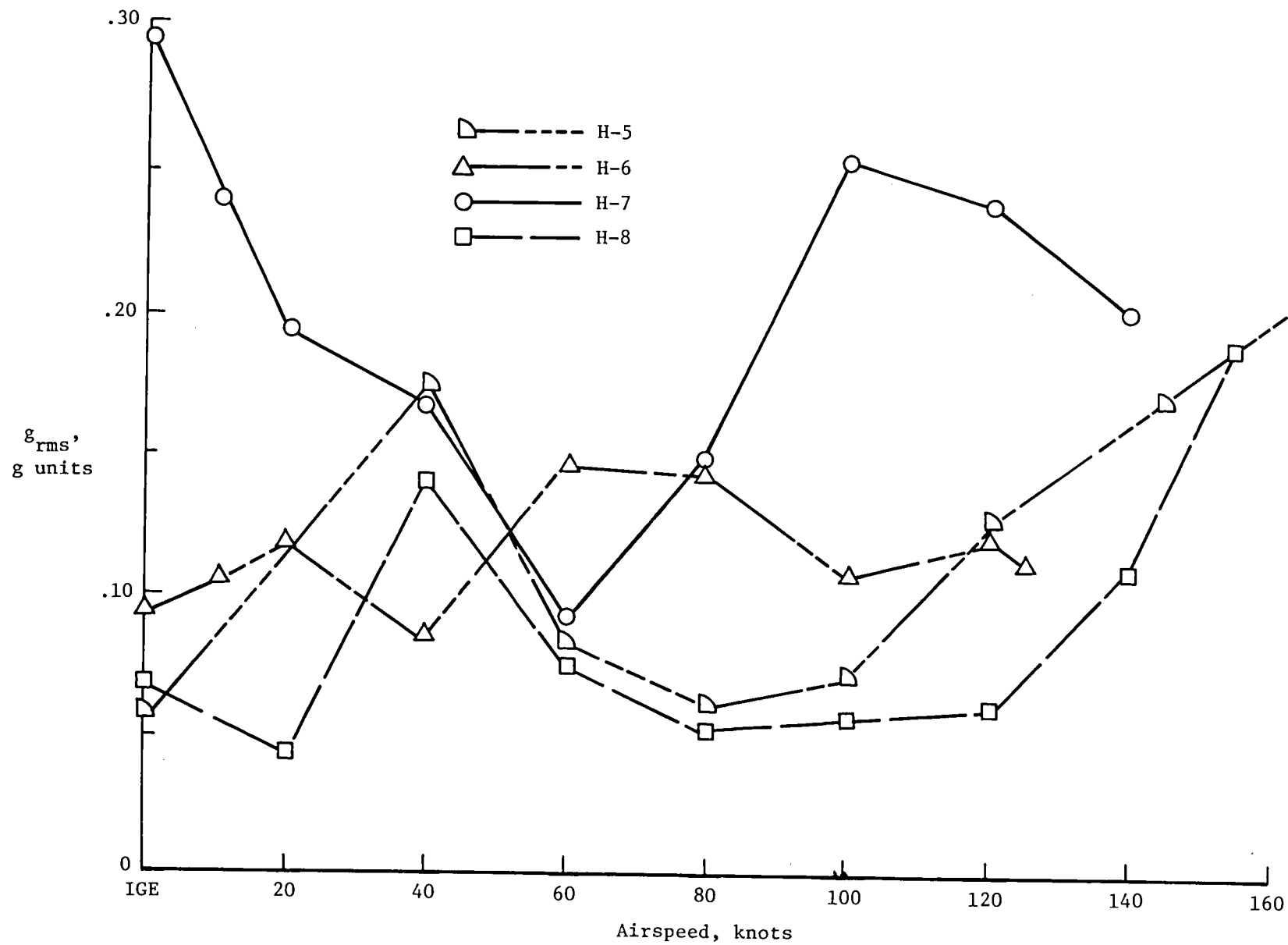
(h) Aircraft H-8.

Figure 4.- Concluded.



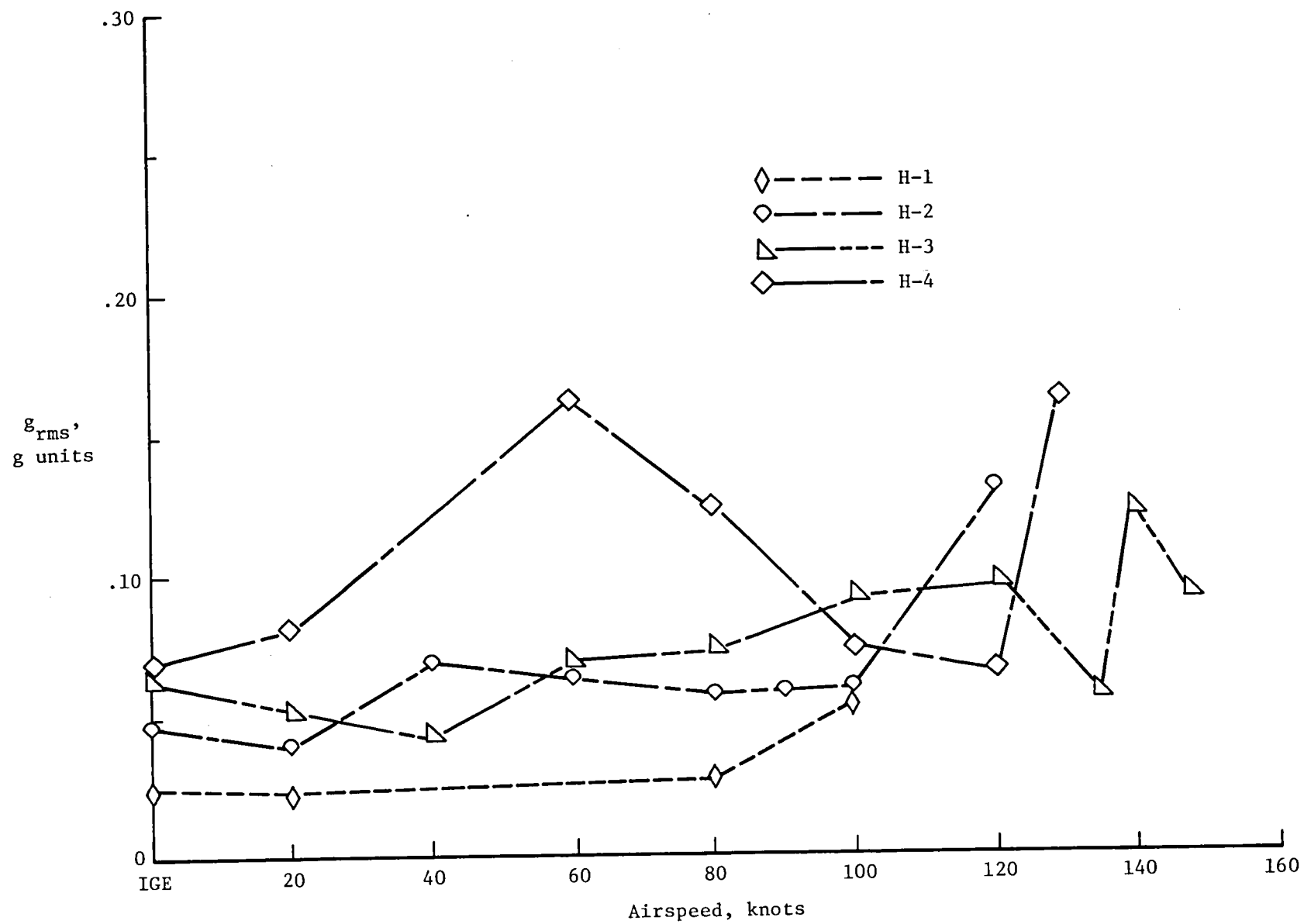
(a) Vertical direction.

Figure 5.- Overall root-mean-square acceleration levels as function of airspeed.



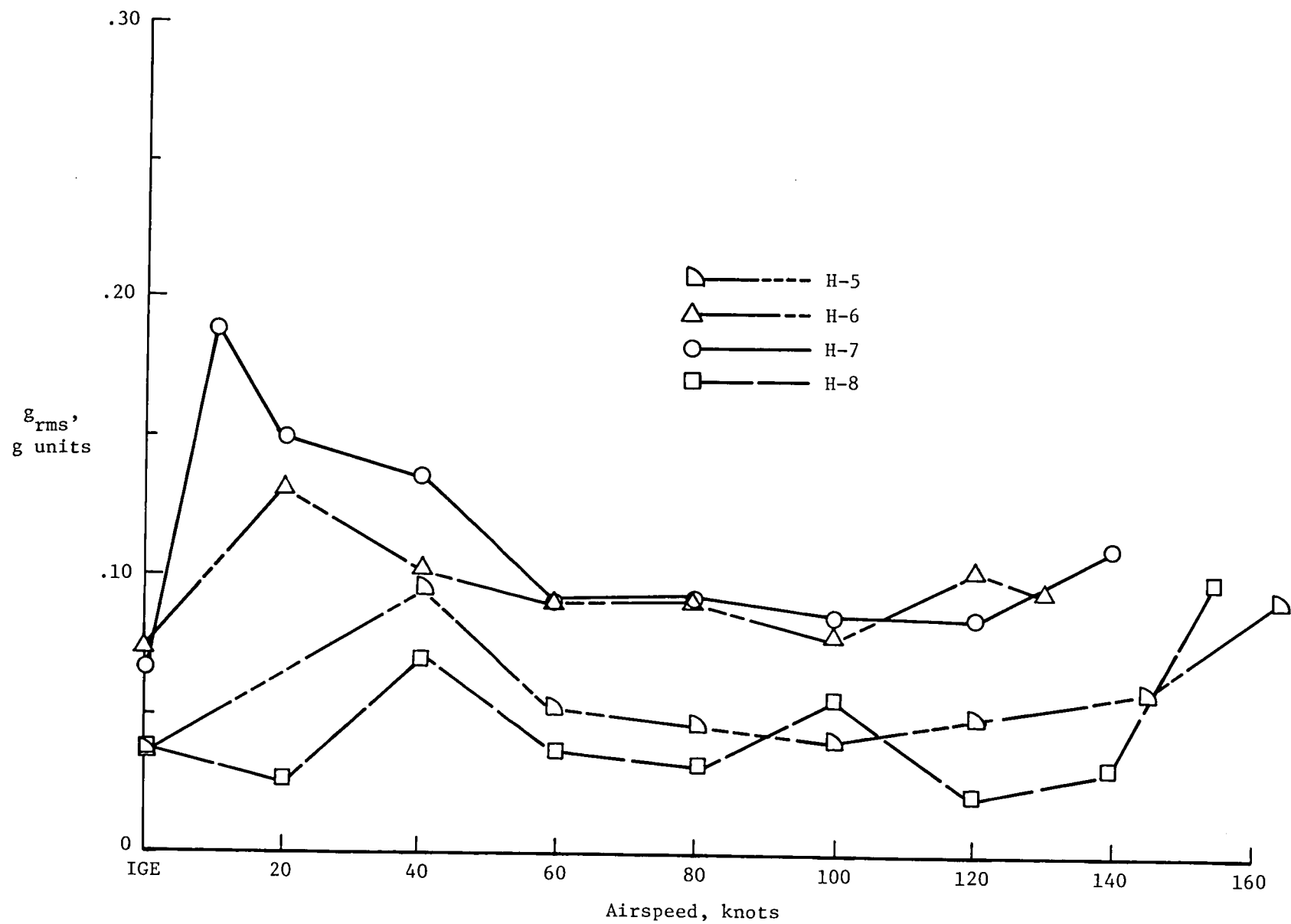
(a) Concluded.

Figure 5.- Continued.



(b) Lateral direction.

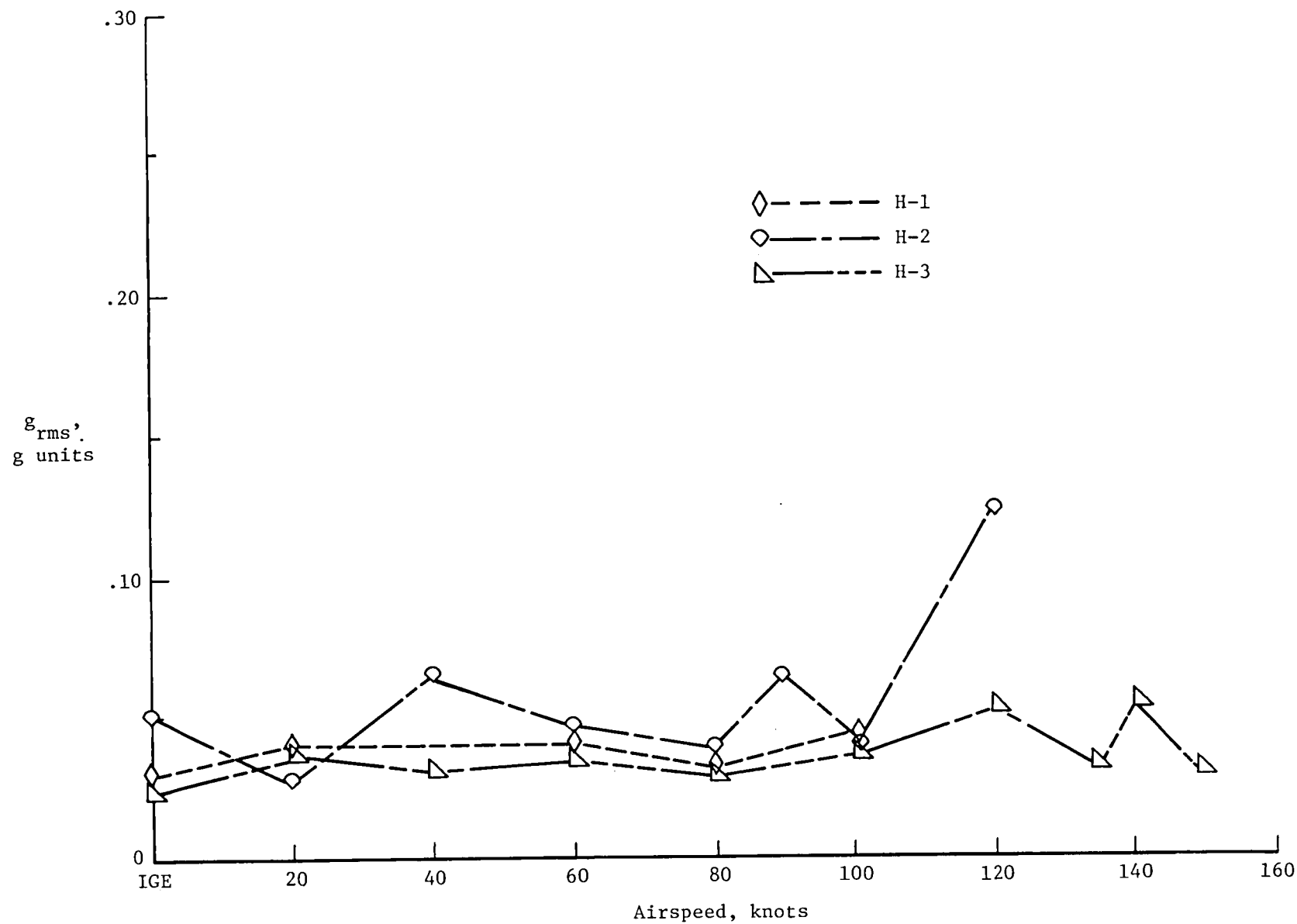
Figure 5.- Continued.



(b) Concluded.

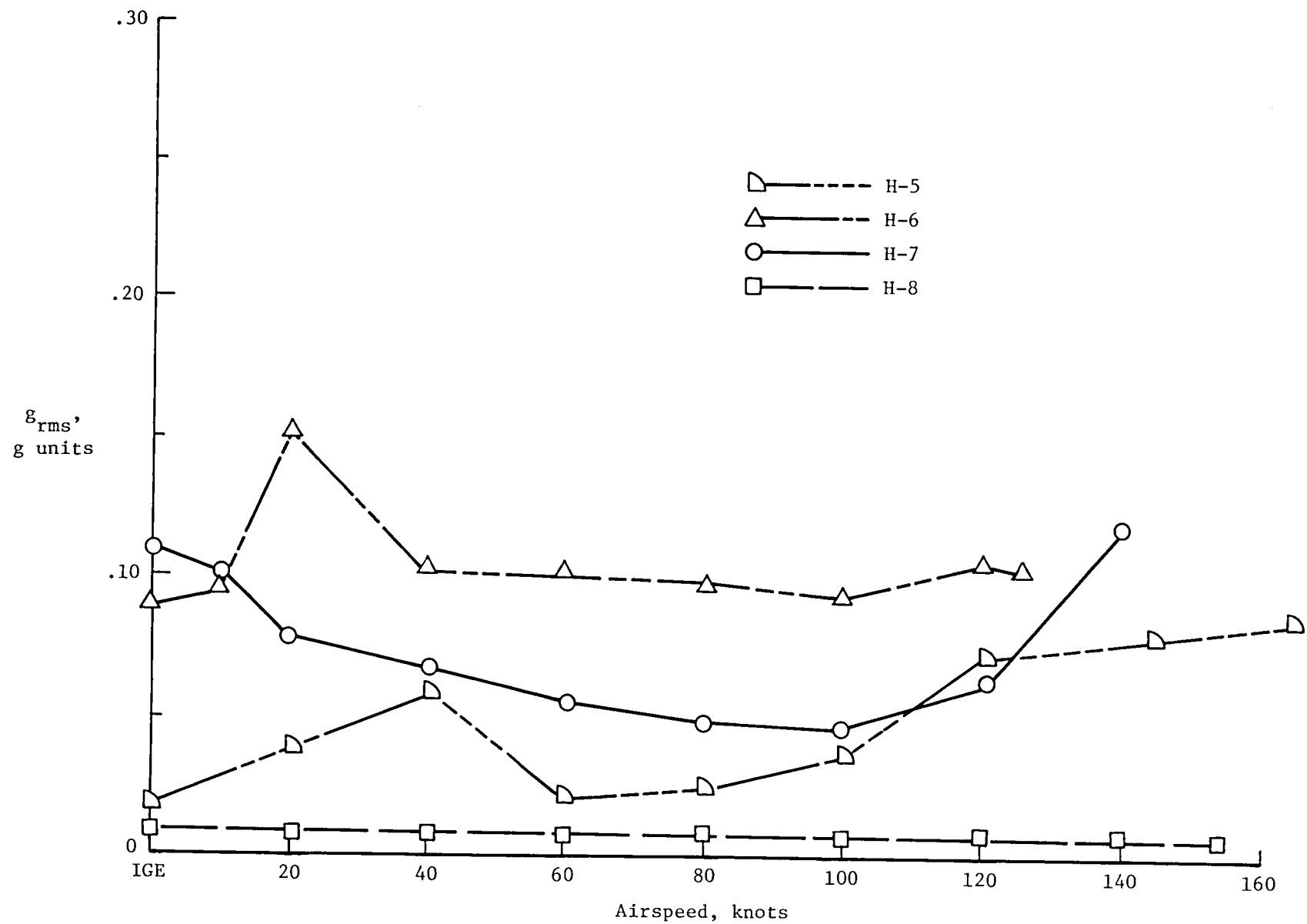
Figure 5.- Continued.





(c) Longitudinal direction.

Figure 5.- Continued.



(c) Concluded.

Figure 5.- Concluded.

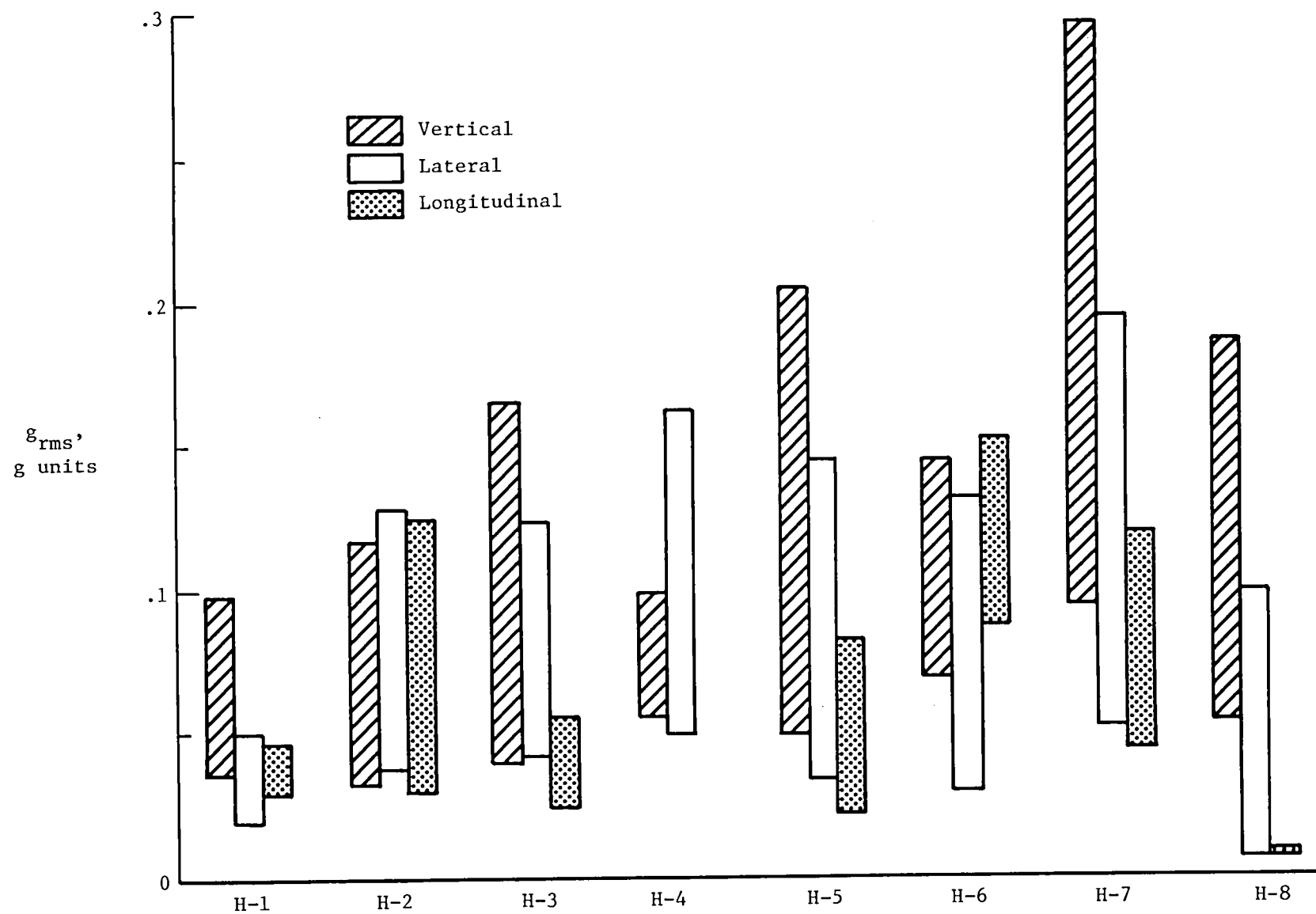
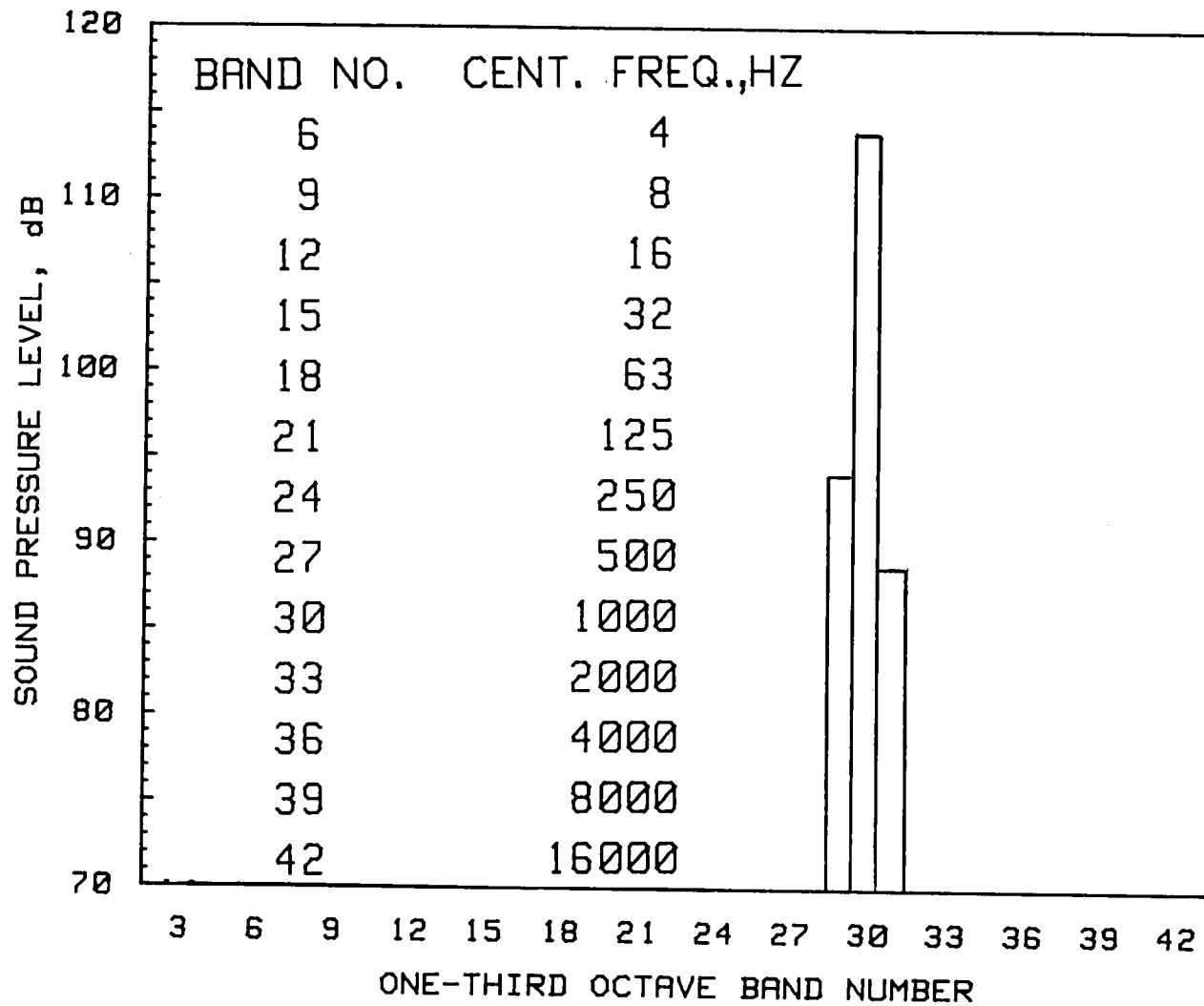
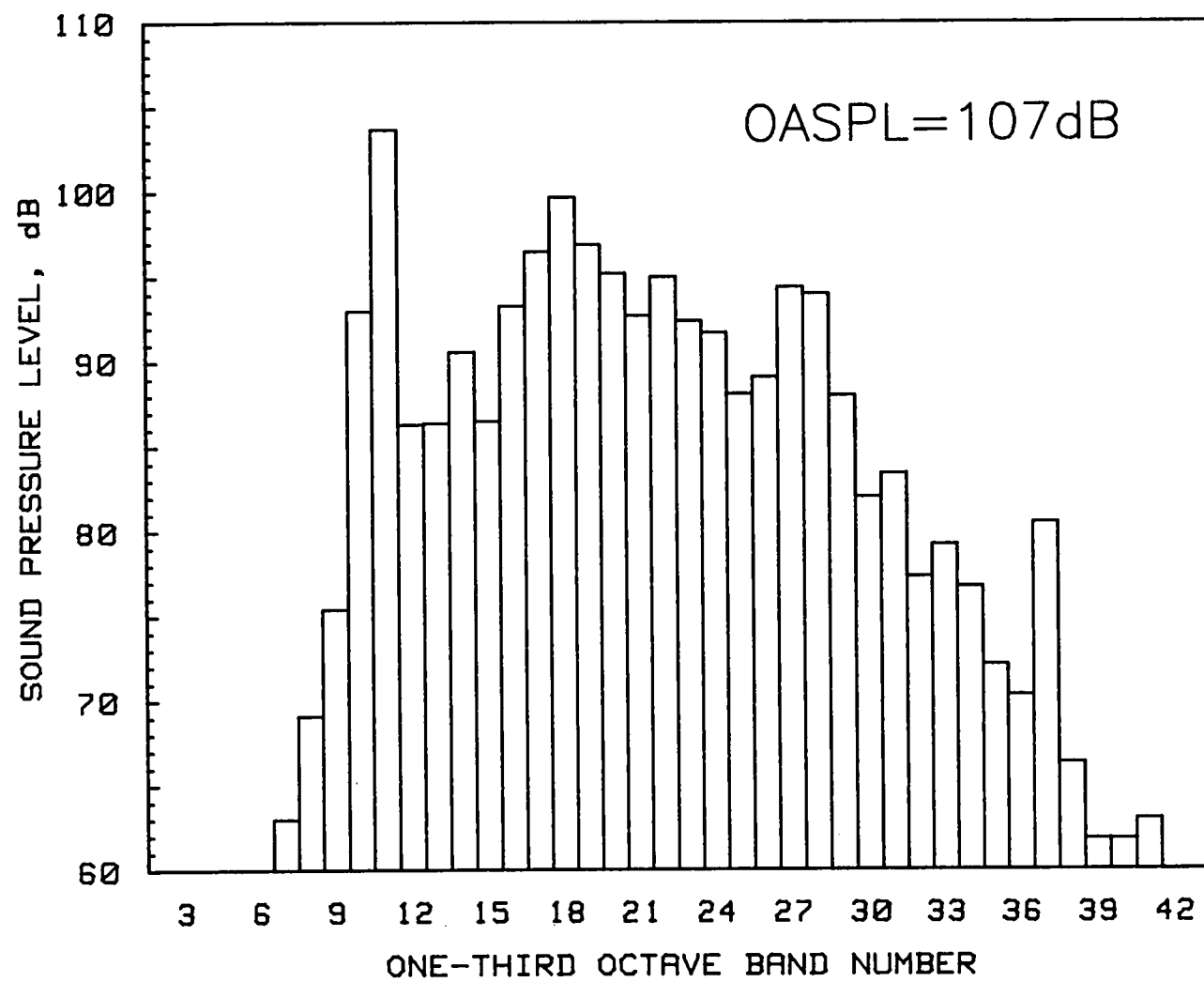


Figure 6.- Flight range of overall rms acceleration levels.



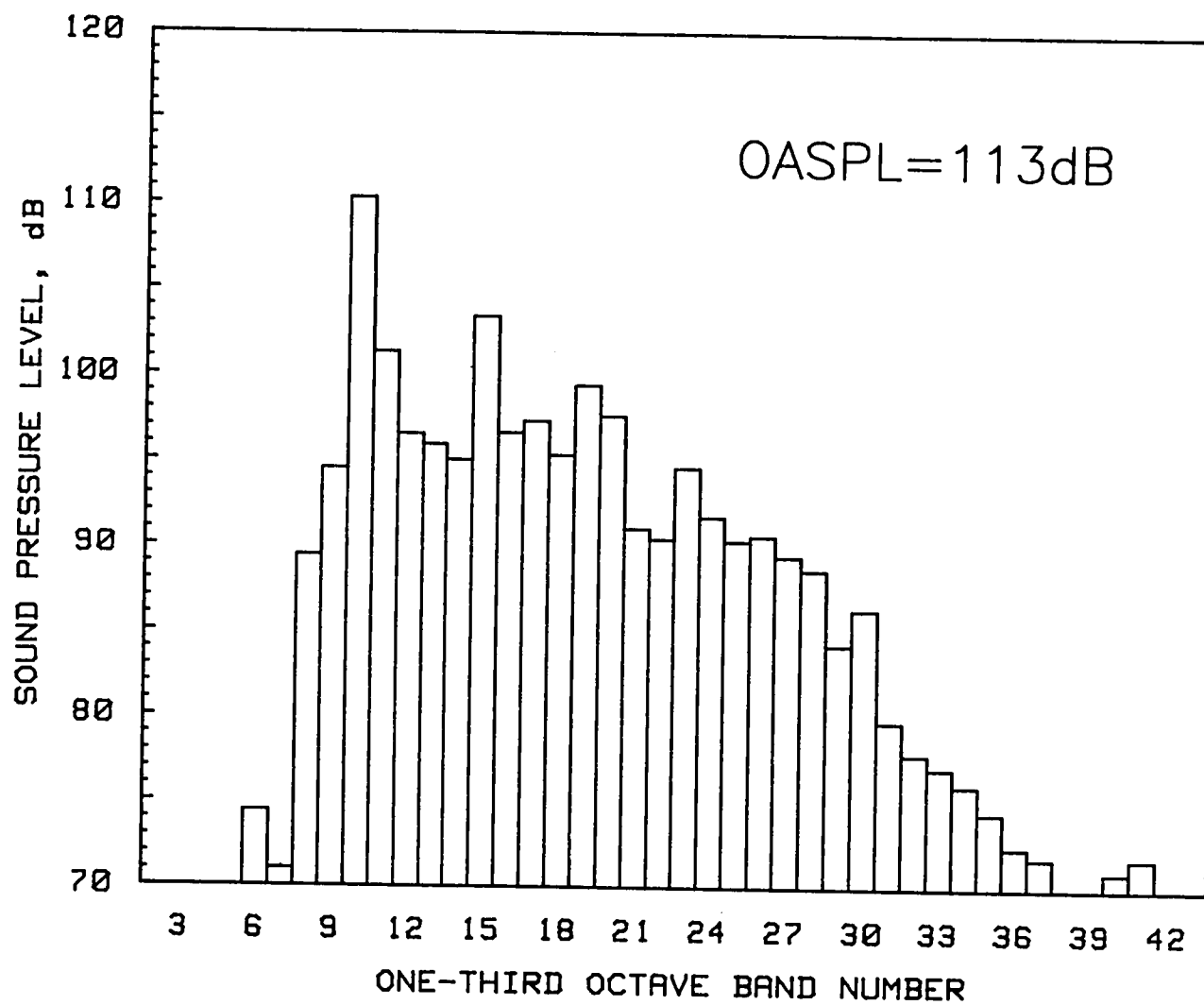
(a) Calibration (114 dB) and band number definition.

Figure 7.- One-third octave band spectra, cruise condition.



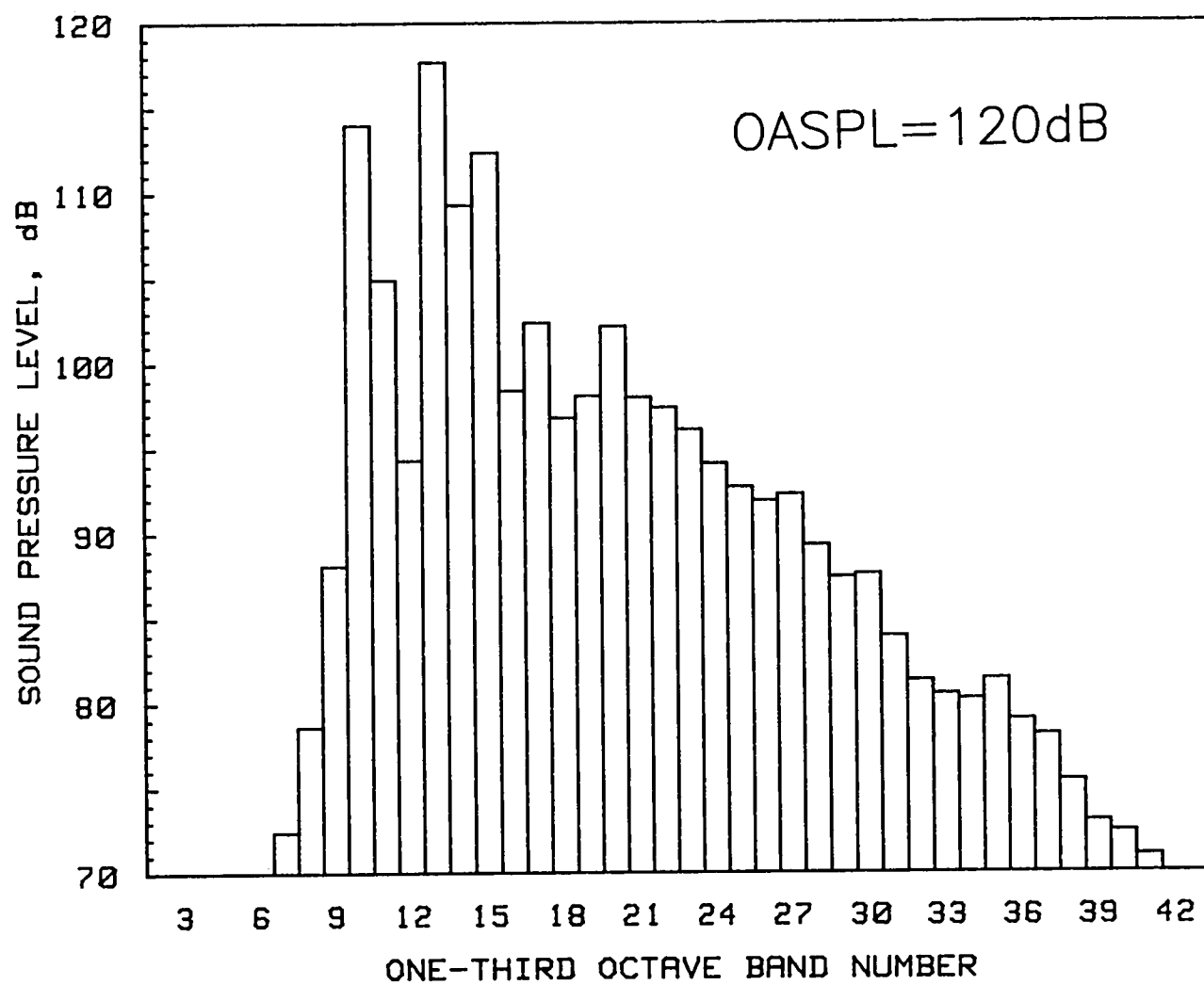
(b) Aircraft H-1.

Figure 7.- Continued.



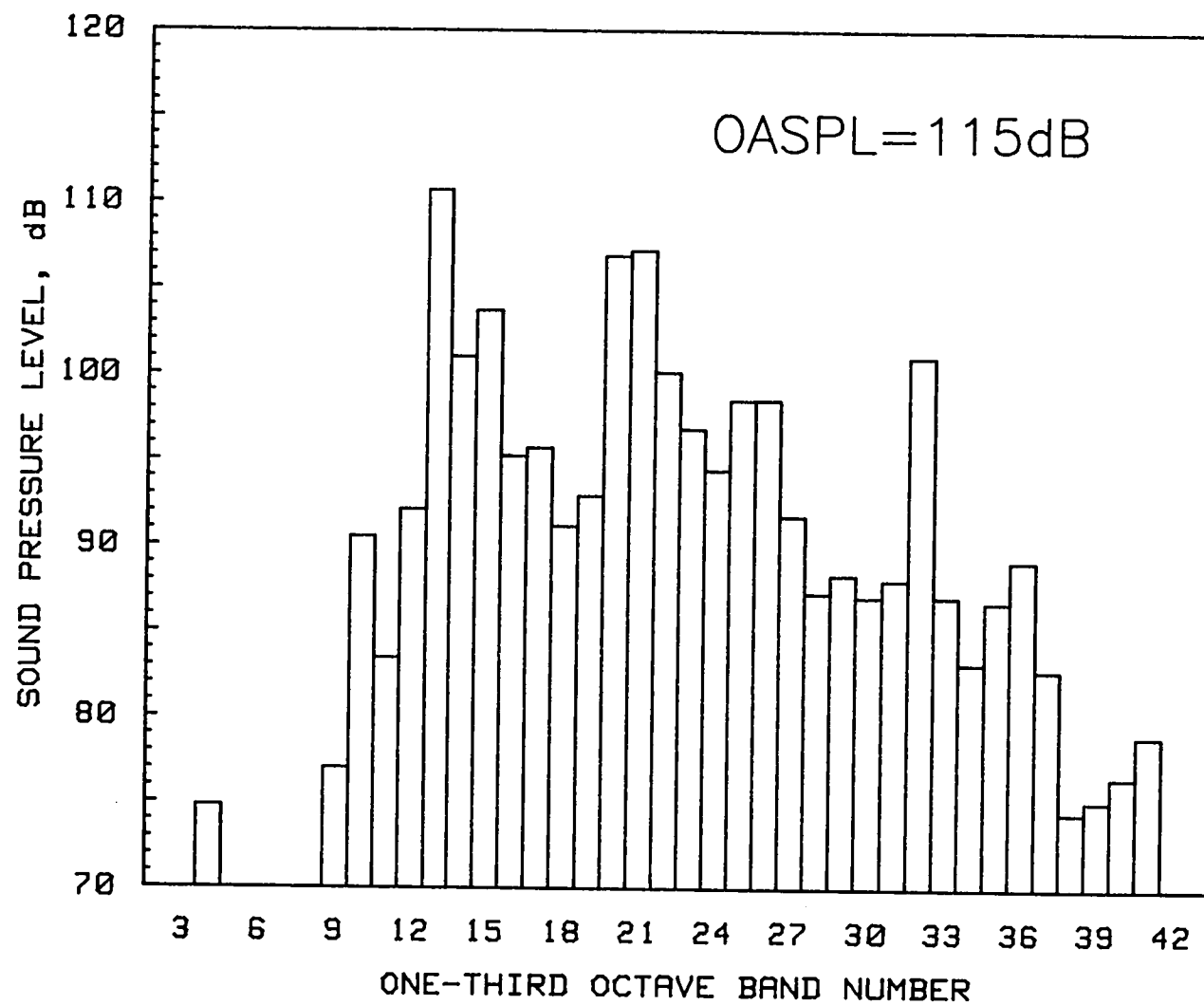
(c) Aircraft H-2.

Figure 7.- Continued.



(d) Aircraft H-3.

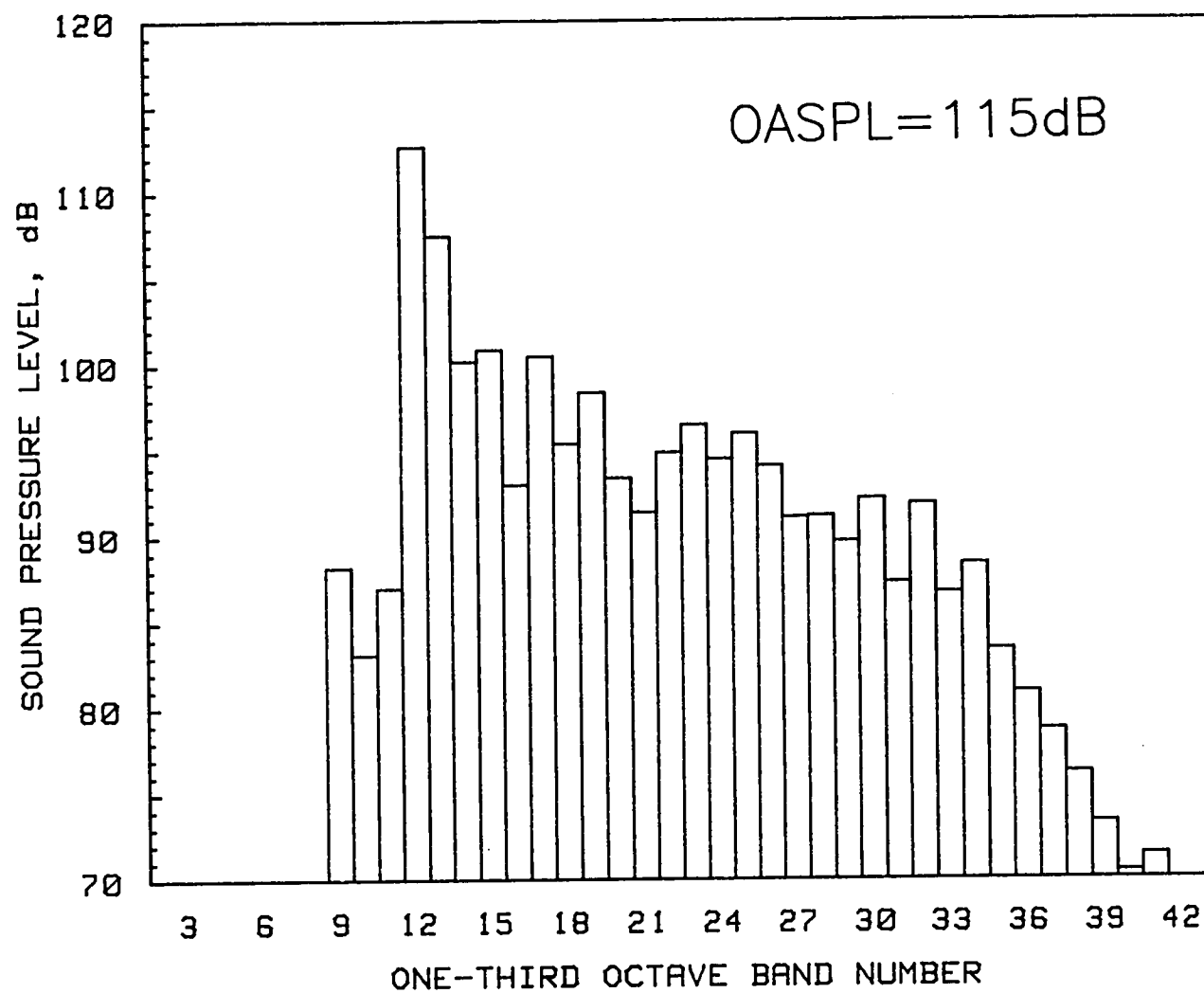
Figure 7.- Continued.



(e) Aircraft H-4.

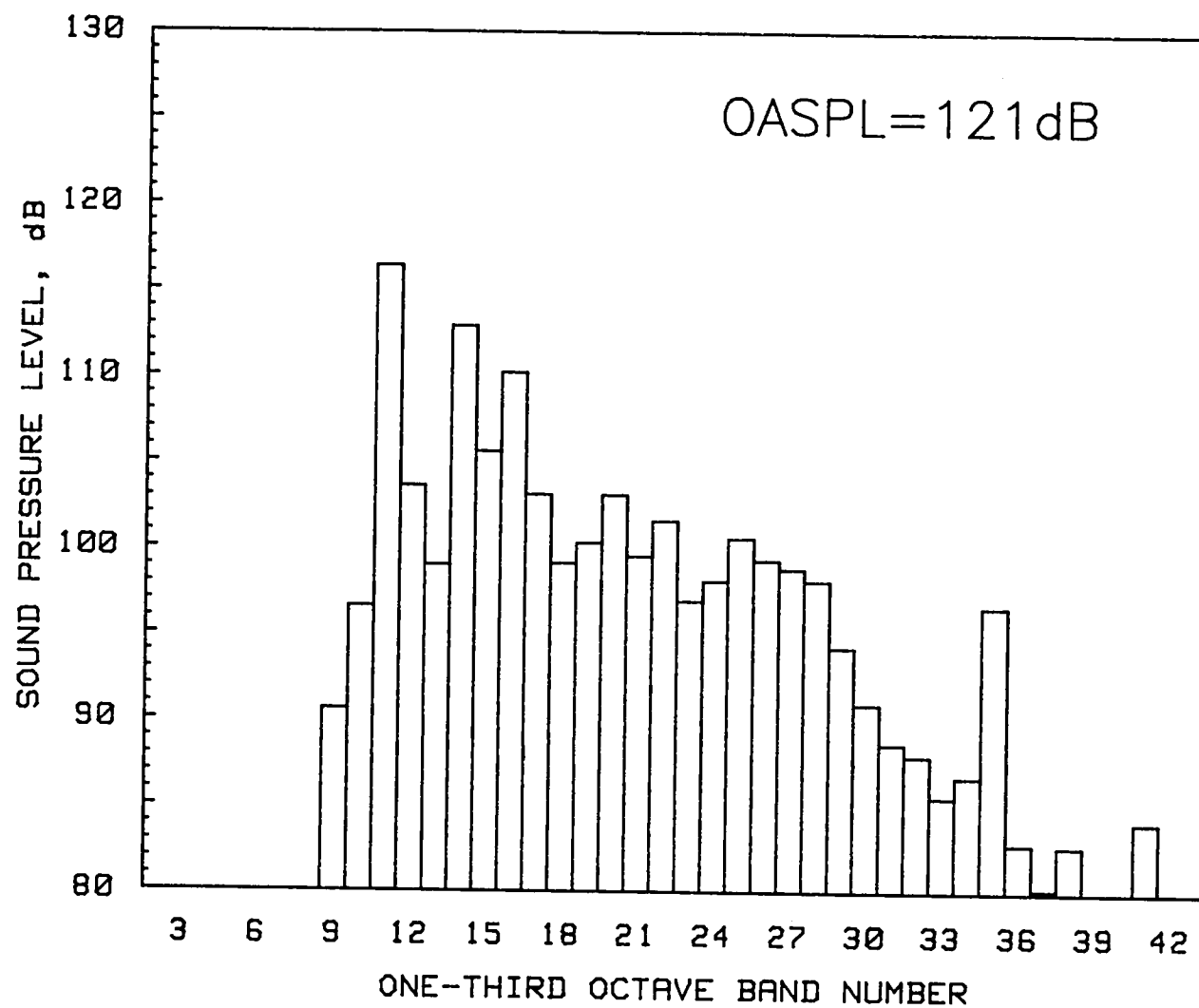
Figure 7.- Continued.





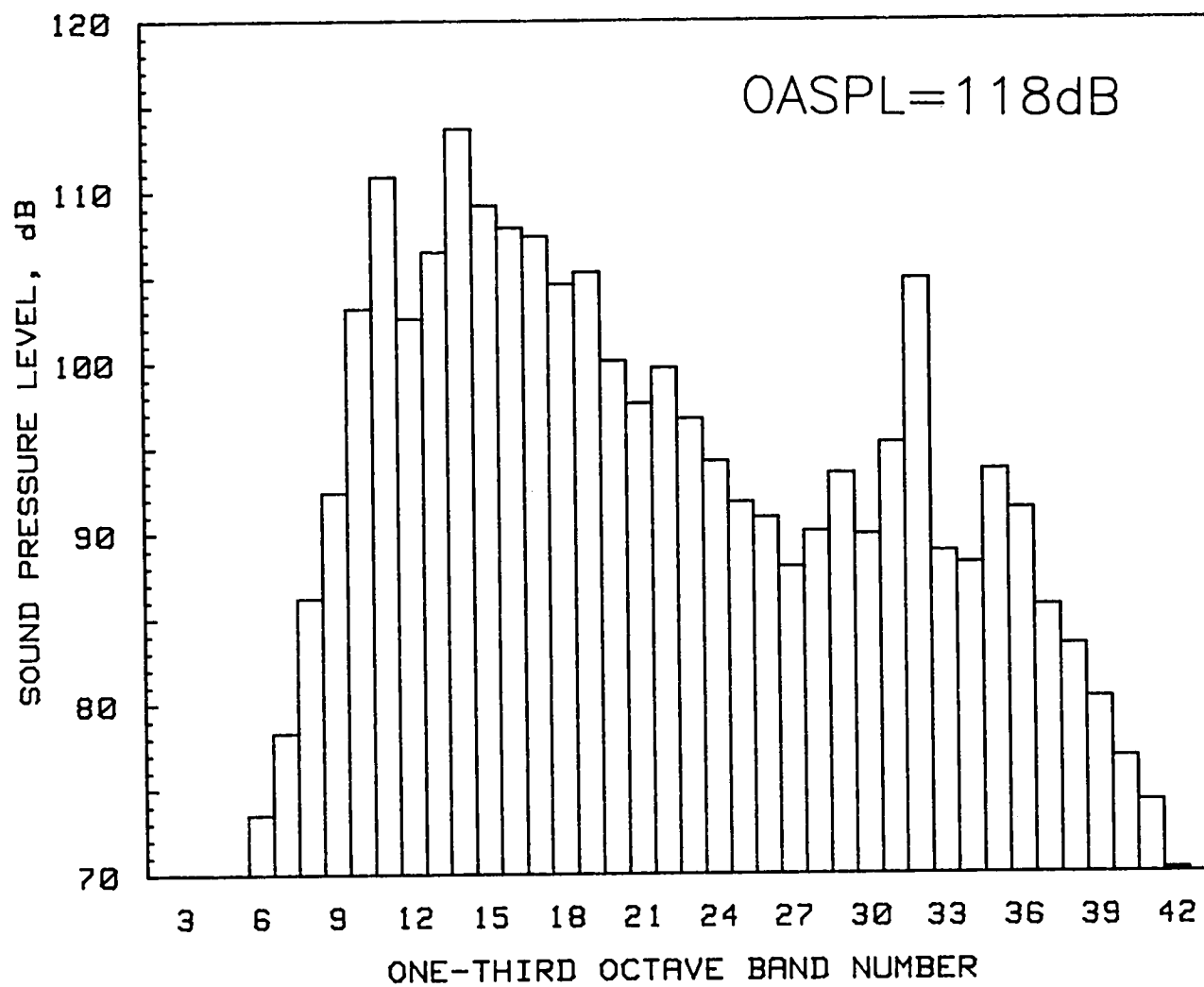
(f) Aircraft H-5.

Figure 7.- Continued.



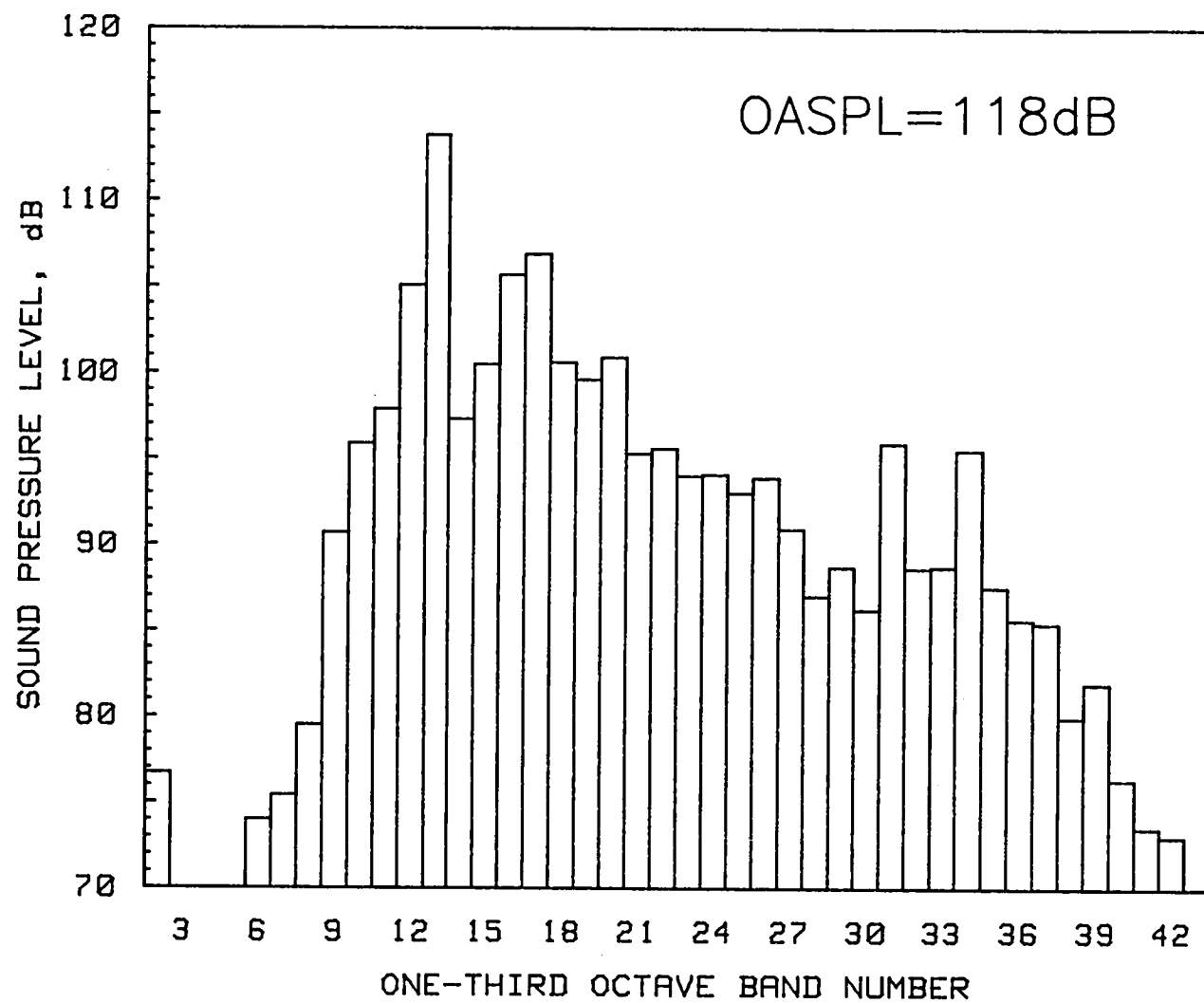
(g) Aircraft H-6.

Figure 7.- Continued.



(h) Aircraft H-7.

Figure 7.- Continued.



(i) Aircraft H-8.

Figure 7.- Concluded.

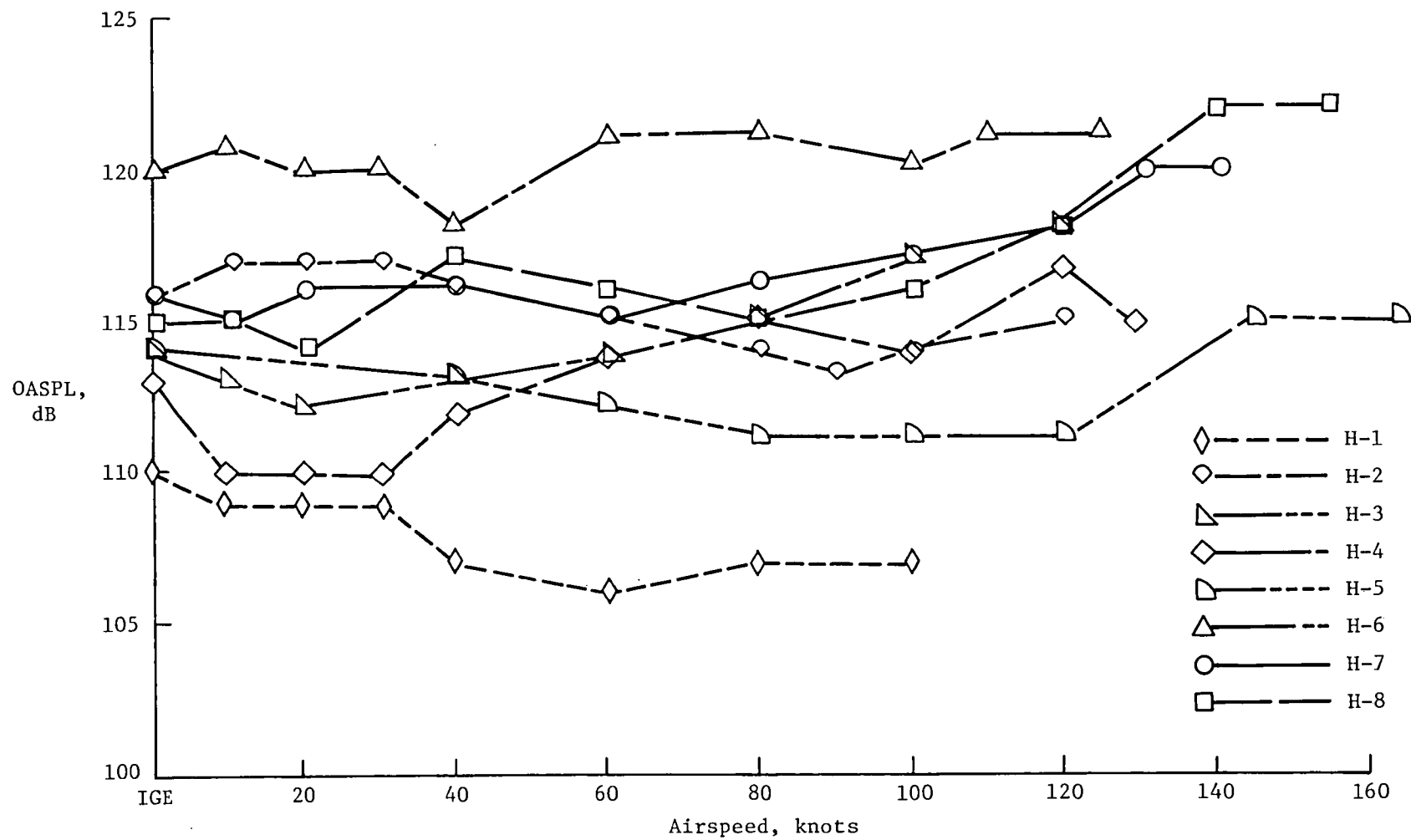


Figure 8.- Variation of overall sound pressure level (OASPL) with airspeed.

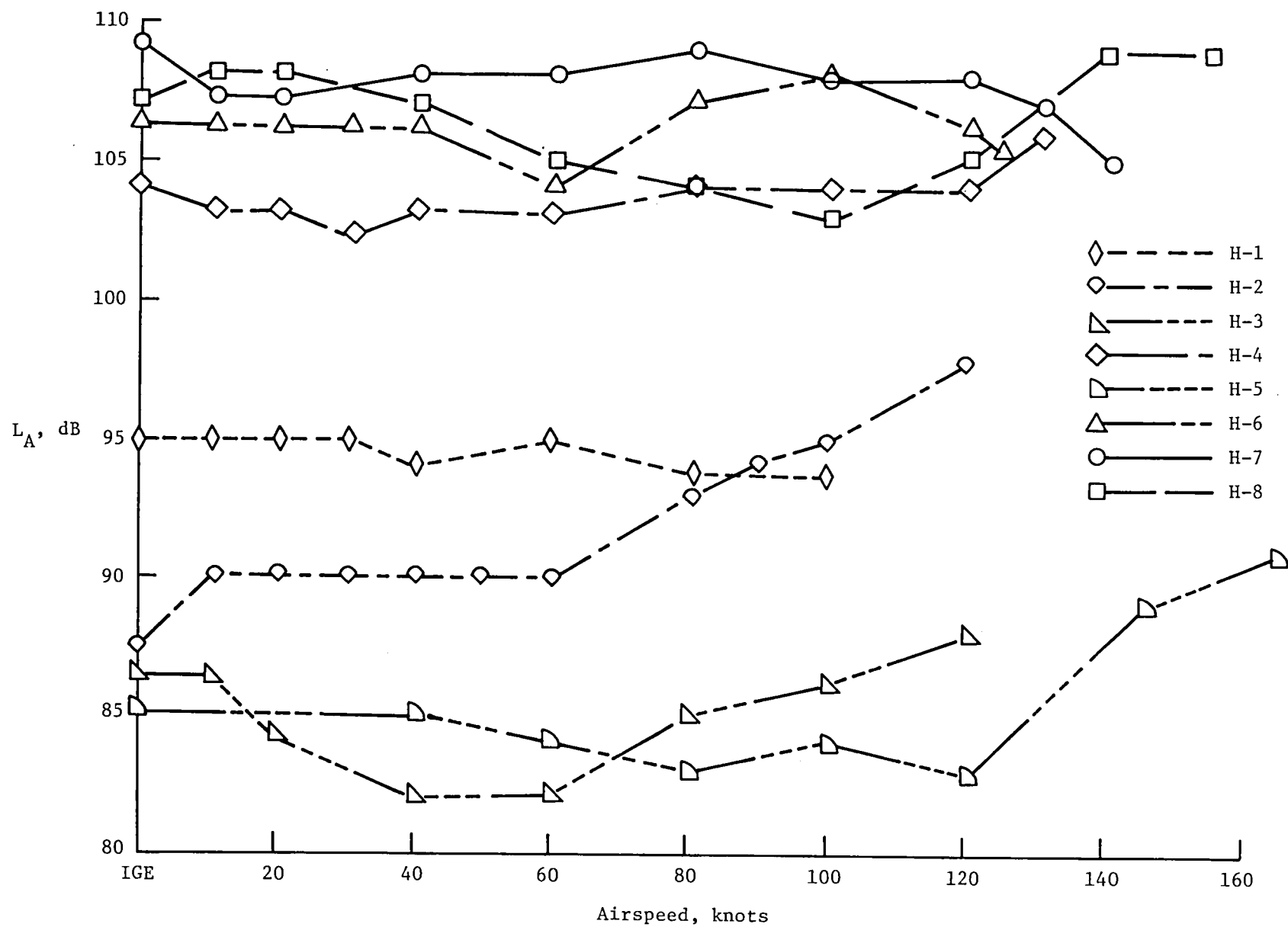
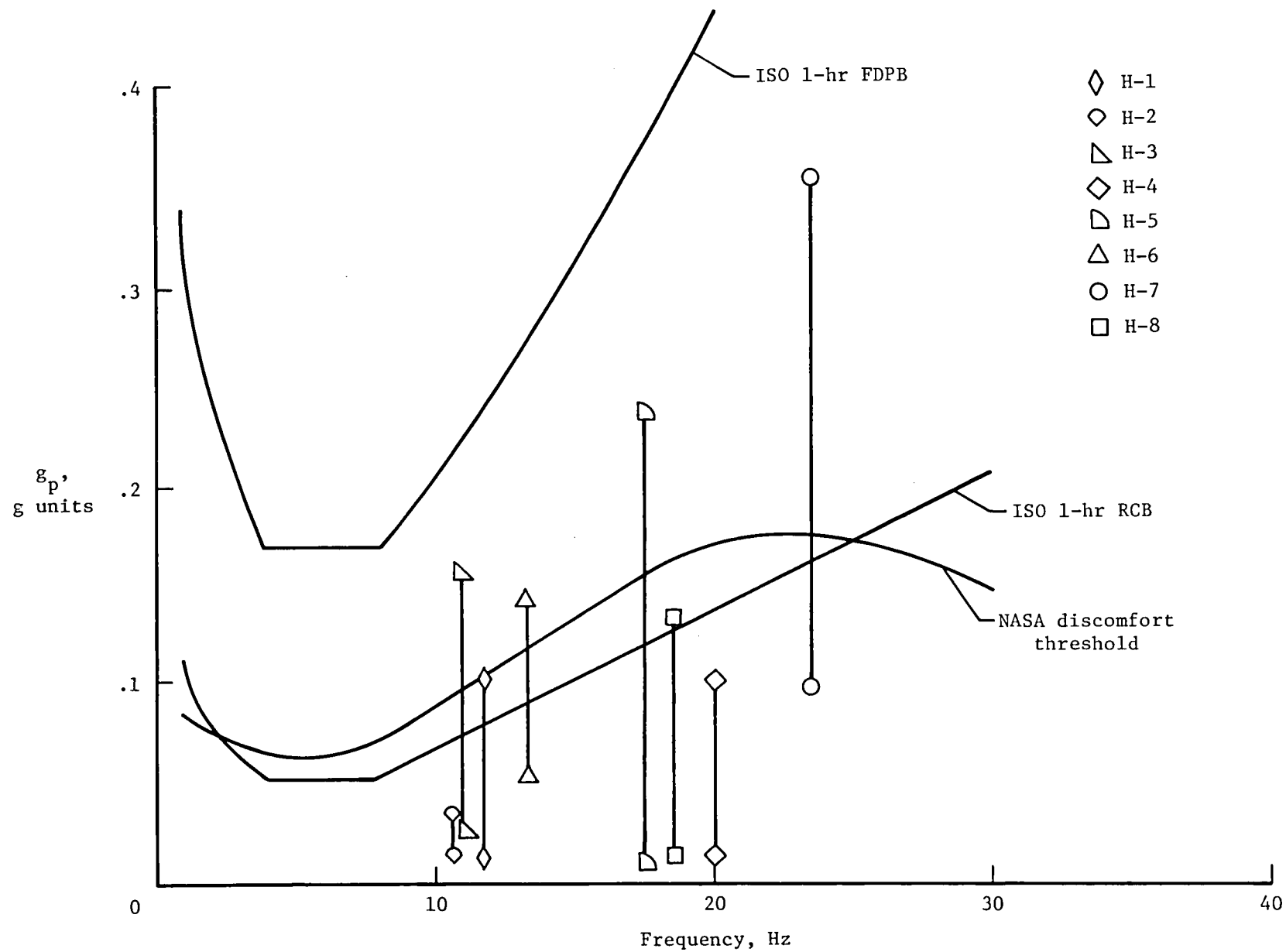
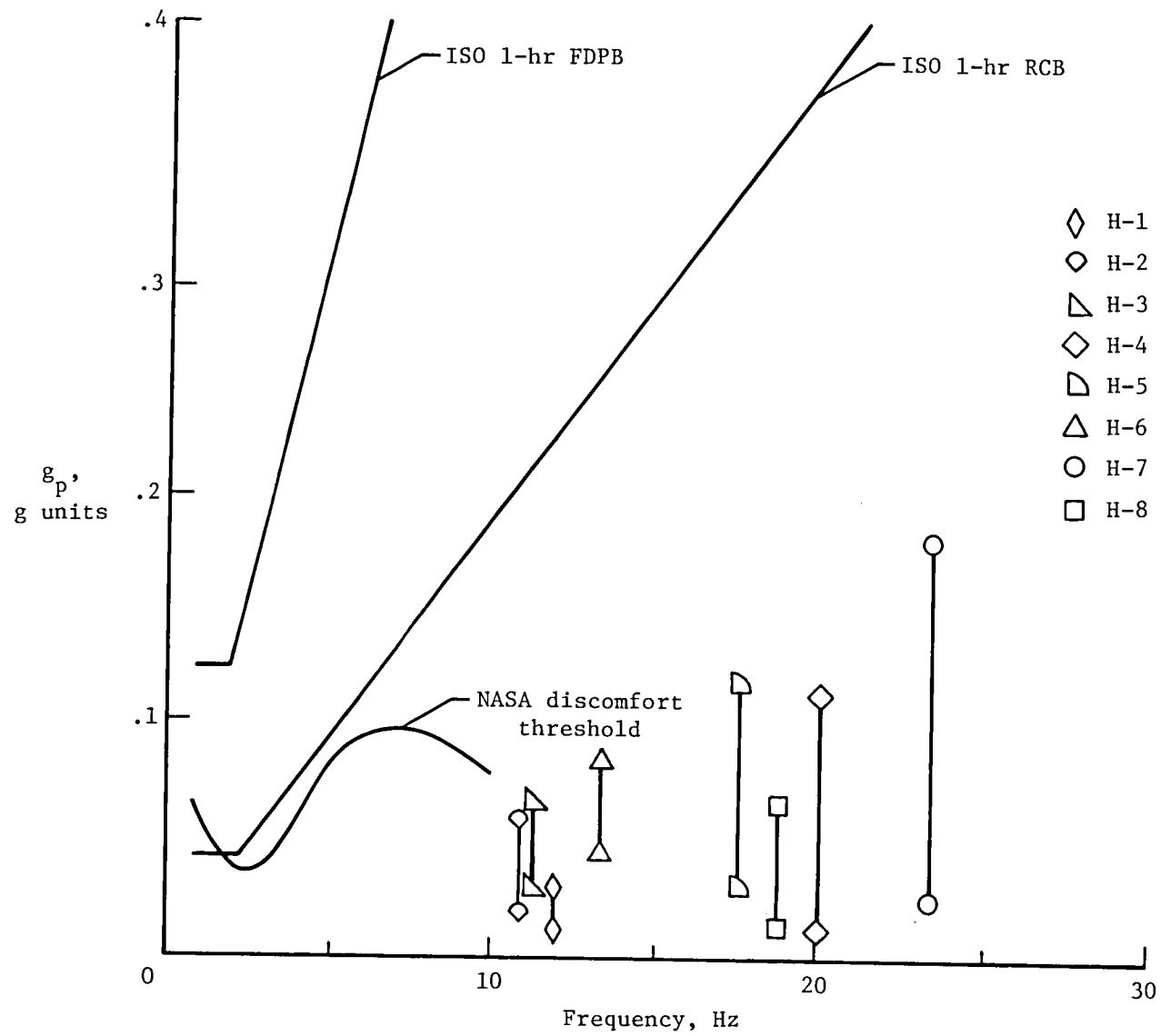


Figure 9.- Variation of "A"-weighted sound pressure level with airspeed.



(a) Vertical direction.

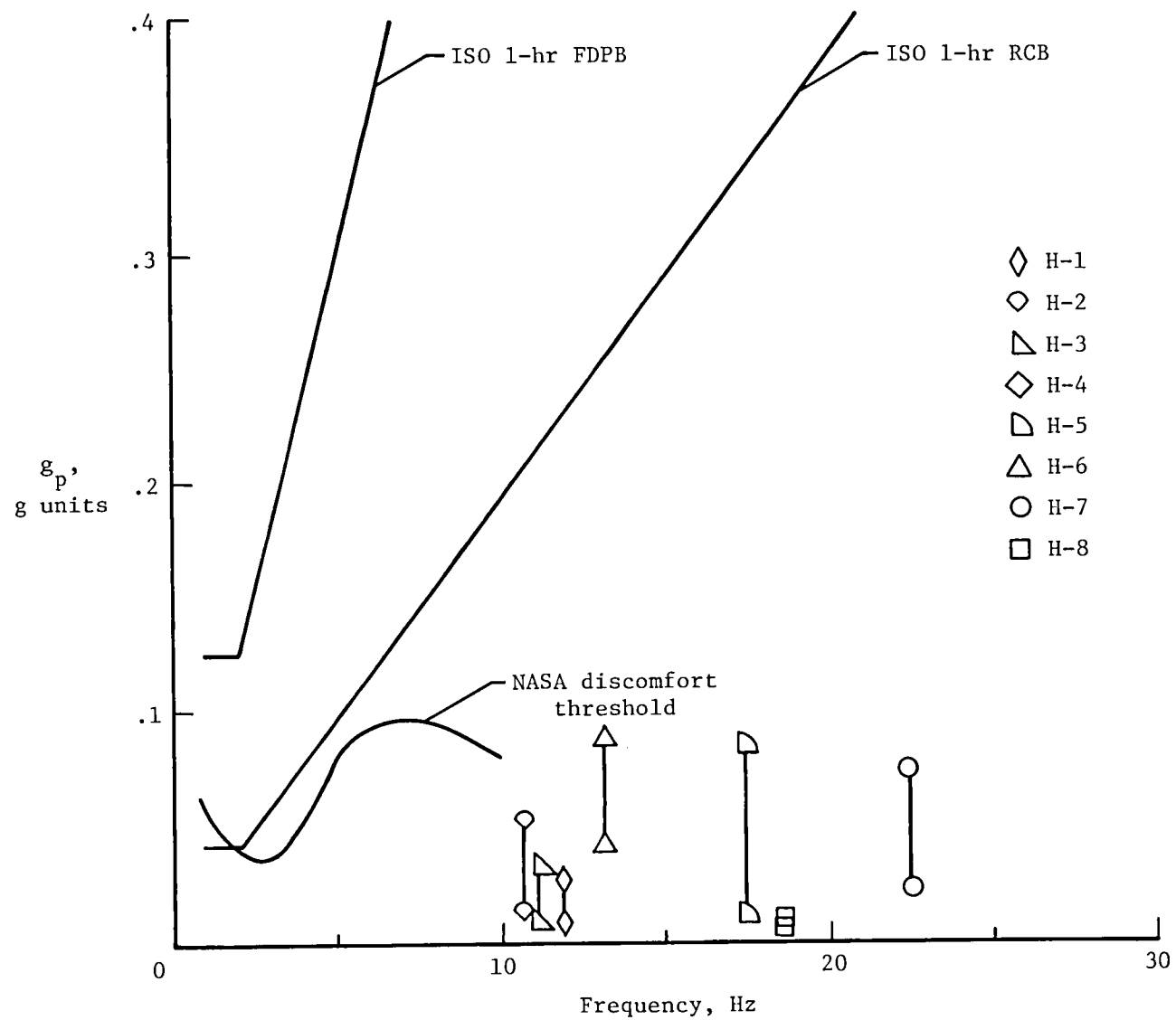
Figure 10.- Comparison of peak acceleration as function of frequency to recommended standards.



(b) Lateral direction.

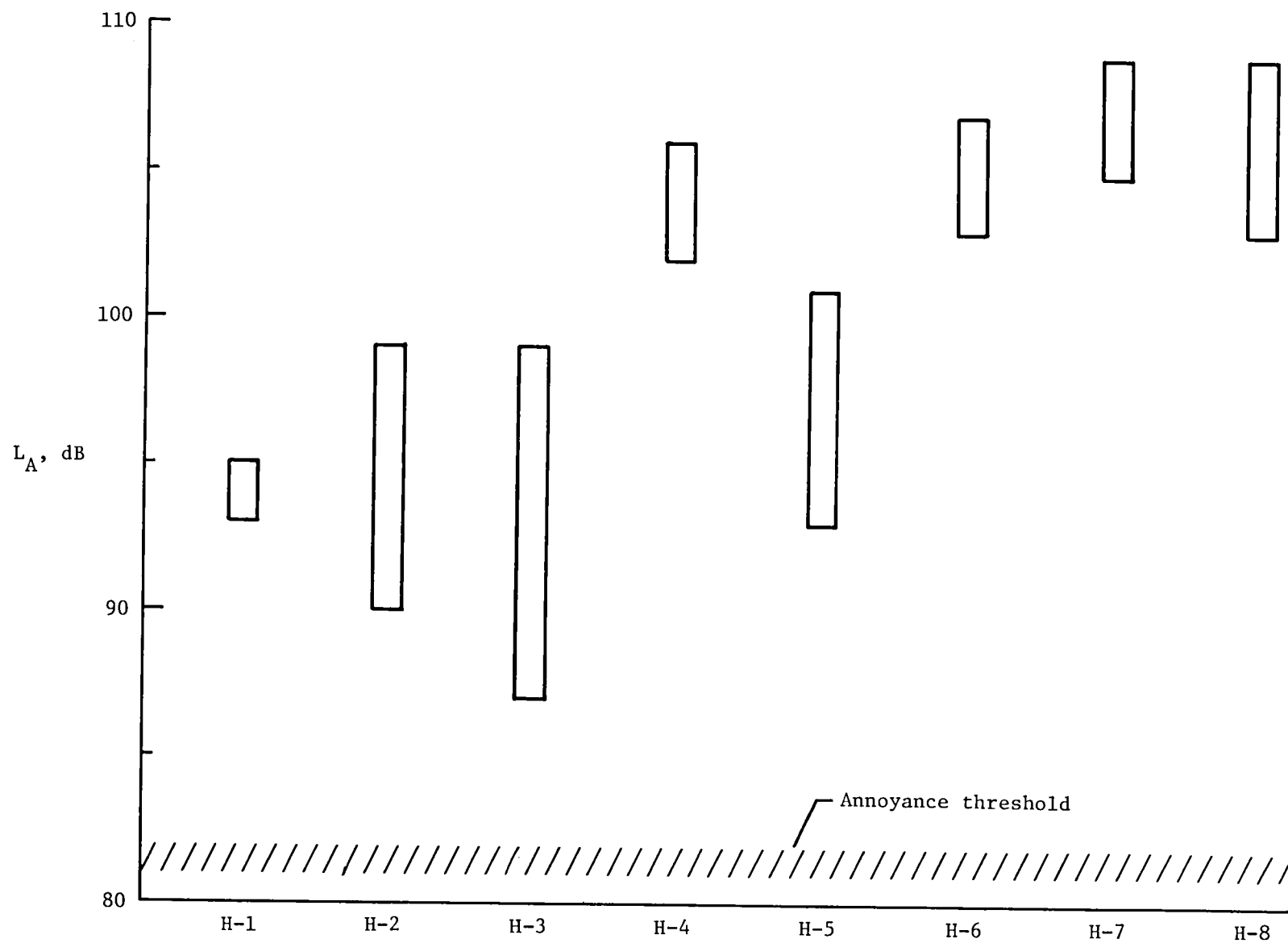
Figure 10.- Continued.





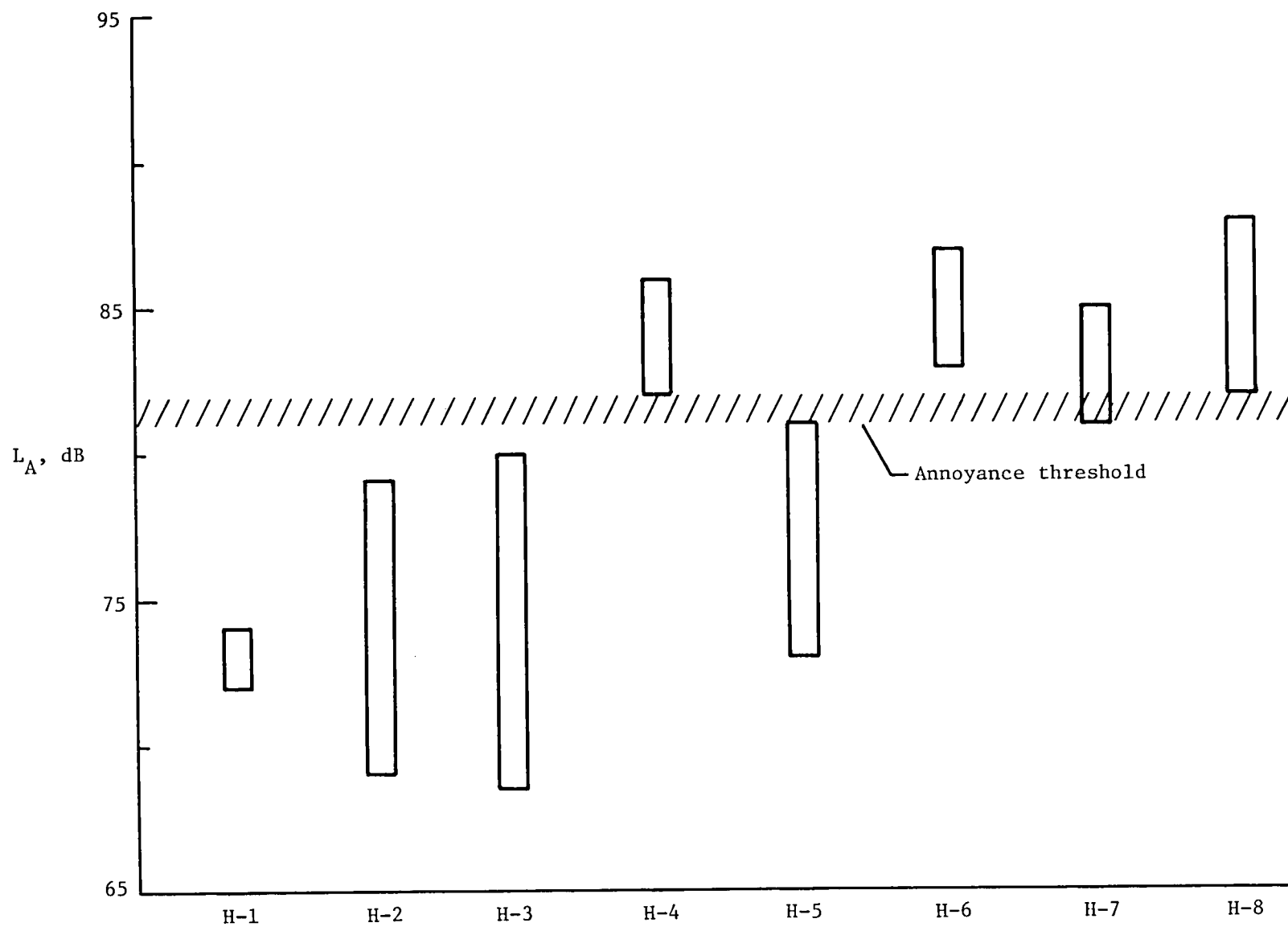
(c) Longitudinal direction.

Figure 10.- Concluded.



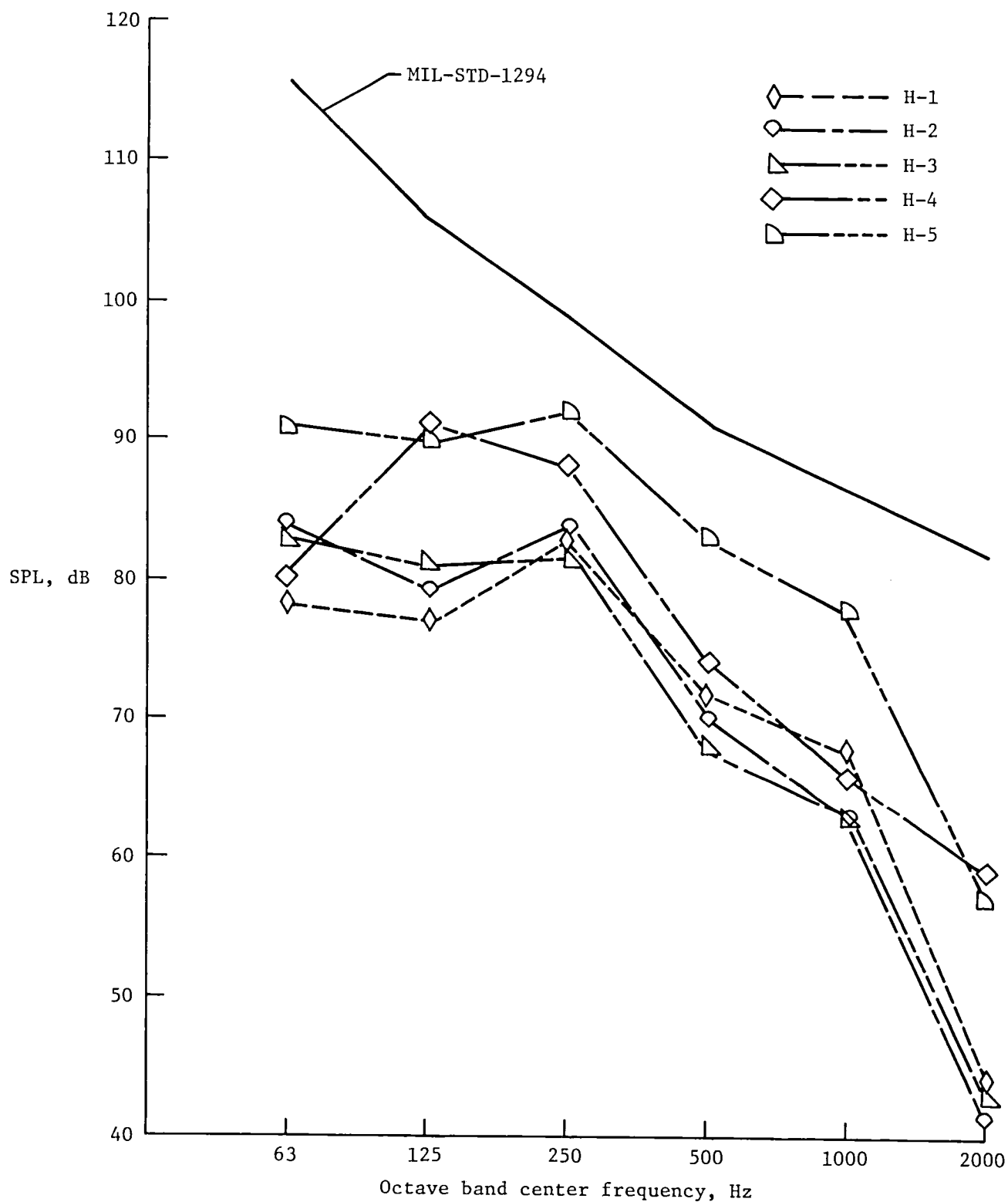
(a) Without ear protection.

Figure 11.- Ranges of interior "A"-weighted noise levels compared to an annoyance threshold (ref. 15).



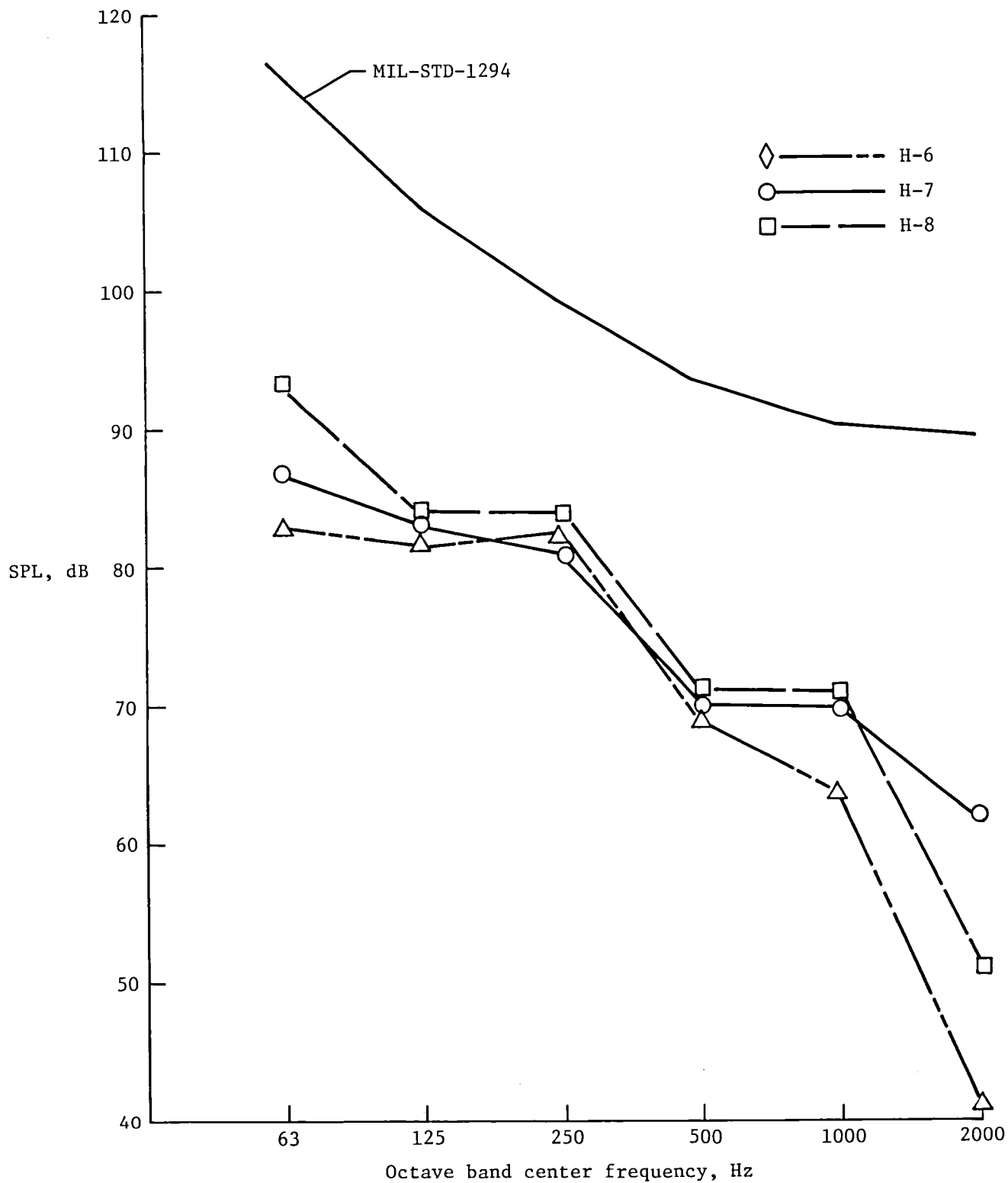
(b) With ear protection.

Figure 11.- Concluded.



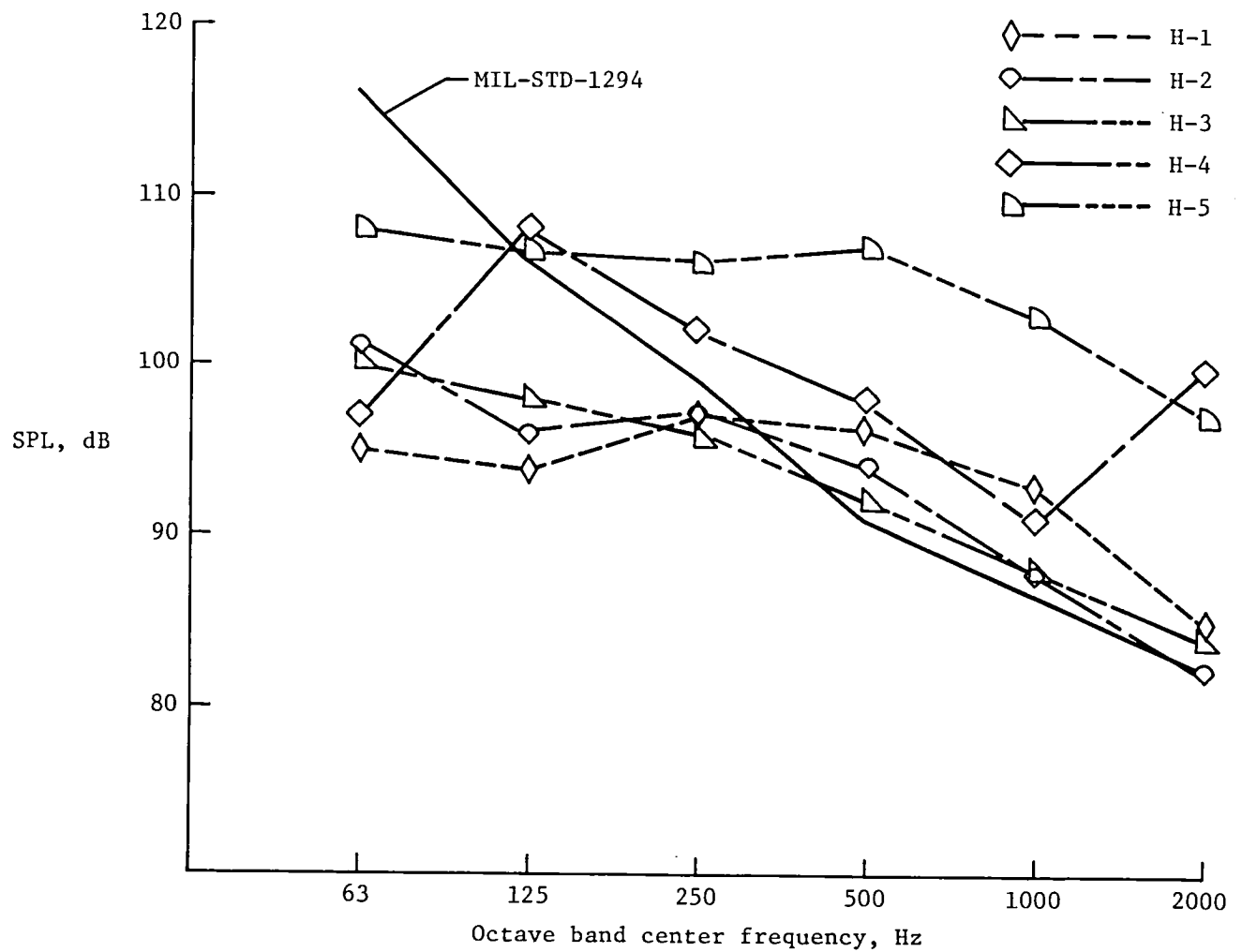
(a) Criteria for helicopter gross weight under 20 000 lb.

Figure 12.- Comparison of interior noise spectra with noise limit design criteria (ref. 14) corrected for helmet attenuation.



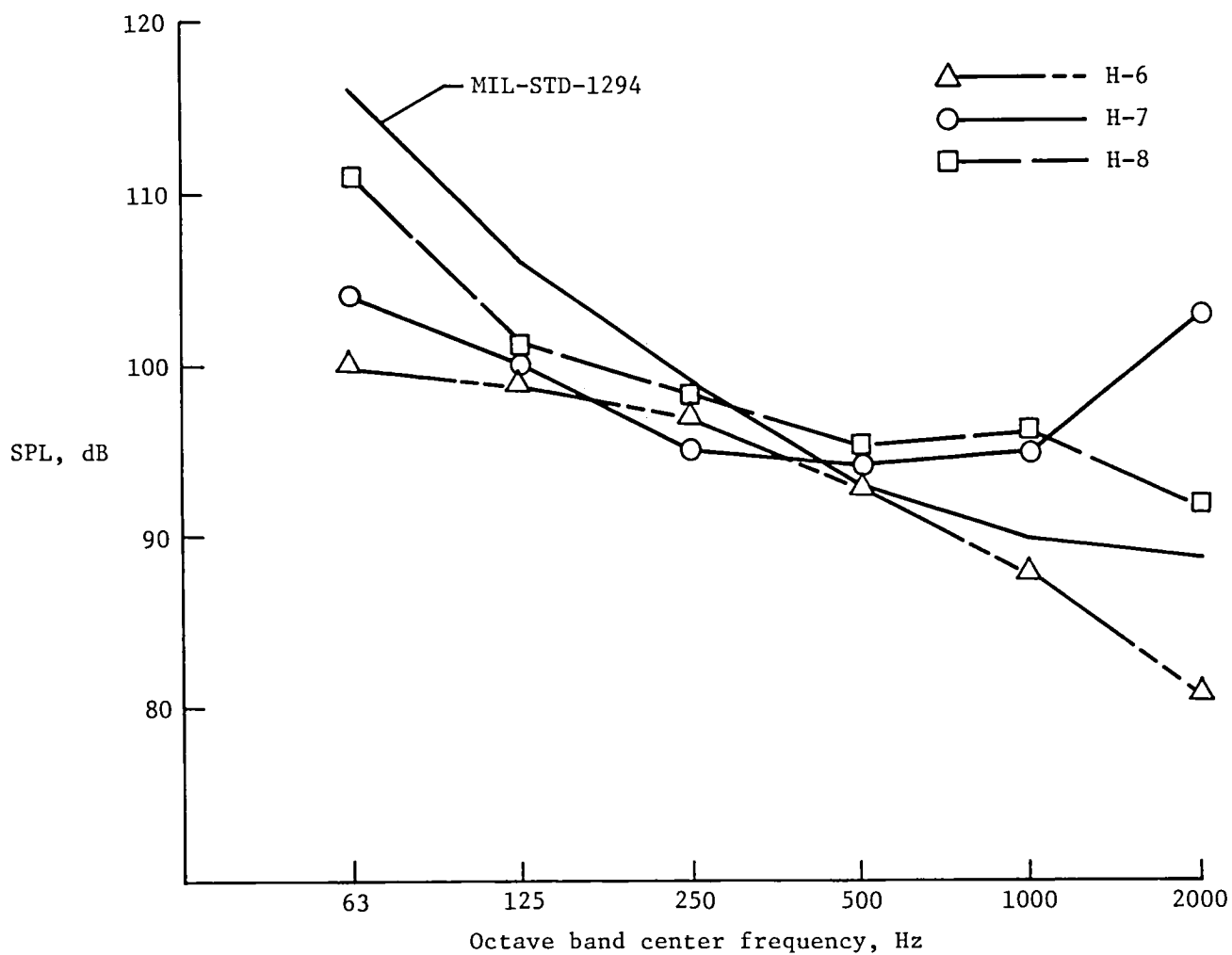
(b) Criteria for helicopter gross weight in excess of 20 000 lb.

Figure 12.- Concluded.



(a) Criteria for helicopter gross weight under 20 000 lb.

Figure 13.- Comparison of interior noise spectra with noise limit design criteria (ref. 14) with no helmet correction.



(b) Criteria for helicopter gross weight in excess of 20 000 lb.

Figure 13.- Concluded.





.

1. Report No. NASA TM-84664 AVRADCOM TR 83-D-21		2. Government Accession No.		3. Recipient's Catalog No.	
4. Title and Subtitle INTERIOR NOISE AND VIBRATION MEASUREMENTS ON OPERATIONAL MILITARY HELICOPTERS AND COMPARISONS WITH VARIOUS RIDE QUALITY CRITERIA				5. Report Date August 1983	
				6. Performing Organization Code 505-35-13-01	
7. Author(s) Sherman A. Clevenson, Jack D. Leatherwood, and Daniel D. Hollenbaugh				8. Performing Organization Report No. L-15598	
9. Performing Organization Name and Address NASA Langley Research Center Hampton, VA 23665 and Applied Technology Laboratory AVRADCOM Research and Technology Laboratories Fort Eustis, VA 23604				10. Work Unit No.	
				11. Contract or Grant No.	
				13. Type of Report and Period Covered Technical Memorandum	
12. Sponsoring Agency Name and Address National Aeronautics and Space Administration Washington, DC 20546 and U.S. Army Aviation Research and Development Command St. Louis, MO 63166				14. Army Project No.  1L262209AH76	
15. Supplementary Notes Sherman A. Clevenson and Jack D. Leatherwood: Langley Research Center. Daniel D. Hollenbaugh: Applied Technology Laboratory, AVRADCOM Research and Technology Laboratories.					
16. Abstract This paper shows the results of physical measurements of the interior noise and vibration obtained within eight operational military helicopters. The data were extensively analyzed and are presented in the following forms: noise and vibration spectra, overall root-mean-square acceleration levels in three linear axes, peak accelerations at dominant blade passage frequencies, acceleration exceedance data, and overall and "A"-weighted sound pressure levels. Peak acceleration levels were compared to the ISO 1-hr reduced comfort and fatigue decreased proficiency boundaries and the NASA discomfort criteria. The "A"-weighted noise levels were compared to the NASA annoyance criteria, and the overall noise spectra were compared to MIL-STD-1294 ("Acoustical Noise Limits in Helicopters"). It is shown that specific vibration components at blade passage frequencies for several aircraft exceeded both the ISO reduced comfort boundary and the NASA passenger discomfort criteria. The "A"-weighted noise levels, corrected for SPH-4 helmet attenuation characteristics, exceeded the NASA annoyance threshold for several aircraft. The spectra of the octave band noise levels for all aircraft exceeded MIL-STD-1294 during cruise, but when corrected for helmet attenuation, fell within the limits of MIL-STD-1294.					
17. Key Words (Suggested by Author(s)) Interior noise Helicopter interior noise Aircraft interior noise Vibration Ride quality				18. Distribution Statement  Unclassified - Unlimited   Subject Category 71	
19. Security Classif. (of this report) Unclassified	20. Security Classif. (of this page) Unclassified		21. No. of Pages 80	22. Price A05	



National Aeronautics and  
Space Administration

Washington, D.C.  
20546

Official Business

Penalty for Private Use, \$300

THIRD-CLASS BULK RATE

Postage and Fees Paid  
National Aeronautics and  
Space Administration  
NASA-451



**NASA**

POSTMASTER: If Undeliverable (Section 158  
Postal Manual) Do Not Return

---